AN ABSTRACT OF THE THESIS OF

John W. Bodnar for the degree of Doctor of Philosophy

in Biochemistry and Biophysics presented on 30 April 1980.

Title: The Kinetics of Adenovirus DNA Replication

Abstract approved: Redacted for Privacy

(George D. Pearson, Associate Professor of Biochemistry)

Methods have been developed to measure the time required to complete replication of an adenovirus DNA molecule and the time between rounds of replication of the viral genomes. These methods show that 22 minutes are required to complete replication of an adenovirus DNA molecule at 37° C and that this time is constant throughout infection. The rate limiting step in DNA replication is initiation of a round of replication. The initiation rate decreases over infection and shows saturable kinetics corresponding to a maximum of 50,000 replication sites per cell. The size of the pool of adenovirus DNA molecules actively replicating is approximately constant over infection, and the DNA molecules in the pool are preferentially replicated. By use of the measured rate parameters based on the strand displacement mechanism of DNA replication (R. L. Lechner and T. J. Kelly, Jr., 1977. Cell, 12, 1007) several

types of experiments were computer simulated to show that this mechanism and measured rate parameters are consistent quantitatively with experimental data. A mechanism is proposed for generation of defective adenovirus DNA inherent in normal replication.

The Kinetics of Adenovirus DNA Replication

by

John W. Bodnar

A THESIS

submitted to

Oregon State University

in partial fulfillment of
the requirements for the
degree of

Doctor of Philosophy

April 1980

Commencement June 1980

APPROVED:

Redacted for Privacy

Associate Professor of Biochemistry in charge of major

Redacted for Privacy

Chairman of Department of Biochemistry and Biophysics

Redacted for Privacy

Dean of Graduate School

Date thesis is presented 30 April 1980.

Typed by Lyndalu Sikes for John W. Bodnar.

ACKNOWLEDGEMENTS

I thank Professor George Pearson for advice, encouragement, and support. Kate Mathews and Mark Engelking provided excellent technical assistance, and I benefitted from discussions with Dr. Michael Schimerlik, Dr. Reginald McParland, Forest Ziemer, and Dr. Walter Baase.

TABLE OF CONTENTS

Table of Contents (Continued)

LIST OF FIGURES

List of Figures (Continued)

List of Figures (Continued)

LIST OF TABLES

FORWARD

The adenoviruses are a group of human respiratory viruses that have been implicated in pharyngitis, conjunctivitis, and respiratory diseases. There are 31 serotypes of these icosahedral viruses divided into five major subgroups (Green et al, 1979). Type 2 and type 5 adenoviruses, group C viruses with 80 percent DNA homology, cause mild respiratory infections in infants, and they have been used extensively as model systems for studying eukaryotic DNA replication and transcription (for reviews see Winnacker, 1978 and Flint, 1977).

Adenovirus contains a linear double stranded DNA with a molecular weight of 23×10^6 (35,000 base pairs). The DNA contains an inverted terminal repetition of approximately 100 base pairs in all serotypes sequenced to date (Tolun et al, 1979). A 55,000 dalton protein, called terminal protein, is covalently linked to each 5' end of the chromosome (Robinson et al, 1973) both in packaged virion DNA (Rekosh et al, 1977) and intranuclear replicating DNA (Girard et al, 1977; Robinson et al, 1979; Stillman and Bellett, 1979; Kelly and Lechner, 1979).

The lytic cycle of adenoviruses has been studied mostly in cultures of HeLa or KB cells using a high multiplicity of infection

(MOI)* to insure synchronous infection (for review see Lindberg et al, 1975). In the first one or two hours of infection the virus is taken up by the cell, transported to the nucleus, and the DNA is uncoated (Lonberg-Holm and Philipson, 1969; Chardonnet and Dales, 1970). Transcription of early gene products then proceeds with about 40 percent of the viral genome being expressed (Tibbetts et al, 1974). Between 6 and 12 hours after infection there is a change to the late phase of infection when viral DNA synthesis begins and transcription changes to expression of about 90 percent of the genome mostly for synthesis of viral structural proteins (Fujinaga and Green, 1970; Tibbetts et al, 1974). Viral packaging begins at 18 to 24 hours after infection (Green, 1962; Strohl and Schlesinger, 1965; Rouse and Schlesinger, 1967), and virus particles are accumulated in the nucleus until cell death. Adenovirus does not normally lyse the cells.

Investigations of the mechanism of adenovirus DNA has centered on study of the biochemical or electron microscopic characteristics of the replicating intermediates. The replicating intermediates have a higher buoyant density in CsCl (Pearson and Hanawalt, 1971; Sussenbach et al, 1972; van der Eb, 1973; Pettersson, 1973) and have

---

* The following abbreviations will be used throughout this thesis: Ad2, Ad5, etc. = adenovirus type 2, 5, etc.; BD-cellulose = benzoylated DEAE cellulose; BUdR = 5 bromodeoxyuridine; FUdR = 5 fluorodeoxyuridine; MOI = multiplicity of infection; PFU = plaque forming units; EM = electron microscope, electron microscopic, or electron microscopy.

large portions of single stranded DNA as assayed by benzoylated-napthylated-DEAE-cellulose chromatography (van der Eb, 1973; Sussenbach and van der Vliet, 1973) or sensitivity to single strand endonucleases (Pettersson, 1973; Pearson, 1975). Replicating molecules sediment faster than mature DNA in neutral sucrose or glycerol gradients (Horwitz, 1971; van der Eb, 1973; Bellett and Younghusband, 1972; Wilhelm et al, 1976). Electron microscope studies of the replicating forms have shown two major types of intermediates: 1) Y-shaped molecules with an arm or arms of single stranded DNA, and 2) linear molecules of unit length with single stranded gaps (van der Eb, 1973; Ellens et al, 1974; Lechner and Kelly, 1977). Pulse labeling experiments have shown that the termini for replication are at both 3' ends of the genome (Horwitz, 1974; Tolun and Pettersson, 1975; Schilling et al, 1975; Horwitz, 1976; Bourgaux et al, 1976; Weingartner et al, 1976; Sussenbach and Kuijk, 1977) and that the origins of replication are at or near both 5' ends (Sussenbach and Kuijk, 1978). No covalently closed circular DNA intermediates have been identified (Doerfler et al, 1973; Bellett and Younghusband, 1972) although the DNA can be circularized by interactions of the terminal proteins (Robinson et al, 1973).

A strand displacement mechanism for adenovirus DNA replication has been suggested by Sussenbach (Sussenbach et al, 1972) based mainly on EM data on replicating forms. This mechanism has been

modified by Lechner and Kelly (1977) based on their methodical classification of the replicating structures by EM. This revised model for adenovirus DNA replication is shown in Figure 1. We will examine this mechanism in detail, since we will use this scheme as our basis for study of the kinetics of adenovirus DNA replication. Initiation of a round of replication can begin at or near either end of the adenovirus genome. The presence of an inverted terminal repetition and terminal proteins on both 5' ends of the DNA suggests that either or both of these features may be involved in the initiation step. Synthesis proceeds by strand displacement, where the growing point moves to the 3' end of the DNA yielding a mature daughter molecule and a completely displaced single stranded DNA. This displaced single stranded DNA then can initiate a round of complementary synthesis in which the growing point moves from the 5' to 3' end of the single strand filling in a daughter strand to complete the second mature daughter molecule. Lechner and Kelly suggest that the initiation step of complementary synthesis may involve annealing of the inverted terminal repeats of the single stranded DNA to form a "panhandle" structure as seen in Figure 1. Since this "panhandle" structure has the same double stranded sequence at its end as a mature molecule, the initiation step could be identical for displacement and complementary synthesis.

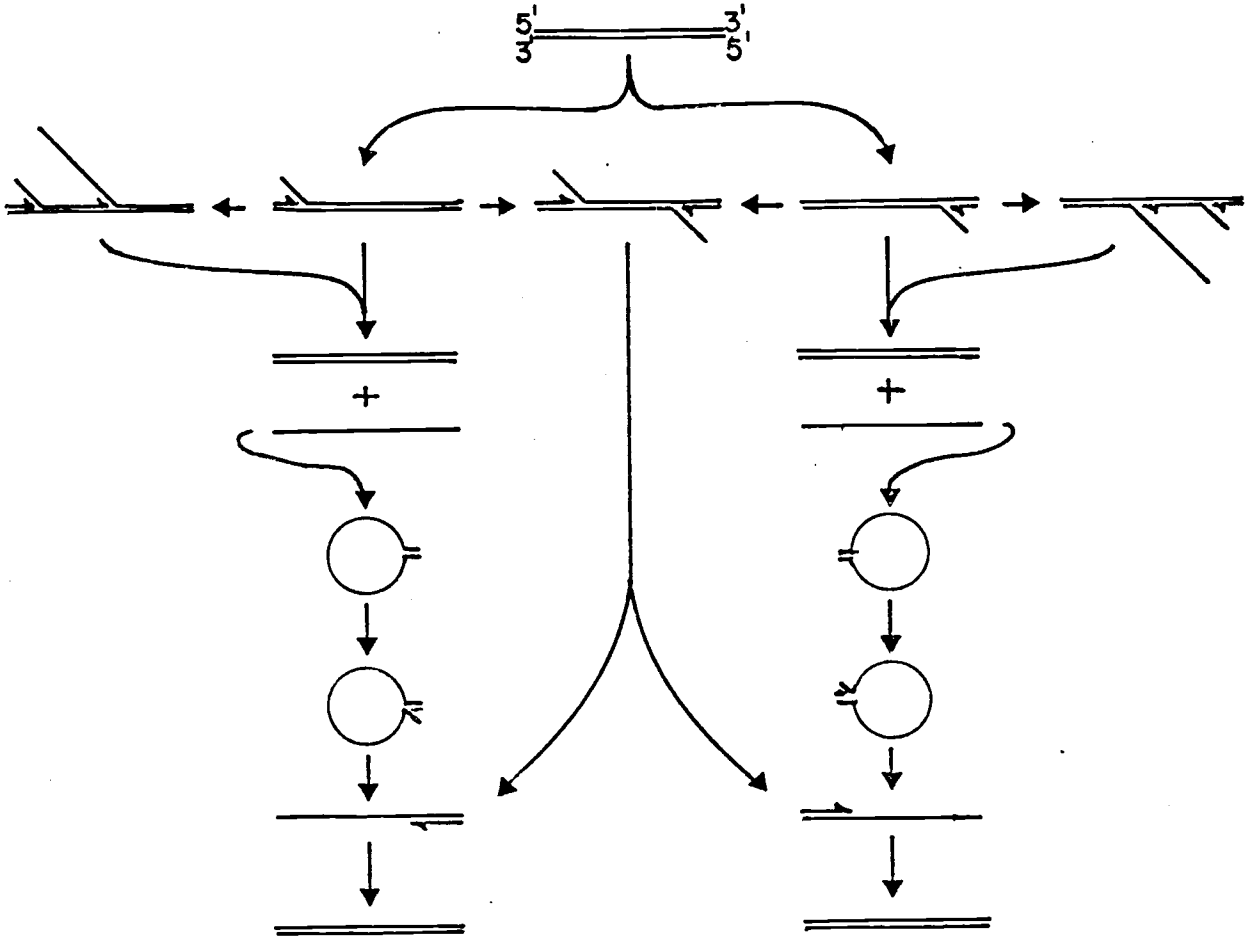

Figure 1. The mechanism for adenovirus DNA replication as proposed by Lechner and Kelly (1977).

The EM studies show many replicative intermediates which have two or more growing points. These can be molecules which initiate a second (or third) round of replication before the first round is completed. These multiply forked molecules accounted for greater than twenty percent of replicating intermediates as seen by Lechner and Kelly.

The mechanism proposed by Lechner and Kelly agrees qualitatively with all experimental data concerning adenovirus DNA replication, but comparing these results we saw what seemed to be contradictions in the kinetics of replication by this scheme. For example, the replication time for one adenovirus DNA molecule has been estimated to be about 20 minutes (Pearson, 1975), but the rate of accumulation of total viral DNA is considerably slower. Early in infection the time to double the DNA concentration is about an hour and later in infection increases to several hours (Green, 1962b; van der Eb, 1973; Flint et al, 1976; Fanning and Doerfler, 1977). This suggests that the time between rounds of replication of the same molecule is long compared with the time to complete one molecule. Supporting this contention are BUdR density labeling experiments in which several hours are required to shift a large fraction of the adenovirus DNA molecules to hybrid density (Vlak et al, 1976; Bellett and Younghusband, 1972; Pearson, unpublished results). However,

Lechner and Kelly have reported that more than 20 percent of the replicating molecules have reinitiated another round of replication before they completed the first. Also, pulse and chase experiments done with tritiated thymidine have shown that it is difficult to chase the activity from the replicating to mature DNA, suggesting that there is substantial re-entry of the adenovirus DNA into the replicating pool prior to completion of replication (Pearson, 1975; van der Eb, 1973). It seems then that the time between rounds of replication is either slow or fast depending on which experiments are to be believed, or perhaps the Lechner and Kelly model does not describe the true picture.

To reconcile these differences, we have described adenovirus DNA replication in terms of its component initiation and chain elongation steps based on the Lechner and Kelly model, measured the individual rates, and compared the kinetics of replication described by these rates with previously published and new data. By using a classical chemical kinetic approach to DNA replication we desired to test the Lechner and Kelly mechanism to see if it could describe DNA replication quantitatively as well as qualitatively. Then by modeling the "contradictory" experiments described above, we hoped to explain the data with one consistent model. Finally, during the course of the kinetic measurements, it became obvious how powerful these

techniques could be in elucidating mechanism, and we were able to propose and test additional aspects of the replication mechanism.

For our kinetic studies we have assumed the mechanism proposed by Lechner and Kelly with component rate constants as shown in Figure 2. The forms shown in this simplified scheme represent greater than 90 percent of the replicating forms (Lechner and Kelly, 1977). Note that for the purposes of the kinetic analysis molecules that are replicating from the left to right end and from the right to left end are equivalent; these will not be described separately unless the particular experiment can distinguish between the two forms. Using the nomenclature suggested by Lechner and Kelly (1977) we name the molecule types as follows: molecules replicating by strand displacement are called type I molecules; molecules replicating by complementary synthesis are called type II molecules; type II molecules which have reinitiated a second round of replication are called type I/II molecules. The rate constants used are as follows: the rate of chain elongation, or the replication rate, has the units of fractional genome lengths per minute; since these may be different for type I and II growing points, r_I is the replication rate for type I molecules, r_{II} for type II molecules, and r the average replication rate where the two types of molecules cannot be distinguished. The probability of a molecule starting a round of replication, or the initiation rate, has

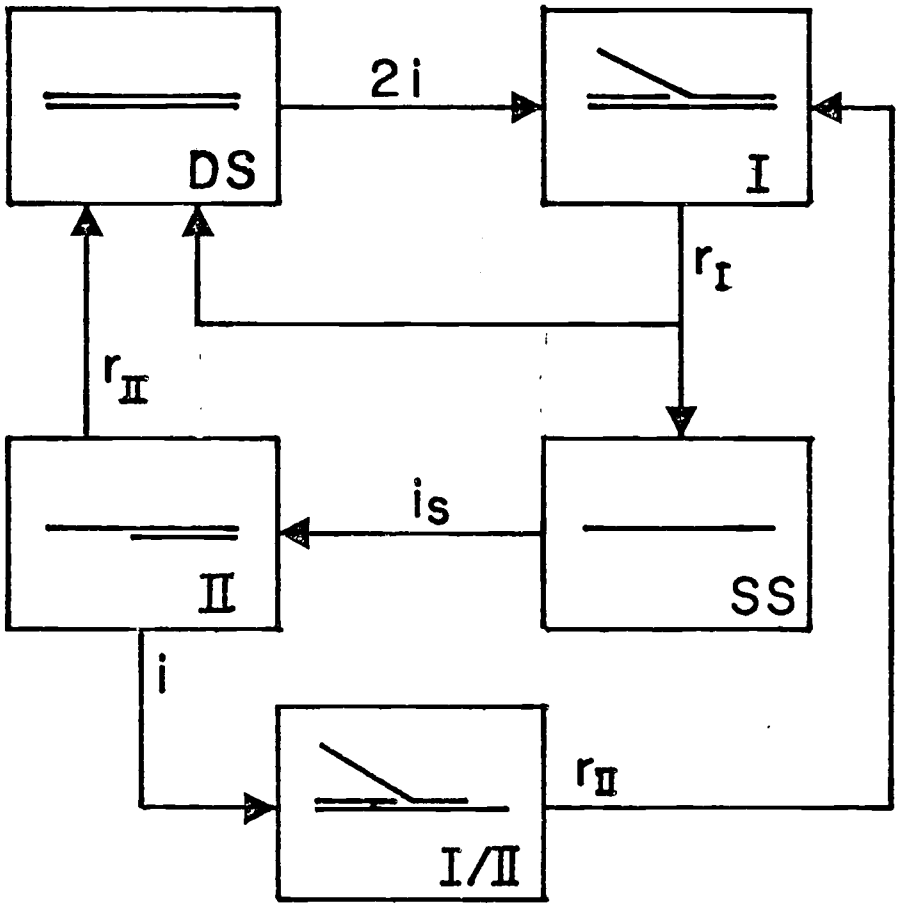

Figure 2. Adenovirus DNA replication. Nomenclature from Lechner and Kelly (1977): I = type I replicating molecules; II = type II replicating molecules; I/II = type I/II replicating molecules; DS = mature double stranded Ad DNA; SS = displaced single stranded DNA. The rate parameters are defined in the text.

the units of initiations per molecular end per minute; the initiation rate for double stranded ends is called i, and the initiation rate for the displaced single stranded DNA will be called i_s. Note that since a mature Ad DNA molecule can initiate a round of replication from either end that its initiation rate will be 2i.

We will divide the kinetic studies into several sections, measure the rate parameters, then use them to model DNA replication. Part I describes several methods to measure the replication rate, and therefore the average time to completely replicate a single Ad DNA molecule. We show that for Ad2 and Ad5 this is about 22 minutes and that this time is constant during infection. In Part II we develop four independent ways to measure the initiation rate (i) and a method to estimate r_I, r_{II}, and i_s. We show that the initiation rate (i) is the rate limiting step in adenovirus DNA replication, that it decreases over infection with saturable kinetics, and that it shows a pooling effect where recently replicated DNA molecules are preferentially replicated. The estimates of the other rate constants show that initiation of complementary synthesis (i_s) is very rapid, and the differences in rate constants suggest a mechanism for generation of defective adenovirus DNA that is inherent in replication. In Part III we use the measured rate parameters to predict the results of several experiments and compare these simulations with the experi-

mental results. We show that the experiments that seemed contradictory are in fact consistent quantitatively with the Lechner and Kelly model. One should note here that while simulations are necessarily simplified to describe such a complex system as adenovirus DNA replication in vivo, the fact that the simple description of replication in four component steps can adequately model experiments as different as the rate of density shifts, the rate of chase of pulse label into mature DNA, and counting relative numbers of replicating forms on an EM grid shows the power of the kinetic techniques used here.

Part IV presents measurement of the kinetic parameters for adenovirus type 7, a serotype which is only 10 percent homologous to Ad2 and Ad5 and which produces three times as much defective DNA. We compare the rate constants to investigate which steps are mediated by cell factors and which are mediated by viral factors, and we test our hypothesis for generation of defective DNA. In Part V we present a kinetic analysis of SV40 DNA replication using the techniques derived for adenovirus and compare the model to the SV40 experiments available in the literature. The results show that these techniques work as well with the SV40 system, and that the Ad and SV40 systems exhibit similar characteristics for the control of DNA replication.

KINETICS OF ADENOVIRUS DNA REPLICATION: I

Determination of Replication Time

ABSTRACT

Methods are presented to determine the replication time for viral DNA. They show that adenovirus type 2 and 5 replicate in 22 minutes at 37° C and that this time is constant throughout infection.

INTRODUCTION

Several methods have been used to estimate the time required to complete replication of a viral genome (Pearson and Hanawalt, 1971; Nathans and Danna, 1972; Danna and Nathans, 1972; Pearson, 1975). We present a mathematical description that can be applied to pulse labeling experiments to determine the replication time for viral DNA. These techniques follow the time course of a pulse label in (a) the relative specific activity of restriction fragments of newly completed DNA, or (b) the fraction of pulse label in replicating molecules or (c) the activity in mature and replicating molecules. By the shapes of the resulting curves we can calculate the time to complete one adenovirus DNA molecule which is 22 minutes for Ad 2 and Ad 5, and this time is constant throughout infection.

THEORY

We define the following terms: t = time in min; x = position along the adenovirus genome in fractional length units where $0 \leq x \leq 1$; and r = average rate of replication expressed as fractional lengths per minute. We also define subscript notations used in equations as follows: C = completed molecules; R = replicating molecules; T = total molecules (i.e. completed plus replicating molecules); r = r strand and l = l strand (strand designations are discussed in an article signed by 36 scientists: J. Virol. 22, 830-831, 1977). We assume adenovirus replicates by a strand displacement mechanism (Lechner and Kelly, 1977) with origins and termini of replication at both molecular ends (Figure 2B in Weingartner et al, 1976). We can write equations describing the relative accumulation of radioactive label at any point along either strand of adenovirus DNA molecules completed during a short time interval.

During a [^{3}H] thymidine pulse of length t all molecules that have a nascent strand longer than (1 - rt) at the beginning of the pulse will be completed during the pulse. The shortest strand will be (1 - rt) long, and longer strands will be equally likely. Therefore, the distribution will be as shown below.

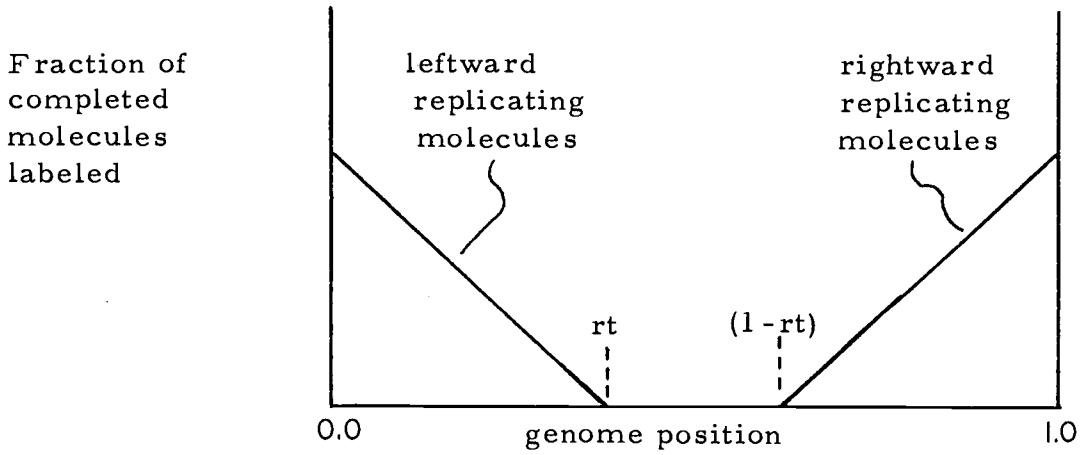

At one complete replication time the 3' end of each strand will be labeled, and the distribution of radioactive label will be as A below for the leftward replicating strand.

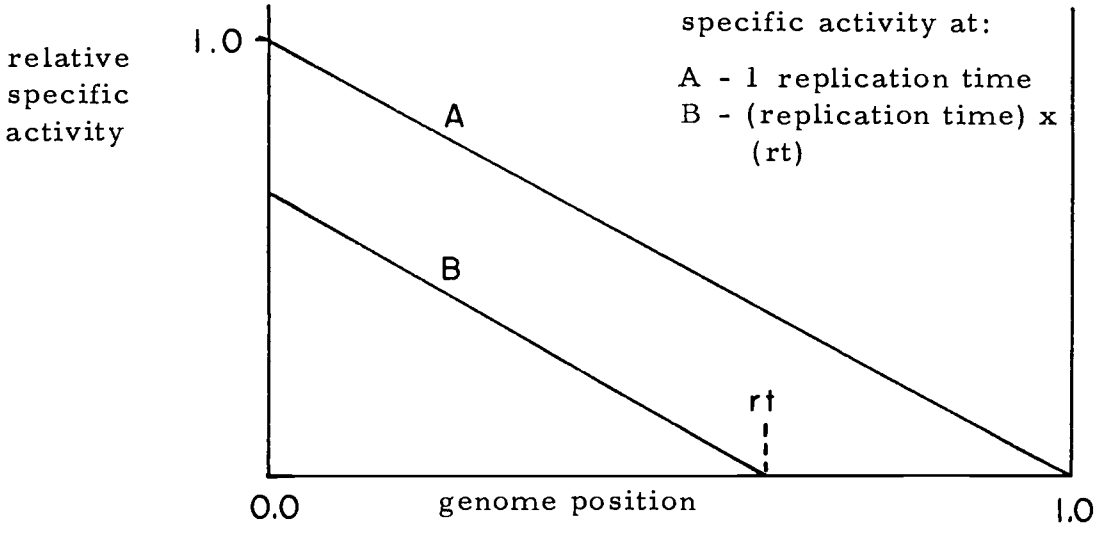

The equation for these lines can be shown to be:

$$f_{C\,r}(x,t) = rt - x \qquad ; \quad 0 \leq x \leq rt$$

$$f_{C\,r}(x,t) = 0 \qquad ; \quad x \geq rt$$

Similarly, the relative specific activity in the molecules replicating rightward will be:

$$f_{C\,1}(x, t) = x - (1 - rt) \quad ; \ (1 - rt) \leq x \leq 1$$

$$f_{C\,1}(x, t) = 0 \quad ; \ x < (1 - rt)$$

Note that the right strand replicates to the left, and also that throughout the calculations boundary values must be rigorously observed to avoid negative values.

The total relative radioactivity in a fragment of the genome will be the integral of the above expressions evaluated between the endpoints.

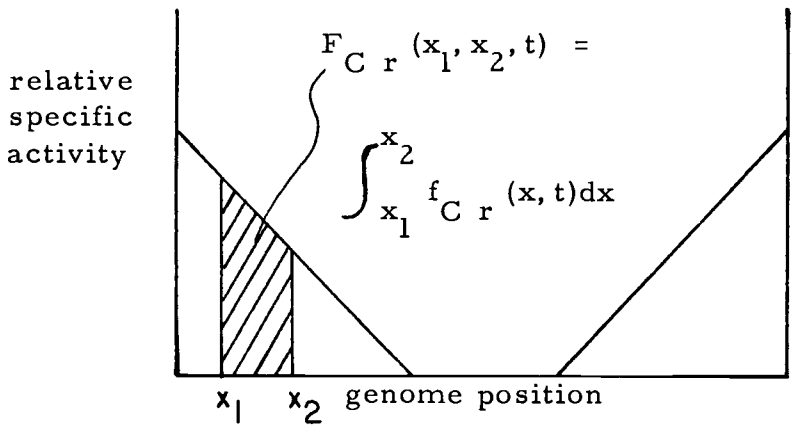

$$F_{Cr}(x_1, x_2, t) = \int_{x_1}^{x_2} f_{Cr}(x, t)\, dx = 0.5([2rt-(x_1+x_2)]\,[x_2-x_1]);$$

$$F_{Cr}(x_1, x_2, t) = 0 \quad ; x > rt \qquad 0 \leq x \leq rt$$

and

$$F_{Cl}(x_1, x_2, t) = \int_{x_1}^{x_2} f_{Cl}(x, t)\, dx = 0.5([(x_1+x_2)-2(1-rt)]\,[x_2-x_1])$$

$$; \ (1 - rt) \leq x \leq 1$$

$$F_{Cl}(x_1, x_2, t) = 0 \qquad ; x < (1 - rt)$$

The average relative radioactivity in a fragment will be the total relative radioactivity divided by the length of the fragment.

$$\overline{F}_{Cr}(x_1, x_2, t) = F_{Cr} / (x_2 - x_1) = 0.5[2rt - (x_1 + x_2)]$$

$$; 0 \leq x \leq rt$$

$$\overline{F}_{Cr}(x_1, x_2, t) = 0 \qquad ; x > rt$$

and

$$\overline{F}_{Cl}(x_1, x_2, t) = F_{Cl} / (x_2 - x_1) = 0.5[(x_1 + x_2) - 2(1 - rt)]$$

$$; (1 - rt) \leq x \leq 1$$

$$\overline{F}_{Cl}(x_1, x_2, t) = 0 \qquad ; x < (1 - rt)$$

Of course the average relative radioactivity in a <u>double stranded</u> fragment will be:

$$\overline{F}_C = \overline{F}_{Cr} + \overline{F}_{Cl}$$

For given values of r and t, the above equations can be evaluated readily for any restriction endonuclease fragment using a program designed to account for the boundary conditions. (See Appendix II for a program for the Hewlett Packard 9821A calculator.)

If we consider <u>all</u> the molecules labeled during a short time interval (i.e., replicating as well as newly completed molecules),

the relative accumulation of radioactivity into both strands at any given point on the genome is:

$$f_T(x,t) = 2rt$$

The total relative radioactivity in fragment i of all the molecules is given by integrating at constant t:

$$F_T(x_1, x_2, t) = \int_{x_1}^{x_2} f_T(x,t)\, dx = 2rt\,(x_2 - x_1)$$

and the average relative radioactivity in fragment i of all the molecules is:

$$\overline{F}_T(x_1, x_2, t) = F_T / (x_2 - x_1) = 2rt$$

Therefore, we can calculate the average relative radioactivity in fragment i in replicating molecules from the expression:

$$\overline{F}_{Ri} = \overline{F}_{Ti} - \overline{F}_{Ci}$$

RESULTS AND DISCUSSION

Numerous experiments have been reported to establish the termini of adenovirus DNA replication using the method of Nathans and Danna, 1972 (Horwitz, 1974; Tolun and Pettersson, 1975; Schilling et al, 1975; Horwitz, 1976; Bourgaux et al, 1976; Weingartner et al, 1976; Sussenbach and Kuijk, 1977). We have applied the functions described in the Theory to this type of experiment and see that the model can describe the specific activities of pulse labeled restriction fragments in terms of pulse length and replication rate. An example is shown in Figure 1.

HeLa S_3 cells were infected with Ad5, exposed to 10^{-6} M fluorodeoxyuridine (FUdR) for 30 minutes at various times post infection, concentrated to 1.5×10^7 cells/ml, and pulse labeled with [^{3}H] thymidine at 25 μCi/ml. Aliquots were removed and fixed in NaCN (final concentration 0.01 M) on ice. Adenovirus chromatin was extracted from cell nuclei with 200 mM ammonium sulfate by using the method of Wilhelm et al, 1976 (Robinson et al, 1979), adenovirus DNA was prepared proteolytically and digested with Hsu endonuclease as previously described (Pearson, 1975). Fragments were mixed with [^{32}P] labeled viral DNA fragments, separated on 1 percent agarose gels at 40 volts for 12 hours, and the specific activity ([^{3}H] / [^{32}P]) corrected for relative thymidine

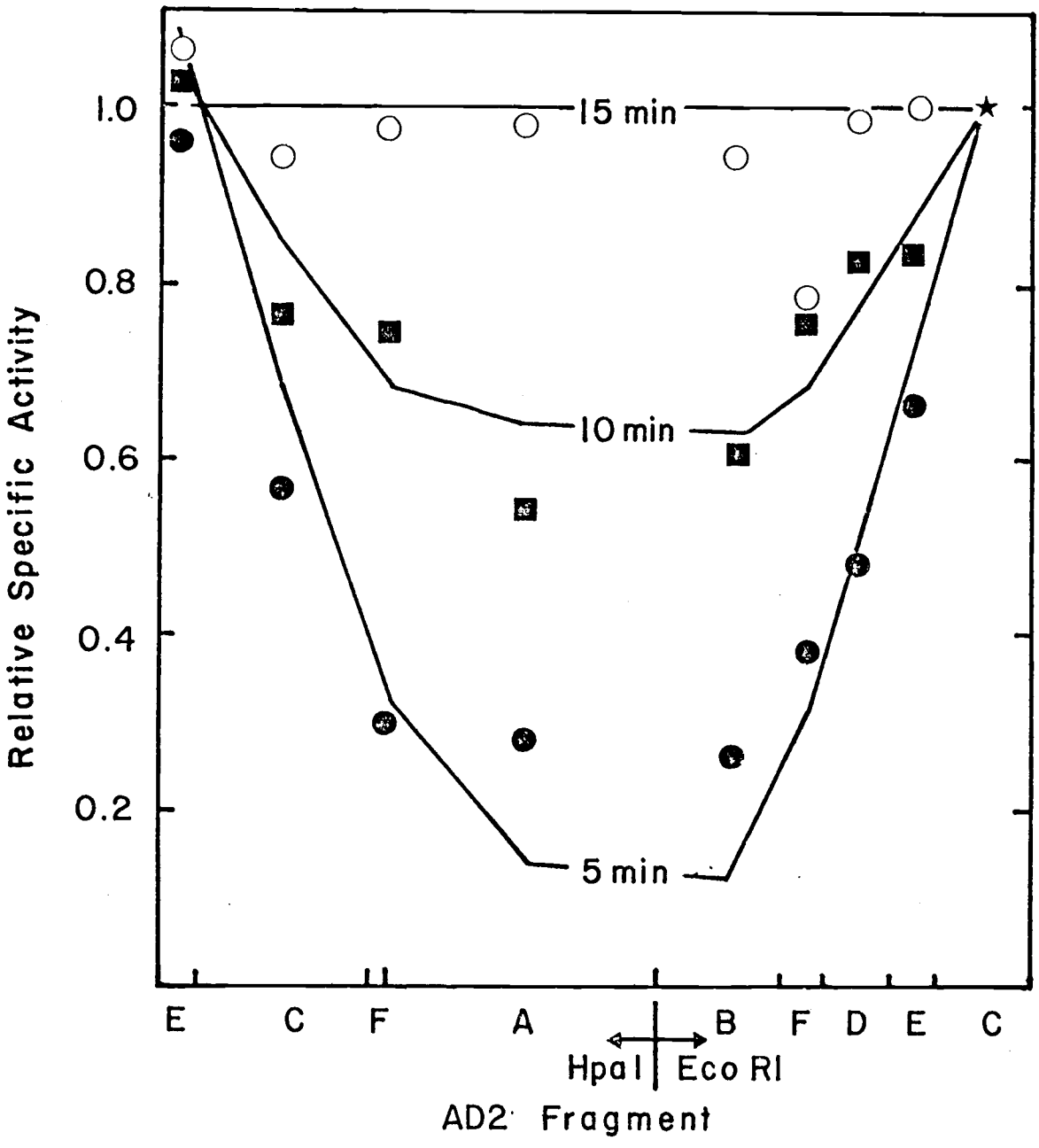

Figure 1. Data from Horwitz (1976) for specific activity of pulse labeled restriction fragments of newly completed Ad2 DNA are compared with calculated curves for pulse incorporation. Pulse lengths are 5 min (●), 10 min (■), and 15 min (○). Curves are calculated for r = 0.07 genome/min or 14.2 min replication time. All data are normalized to the specific activity of the EcoRI C fragment (★). The DNA was first cut with EcoRI then EcoRI^{A} fragment was further digested with HpaI.

content was determined. The replication rate was determined by comparing calculated curves for various replication rates with the experimental data and selecting the best fit by eye, as shown in Figure 2.

Inspection of the calculated curves indicated a similar method to determine replication rate from the data. If a line is drawn through the specific activities of the fragments at either end of the genome where there is labeling of one strand only, this line will intersect zero specific activity at the maximum distance that the genome has been completed during the pulse. The average of the two lengths from either end of the genome divided by the pulse length will give the replication rate in fractional genome lengths per minute; the reciprocal of this is the time to complete the entire genome. We applied this technique to available data in the literature, then determined the replication rate by finding the best fit of each experiment with calculated curves for various replication rates. The two methods gave comparable results which are shown in Table I.

To determine if the replication rate varies over infection, we applied this method to measure replication rate over the course of an infection. Replication time was determined as described above between 14 and 23 hours post infection with the results shown in Table 2. The average rate calculated from the experiments with

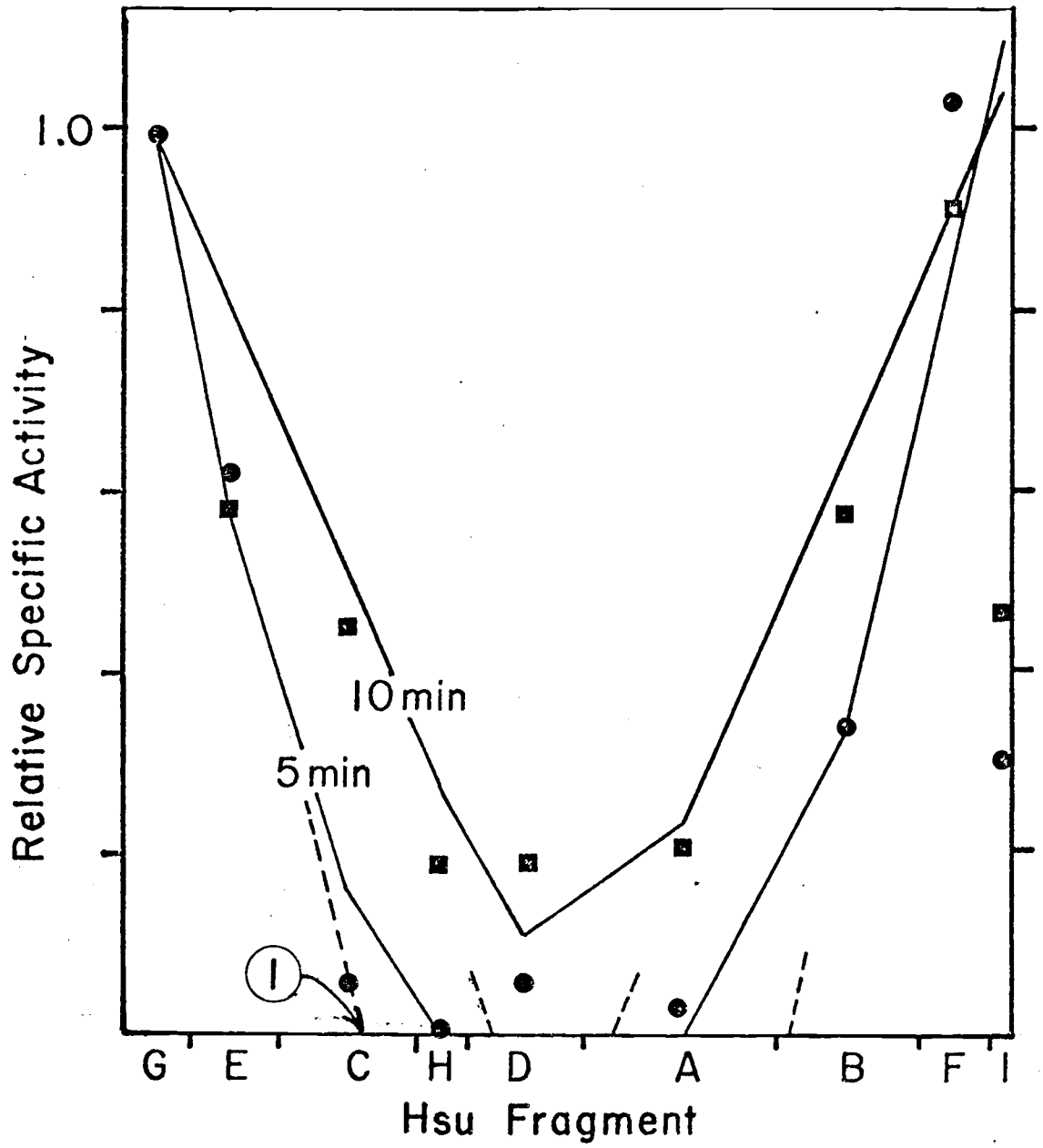

Figure 2. Calculation of replication rate from pulse labeled Ad5 replication fragments. Adenovirus type 5 was pulse labeled at 14 hours post infection with [^{3}H]thymidine. Cells were removed at 5 min (●) and 10 min (■), fixed in 0.01 M NaCN, total intracellular DNA isolated and purified by BD-cellulose column chromatography. The mature DNA was digested with Hsu (Hind III isoschizomer) along with [^{32}P]viral DNA and the fragments separated on 1% agarose gels. The relative specific activity ([^{3}H]/[^{32}P]) is shown compared to calculated curves for a replication time of 21 min. Replication time can also be measured by drawing straight lines through the specific activities at either end of the genome (– – –), and the intercept will give the portion of the genome that has been completed during the pulse (e.g., (1) above; 0.27 genome/5 min = 0.051 genome/min or 20 min replication time).

Table 1. Determination of Ad2 replication time from previously published experiments measuring specific activity of pulse labeled restriction fragments.

Reference	Endonuclease	Time of Pulse (Hr P. I.)	Pulse Length (min)	Replication Time (min)*
Bourgaux et al, 1976	EcoRI	16.25	3	11
			6	13
			9	17
Tolun et al, 1975	EcoRI	13-14	5	12
			10	15
	Hpa I	13-14	5	12
			10	17
Schilling et al, 1975	EcoRI	20	5	25
			10	20
	Hpa I	20	5	33
	Hin d III	20	5	25
			10	25
Horwitz, 1976	EcoRI/Hpa I	18	5	12
			10	14
Pearson, 1976	EcoRI	14	5	14
			10	17
Weingartner et al, 1976	Hpa I	14	4	17
	EcoRI	14	4	17
	Hin d III	14	4	17
Sussenbach and Kuijk, 1977 (Ad5)	Hin d III	18	5	12
			10	25
Jones & Pearson (unpublished data)	EcoRI	17	10	17
			Average =	16 min
Separated Strands				
Horwitz, 1976	EcoRI	18	5	h=17
			10	h=10
Sussenbach and Kuijk, 1977 (Ad5)	EcoRI/Hin d III	18	10	h=24 l=23

* Replication time is measured as described in Figure 2.

Table 2. Replication time of Ad DNA as a function of time post infection.

	Time (P. I.) (hr)	Pulse Length (min.)	Measured Replication Time (min.)*
Ad2	14	5	19
		10	23
	18	5	25
	22	5	21
		10	21
Ad5 (Expt. I)	14	6	22
		12	24
	17	6	20
		12	24
	20	6	24
		12	24
	23	6	21
		12	26
Ad5 (Expt II)	14	3	15
		6	18
	18	3	15
		6	20

* Replication time was measured as described in Figure 2.

shorter labeling times (5 or 6 minutes) was 0.048 ± 0.005 fractional lengths per min., whereas the average rate determined from the longer pulses (10 or 12 minutes) was 0.042 ± 0.003 fractional lengths per minute. Since these rates did not differ significantly, they were pooled to give an average rate of 0.046 ± 0.005 fractional lengths per minute or 1600 ± 170 nucleotides per minute. From the rate of replication we calculated that the time to synthesize an adenovirus DNA molecule was 21.7 ± 2.4 minutes. More importantly Figure 3 clearly shows that the rate of adenovirus DNA replication is constant throughout the course of infection.

The rate of replication calculated from previously published experiments as described above was 0.066 ± 0.002 fractional lengths per minute for experiments with short pulses (3 to 6 minutes), while the average rate determined from longer pulses (9 or 10 minutes) was 0.058 ± 0.002 fractional lengths per minute in reasonable agreement with the value calculated above. Estimates for the rate of replication of type 2 and type 5 adenoviruses also did not differ significantly. Likewise, although there was much greater scatter in the calculated values, the rate was constant over the period ranging from 14 to 20 hours post infection.

It has been reported (Dintzis, 1961; Manteuil et al, 1973) that the replication time can be estimated by measuring the percent of radioactivity that is associated with replicating DNA during a

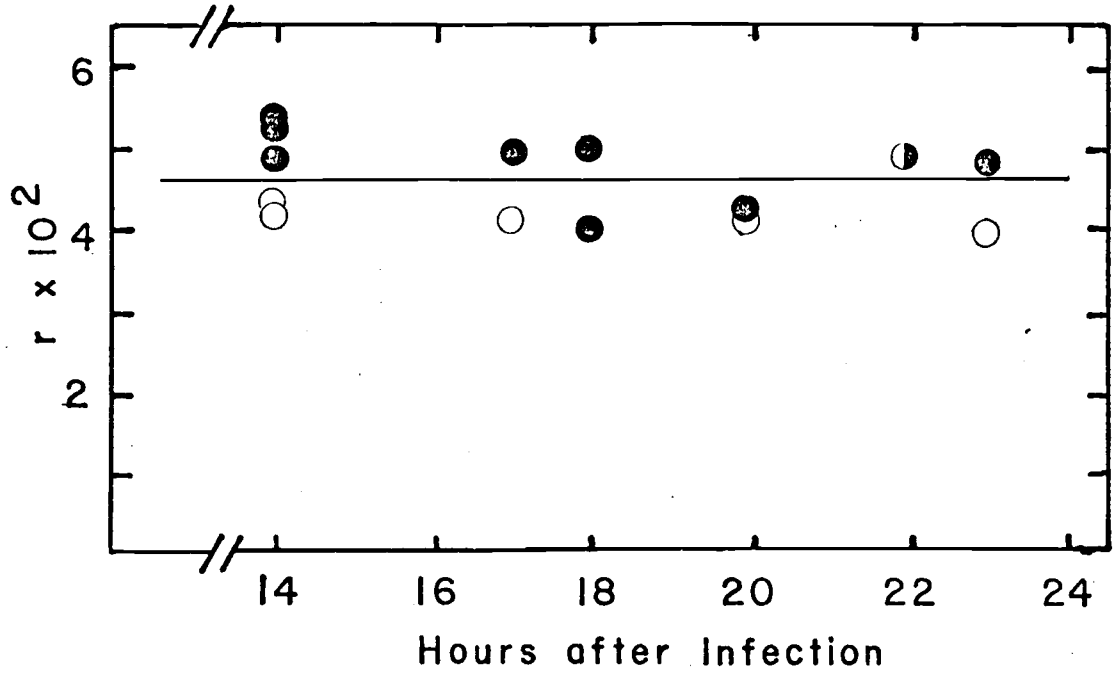

Figure 3. Rate of adenovirus DNA replication during infection. Rates were calculated as described in Figure 1. Pulse-labeling with [^{3}H]thymidine was started in each experiment at the indicated times after infection. ● , 5 or 6 min pulses; O , 10 or 12 min pulses. The solid line represents the average rate of replication (r = 0.046 fractional lengths/min or 1,600 nucleotides/min).

[^{3}H] thymidine pulse and looking at the time required for that value to fall to 50 percent. To verify this method we define a function which would show the percent of all DNA as replicating DNA during a pulse: $(100 \times F_R(0, 1, t)/F_T(0, 1, t))$ where F_R and F_T are the relative [^{3}H] activities of full length replicating and total DNA molecules as described in the Theory. This function showed that the percent replicating DNA does in fact start at 100 percent and falls linearly to 50 percent in one replication time, then drops slowly beyond that as shown in Figure 4.

We further noted that the shape of the relative radioactivity curves for the entire genome could themselves be used to estimate replication time. The relative radioactivity incorporated into mature DNA ($F_C(0, 1, t)$) builds up parabolically for one replication time then increases linearly. The function for replicating DNA ($F_T(0, 1, t)$) builds up rapidly and levels out to a constant value also at one replication time, while the function for total DNA ($F_T(0, 1, t)$) is linear as long as the concentration of DNA does not change markedly. These curves are shown in Figure 5.

We tested these methods for measuring replication rate using different methods to fractionate replicating and mature DNA to also test the equivalency of the separation techniques. Results were already available for such experiments using CsCl/ethidium bromide equilibrium gradients for separation of the DNA (Pearson, 1975).

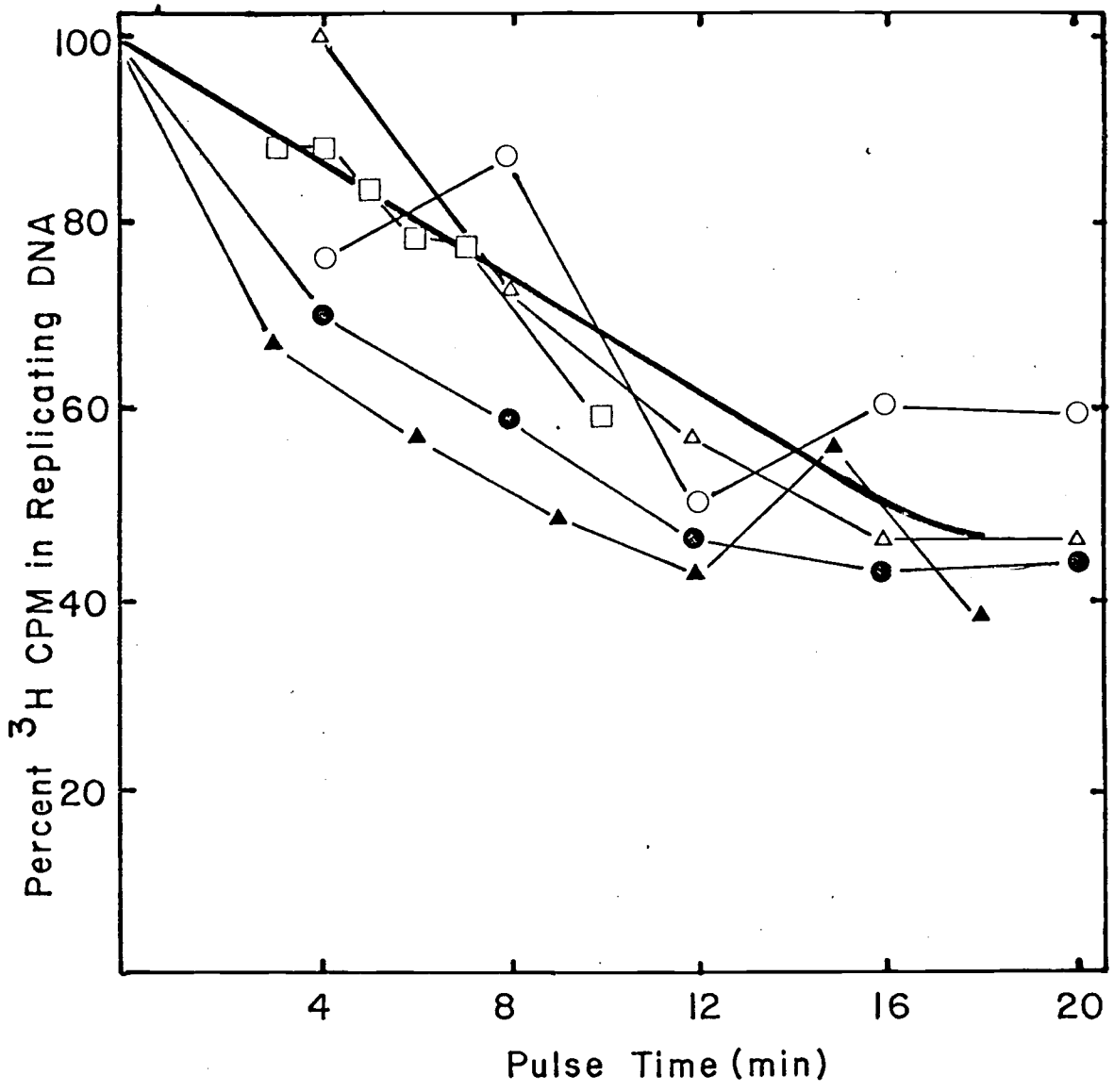

Figure 4. Calculation of replication rate from percent of a pulse label in replicating DNA. Adenovirus type 2 (□, ○, and △) and type 5 (● and ▲) was pulsed with [^{3}H]tymidine at 17 hours post infection. Cells were removed and fixed in 0.01 M NaCN at the times indicated, and replicating molecules were separated from mature DNA by BD-cellulose column chromatography (▲ and △), centrifugation on glycerol gradients by the method of Wilhelm et al, 1976 (● and ○), or CsCl/ethidium bromide equilibrium gradients (□ ; data from Pearson, 1975). The percent of radioactivity associated with the replicating molecules is compared with the calculated curve (= 100 x $F_R(0,1,t)/F_T(0,1,t)$) for a replication time of 17 minutes. Theoretically the percent will drop linearly from 100 percent to 50 percent in one replication time then slowly fall to a steady state value.

Figure 5. Calculation of replication rate from pulse label incorporation into mature and replicating DNA. Adenovirus type 2 (▲) and type 5 (● and ■) were pulse labeled with [^{3}H]thymidine at 17 hours post infection. Cells were removed and fixed in 0.01 M NaCN at the times indicated, total intracellular DNA was isolated, and the replicating and mature molecules were separated. Buildup of [^{3}H] activity was established relative to a [^{14}C] internal DNA marker, and normalized by setting the total activity at the point listed below equal to the theoretical $F_T(0, 1, t)$ at that time.

Separation Method	DNA Activity			Normalized at time =	Internal Marker DNA
	Total	Mature	Replicating		
BD-cellulose	●	○	◐	15 minutes	[^{14}C] HeLa DNA
Glycerol gradient	■	□	◨	16 minutes	[^{14}C] Ad5 DNA
*$CsCl_2$/EtBr gradient	▲	△	◭	10 minutes	[^{14}C] HeLa DNA

Theoretical curves are for relative activity of total DNA (F_T), mature DNA (F_c) and replicating DNA (F_R) in the entire genome with a replication time of 15 minutes.

* Data from Pearson (1975).

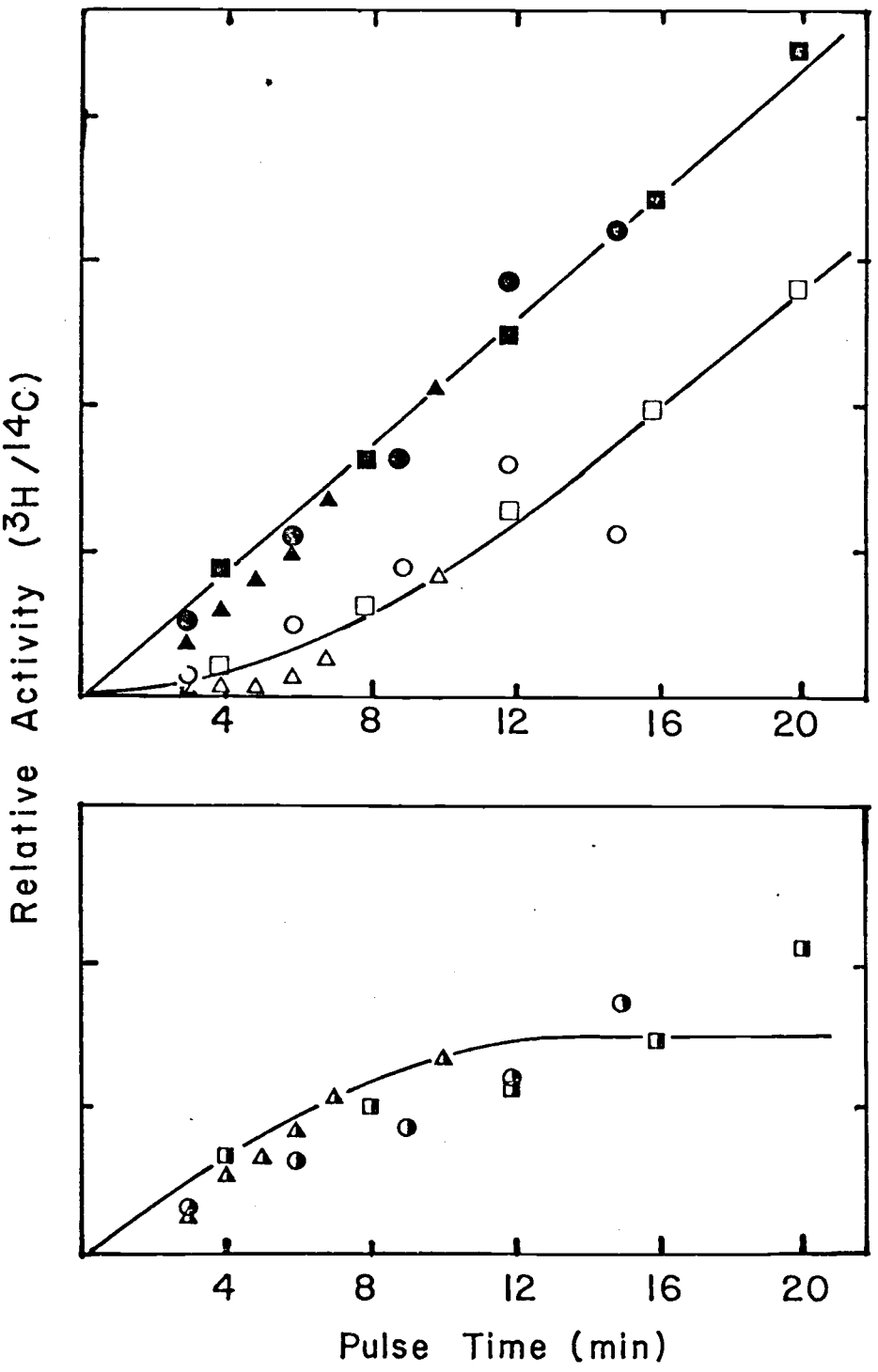
Relative Activity ($^3H/^{14}C$)
4
8
12
16
20
4
8
12
16
20
Pulse Time (min)

To use BD-cellulose column chromatography cells were prelabeled for 24 hr with [^{14}C] thymidine as a recovery marker, the [^{14}C] washed out prior to infection, then Ad2- or Ad5-infected cells were pulse labeled at 17 hours post infection as above. Total intracellular DNA was phenol extracted from SDS- and Pronase-disrupted cells as previously reported (Pearson, 1975), and replicating and mature DNA were separated with BD-cellulose chromatography (Robinson et al, 1979). In the second experiment the Ad2 or Ad 5 DNA was labeled with [^{14}C]thymidine from 11 to 17 hours post infection for a recovery marker, and the DNA was pulse labeled at 17 hours post infection as above. Adenovirus chromatin was extracted with ammonium sulfate from cell nuclei, and replicating and mature DNA were separated on 10 to 40 percent glycerol velocity gradients (Wilhelm et al, 1976; Robinson et al, 1979).

The results of these experiments and data from Pearson (1975) are shown in Figures 4 and 5, which indicate that BD-cellulose chromatography, glycerol gradient centrifugation, and CsCl/ethidium bromide equilibrium centrifugation are consistent in fractionation of replicating and mature DNA. In Figure 4 all experimental curves reflected the linear drop of percent of activity in the replicating DNA during the first replication time of the pulse and showed a replication time of 8 to 16 minutes as judged by the time to decrease below 50 percent. Figure 5 shows that the

experimental data are consistent with a replication time of 15 minutes, but this type of plot is probably the least satisfactory for determining adenovirus replication time. However, these data do show some important points about the assumptions made in derivation of the functions. The total incorporation curve (F_T) is linear as expected, indicating that the concentration of adenovirus DNA did not change markedly during the pulse; such a large growth would cause this curve to be exponential. Also, a straight line through the experimental points which intersects the time axis between 0 and 2 minutes indicates that nucleotide pool equilibration is not a problem since incorporation is linear within 2 minutes of addition of [^{3}H]thymidine. The curve for tritium incorporation into replicating DNA does not approach a constant value; this indicates the assumption of little return of completed molecules into the replication pool during the pulse is weak within 20 minutes after the start of the pulse and that significant reinitiation is seen during the pulse.

We have demonstrated methods to measure replication rate of adenovirus DNA. These methods with slight modifications may be useful in measuring replication rates of other viruses. We have shown that the rate of adenovirus DNA replication is constant. Since the rate of total Ad DNA accumulation varies during infection

(van der Eb, 1973), factors other than the rate of replication must play a role in this modulation. In the following section we describe methods to estimate these factors.

KINETICS OF ADENOVIRUS DNA REPLICATION: II

Measurement of Initiation Rate

ABSTRACT

Methods are presented to measure the rate of initiation of rounds of replication of viral DNA. These methods show that initiation is the rate-limiting step for adenovirus DNA replication, that the initiation rate decreases over infection with saturable kinetics, and that recently replicated molecules are preferentially reinitiated.

INTRODUCTION

We have shown that the time to complete replication of a single adenovirus genome is 22 minutes (Bodnar and Pearson, 1980a; Part I). This would suggest that the total amount of adenovirus (Ad) DNA should double in about 20 minutes, but it has been shown that the accumulation of adenovirus DNA is considerably slower than this (Green, 1962b; Philipson et al, 1975; van der Eb, 1973; Flint et al, 1976). We hypothesized that this was due to a low probability of a particular molecule reinitiating a round of DNA replication. To investigate this theory we have developed methods to measure the rate at which Ad DNA molecules initiate new rounds of replication. Two of these methods assume the strand displacement replication model (Lechner and Kelly, 1977): (1) measurement of the rate of accumulation of mature DNA, (2) steady-state kinetic analysis of electron microscopy of replicating forms. The other methods assume only semi-conservative DNA replication and that initiation is the slow step in kinetics: (3) initiation rate measurement by BUdR density shift kinetics, and (4) measurement of V_{max} and K_m for saturable kinetics of DNA replication. Since the latter two methods do not assume a replication model, they are directly applicable to other viral systems.

These kinetic methods show that initiation is the rate limiting step in adenovirus DNA replication. The initiation rate decreases

over infection, showing saturable kinetics as the substrate DNA concentration increases. Also, recently replicated molecules are preferentially initiated; this preference is slight early in infection but increases markedly later in infection.

THEORY

Numerical Estimation of the Initiation Rate from Saturable Kinetics

Assume that the initiation rate (i) is dependent on some intracellular factor such that the initiation rate shows saturable kinetics as shown in Figure 6. Using the HP 2851A programmable calculator, we simulated the kinetics of Ad5 total DNA accumulation numerically by approximating the rate of change of each pool by using the total change in that pool each minute. The type I molecules are divided into m pools where $m = 1/r_I$ so that we have pool 1 representing the type I molecules in the first minute of replication through pool m representing the type I molecules in the last minute of replication. Similarly, the type II molecules are divided into n pools where $n = 1/r_{II}$.

We then approximate:

$$\Delta [DS] = \frac{-V_{max} [DS]}{K_m + [DS]} + [I]_m + [II]_n$$

$$\Delta [I]_1 = \frac{V_{max} [DS]}{K_m + [DS]} - [I]_1$$

$$\Delta [I]_x = [I]_{(x-1)} - [I]_x \text{ for } x = 2, 3, \ldots, m$$

$$\Delta [II]_1 = i_s [SS] - [II]_1$$

$$\triangle [II]_y = [II]_{(y-1)} - [II]_y \quad \text{for } y = 2, 3, \ldots, n$$

$$\triangle [SS] = [I]_m = i_s [SS]$$

Then for each minute $[DS] = \triangle [DS] + [DS]$, etc.

The value for v is calculated graphically by plotting $[DNA_{total}]$ versus time where $v = d [DNA_{total}]/dt$. Plotting $(1/v)$ versus $(1/[DNA_{total}])$ the $(1/v)$ intercept is equal to $(1/V_{max})$ and the abscissa intercept is $(-1/K_m)$. These rough values are then inserted into the numerical program above and adjusted for a best fit of the experimental curve. The values of V_{max}, K_m, and $[DS]$ can then be used to estimate the initiation rate (i) at any time by using the relationship:

$$2i = V_{max} [DS] / (K_m + [DS])$$

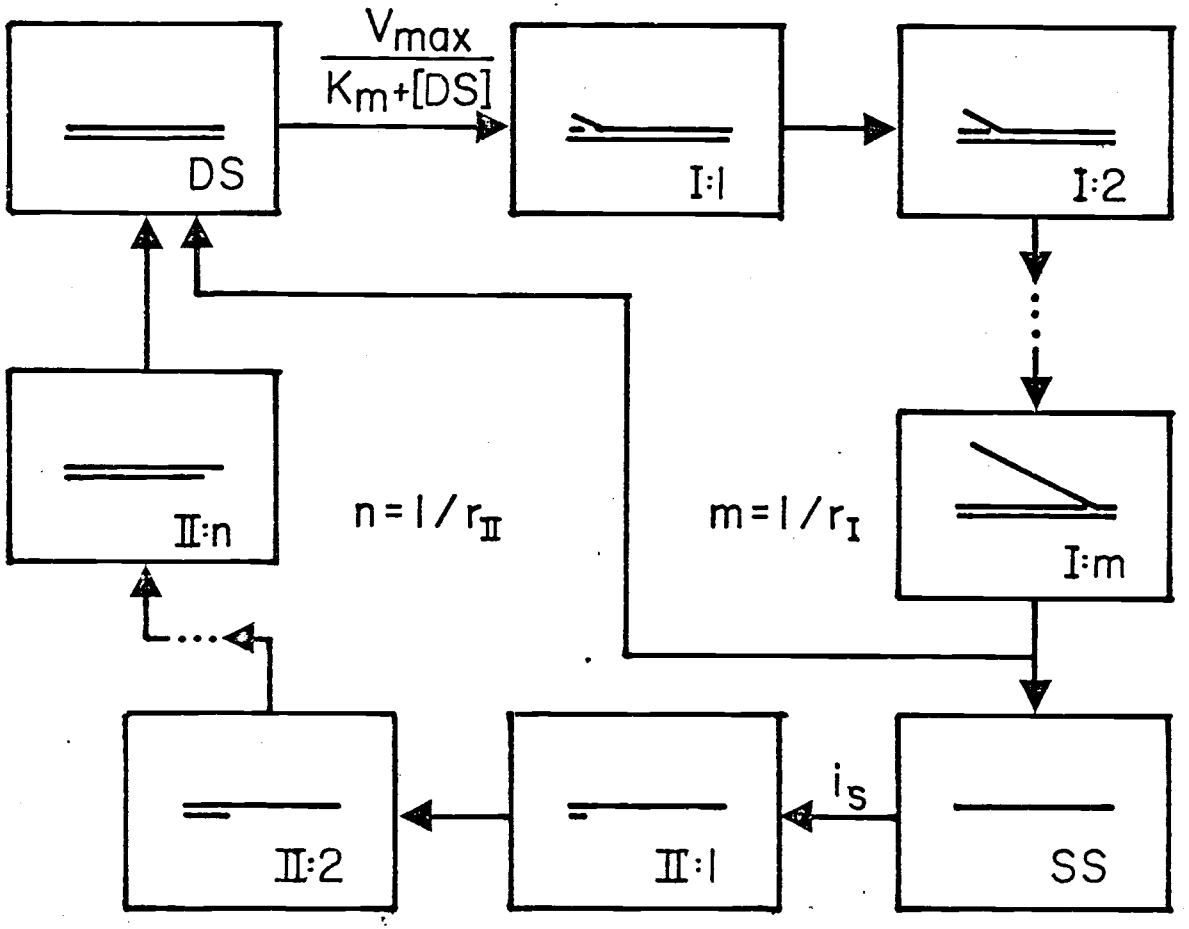
Vmax
Km+[DS]
DS
I:1
I:2
I:m
II:n
n=1/rII
m=1/rI
II:2
II:1
is
SS

RESULTS

Measurement of the Initiation Rate by Density-shift Experiments

The initiation rate of adenovirus DNA replication can be calculated in experiments that measure consecutive replications of the same viral molecule, that is, density-shift experiments. Infected cells growing in heavy (H) medium containing 5-bromodeoxyuridine (BUdR) were shifted to light (L) medium lacking BUdR. This makes it possible to measure the fraction of viral molecules that have not replicated (HH), have replicated once (HL), or have replicated two or more times (LL) at various times after the density shift (see Figure 1). The following reactions occur during a density shift:

$$HH + dNTPs \xrightarrow{2i} 2\,HL \qquad (1)$$

$$HL + dNTPs \xrightarrow{2i'} HL + LL \qquad (2)$$

$$LL + dNTPs \xrightarrow{2i'} 2\,LL \qquad (3)$$

where i = rate of initiation of molecules that have not yet been replicated, i' = rate of initiation of molecules that have been replicated at least once, and the factor 2 arises from the fact that adenovirus DNA replication initiates at or near either end of double stranded linear molecules (for review see Winnacker, 1978).

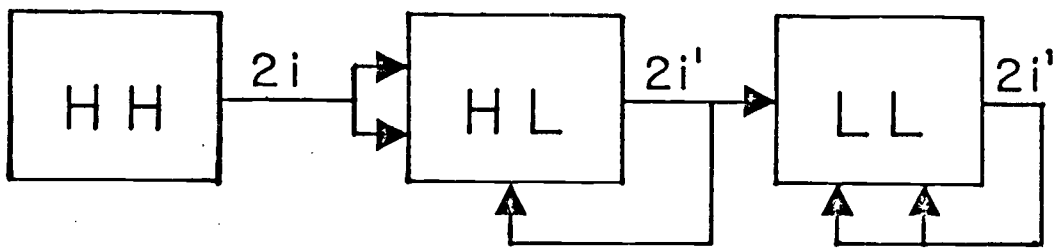

Figure 1. Kinetic relationship between density-labeled adenovirus DNA molecules during a density-shift experiment. HH = fully heavy molecules containing BUdR in both strands. HL = hybrid molecules containing BUdR in only one strand. LL = fully light molecules containing BUdR in neither strand. i = rate of initiation of molecules that have not yet replicated (HH) during the chase in light medium. i' = rate of initiation of molecules that have been replicated at least once (HL or LL) during the chase in light medium. The factor 2 arises from the fact that adenovirus DNA replication initiates at or near either end of double stranded linear molecules.

We can consider two cases: (a) $i = i'$ where all molecules have an equal chance to initiate replication, and (b) $i \neq i'$ where prior history influences the chance to initiate replication. In the first case, we can describe the rate of change of each species of density-labeled molecule by a system of differential equations:

$$d[HH]/dt = -2i[HH] \quad (4)$$

$$d[HL]/dt = 4i[HH] \quad (5)$$

$$d[LL]/dt = 2i[HL] + 2i[LL] \quad (6)$$

We can calculate the concentrations of density-labeled molecules by integrating equations (4), (5), and (6) and observing the boundary conditions that $[HH] = [HH]_o$ and $[HL] = [LL] = 0$ at $t = 0$ (the start of the density shift):

$$[HH] = [HH]_o e^{-2it} \quad (7)$$

$$[HL] = 2[HH]_o(1 - e^{-2it}) \quad (8)$$

$$[LL] = [HH]_o(e^{2it} + e^{-2it} - 2). \quad (9)$$

We can then define the following expression:

$$\text{Fraction } [HH] = [HH]/([HH] + [HL] + [LL]) = e^{-4it} \quad (10)$$

A plot of ln (fraction [HH]) versus t (time after density shift) will give a straight line (see Figure 4 below) with slope = -4i, or

$$i = -\text{slope}/4. \tag{11}$$

Similarly, we can also define the expression:

$$\text{Fraction } [HL] = [HL]/([HH] + [HL] + [LL]) = 2e^{-2it} - 2e^{-4it}. \tag{12}$$

When $t = t_{max}$, equation (12) passes through a maximum such that

$$d(\text{Fraction } [HL])/dt = -4ie^{-2it_{max}} + 8ie^{-4it_{max}} = 0. \tag{13}$$

Solving for i, we get:

$$i = \ln 2/2t_{max}. \tag{14}$$

It is easy to show that Fraction [HL] = 0.5 when $t = t_{max}$. Thus, a plot of Fraction [HL] versus t (see Figure 5B below) should pass through a maximum value of 0.5 at t_{max}, and i can be calculated from equation (14) using the observed value of t_{max}.

In the case where $i \neq i'$, equations (4), (5), (7), and (8) remain unchanged, but equation (6) becomes

$$d[LL]/dt = 2i'[HL] + 2i'[LL] \tag{15}$$

and equation (9) becomes

$$[LL] = 2[HH]_o \left(\frac{i}{i + i'} e^{2i't} + \frac{i'}{i + i'} e^{-2it} - 1\right). \tag{16}$$

The expressions for Fraction [HH] and Fraction [HL] now become

quite complicated. Since Fraction [HL] will be useful (see below), it is given in detail. Equation (12) now becomes

$$\text{Fraction [HL]} = \frac{2(1-e^{-2it})}{\left(\frac{i'-i}{i'+i}\right) e^{-2it} + \left(\frac{2i}{i'+i}\right) e^{2i't}} \qquad (17)$$

Figure 2 diagrams the protocol for the density shift experiment. Cellular DNA was labeled by growing HeLa cells in medium containing [^{3}H]thymidine for 30 hr, then cells were infected with adenovirus. Starting at 11 hr after infection, adenovirus DNA was labeled with [^{32}P]orthophosphate in medium containing 5 μg/ml of BUdR. Preliminary experiments indicated that neither the rate of accumulation nor the amount of adenovirus DNA were affected by growth in BUdR at this concentration. At 14 hr (Figure 2A), 18 hr (Figure 2B), or 22 hr (Figure 2C) after infection, cells were shifted to medium lacking BUdR but maintaining [^{32}P]orthophosphate at the same concentration. Samples were removed at various times after the density shift, and total intracellular DNA was extracted. Double stranded DNA, selected by chromatography on benzoylated-DEAE-cellulose, was analyzed by CsCl density gradient centrifugation (Figure 3).

Two considerations limited the design of the density-shift experiment: (a) the inhibition of cellular DNA replication, and (b) the density labeling of all or most of the viral DNA. Figure 3

Figure 2. Protocol for density-shift experiments. Cellular DNA was labeled by growing cells in medium containing [^{3}H]thymidine for 30 hr, then cells were infected with adenovirus. Starting at 11 hr after infection, adenovirus DNA was labeled with [^{32}P]orthophosphate in medium containing BUdR (5 μg/ml). At 14 hr (A), 18 hr (B), or 22 hr (C) after infection, cells were shifted to medium lacking BUdR but maintaining [^{32}P] orthophosphate at the same concentration. Density-labeled viral DNA molecules, extracted from cells harvested at various times after the density shift, were analyzed by CsCl gradient centrifugation. Solid bar = growth in heavy (H) medium containing BUdR. Open bar = growth in light (L) medium lacking BUdR. Hatched bar = growth in [^{32}P]orthophosphate.

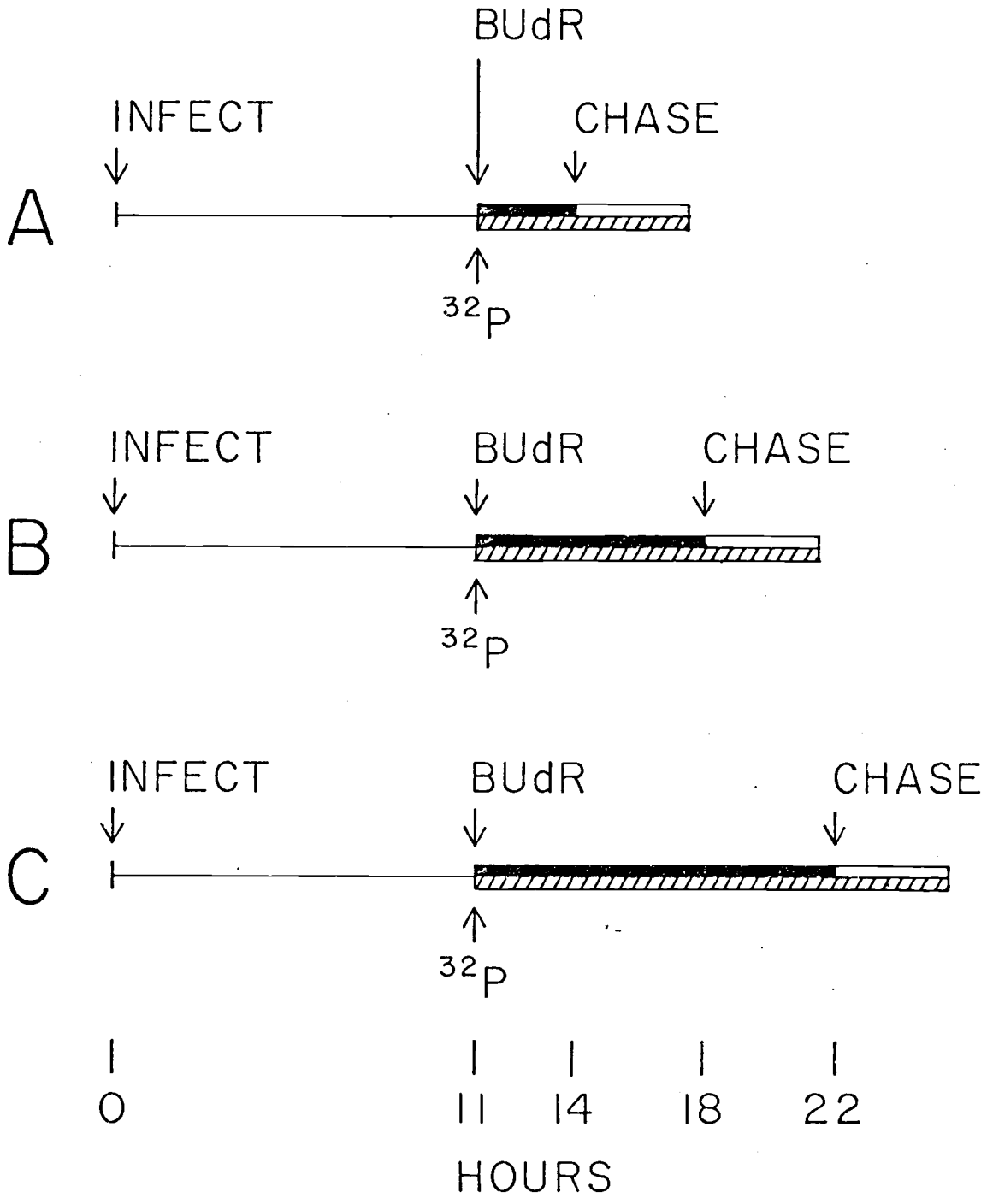
BUdR
INFECT
CHASE
A
32P
INFECT
BUdR
CHASE
B
32P
INFECT
BUdR
CHASE
C
32P
0
11
14
18
22
HOURS

clearly shows that cellular DNA replication had been inhibited by 11 hr after infection (Hodge and Scharff, 1969; Pearson and Hanawalt, 1971): [^{3}H]thymidine-labeled cellular DNA banded at the unreplicated, fully light buoyant density and contained virtually no ^{32}P radioactivity. Thus pre-labeled cellular DNA served in all gradients both as a recovery standard as well as a density marker. Figure 3A shows the CsCl gradient profile of DNA extracted at 14 hr after infection just before the chase in light medium. The peak of fully heavy (HH) adenovirus DNA contained 78% of the ^{32}P radioactivity, whereas the shoulder of hybrid (HL) viral DNA contained 22%. From this distribution of ^{32}P radioactivity, it was possible to calculate that adenovirus DNA had doubled 2.7-times during the 180 min. labeling period, a doubling time of 66 min (compare with Figure 6 below). Moreover, calculations indicated that 85% of the <u>total</u> adenovirus DNA was labeled by 14 hr after infection using the protocol in Figure 2 (i.e., only 15% had been synthesized prior to the addition of [^{32}P]orthophosphate and BUdR at 11 hr after infection). However, virtually all of the adenovirus DNA had become HH by 18 hr (Figure 3D) or 22 hr (not shown) after infection. Finally, it was also important to verify that the incorporation of BUdR was prevented during the chase in light medium. Two observations indicated that the chase was effective: (a) the appearance of hybrid density viral DNA extrapolated back to the

Figure 3. CsCl density gradient analysis of adenovirus DNA. The protocol for the density shift experiments is described in Figure 2. Total intracellular DNA was extracted from cells at various times after the density shift. Double stranded DNA, selected by chromatography on benzoylated-DEAE-cellulose, was centrifuged to equilibrium in CsCl density gradients. The buoyant density increases from right to left in each gradient. The radioactivity in each gradient has been normalized to the peak value for each isotope. O—O , ^{32}P radioactivity; ●—● , ^{3}H radioactivity. In panels (A) through (C) the density shift occurred at 14 hr after infection. (A) No chase: peak ^{32}P = 5173 cpm, peak ^{3}H = 10,454 cpm. (B) 70 min chase: peak ^{32}P = 14,855 cpm, peak ^{3}H = 14,388 cpm. (C) 150 min chase: peak ^{32}P = 17,751 cpm, peak ^{3}H = 5,952 cpm. In panels (D) through (F) the density shift occurred at 18 hr infection. (D) No chase: peak ^{32}P = 65,440 cpm, peak ^{3}H = 13,132 cpm. (E) 100 min chase: peak ^{32}P = 61,499 cpm, peak ^{3}H = 6,367 cpm. (F) 180 min chase: peak ^{32}P = 63,147 cpm, peak ^{3}H = 6,847 cpm.

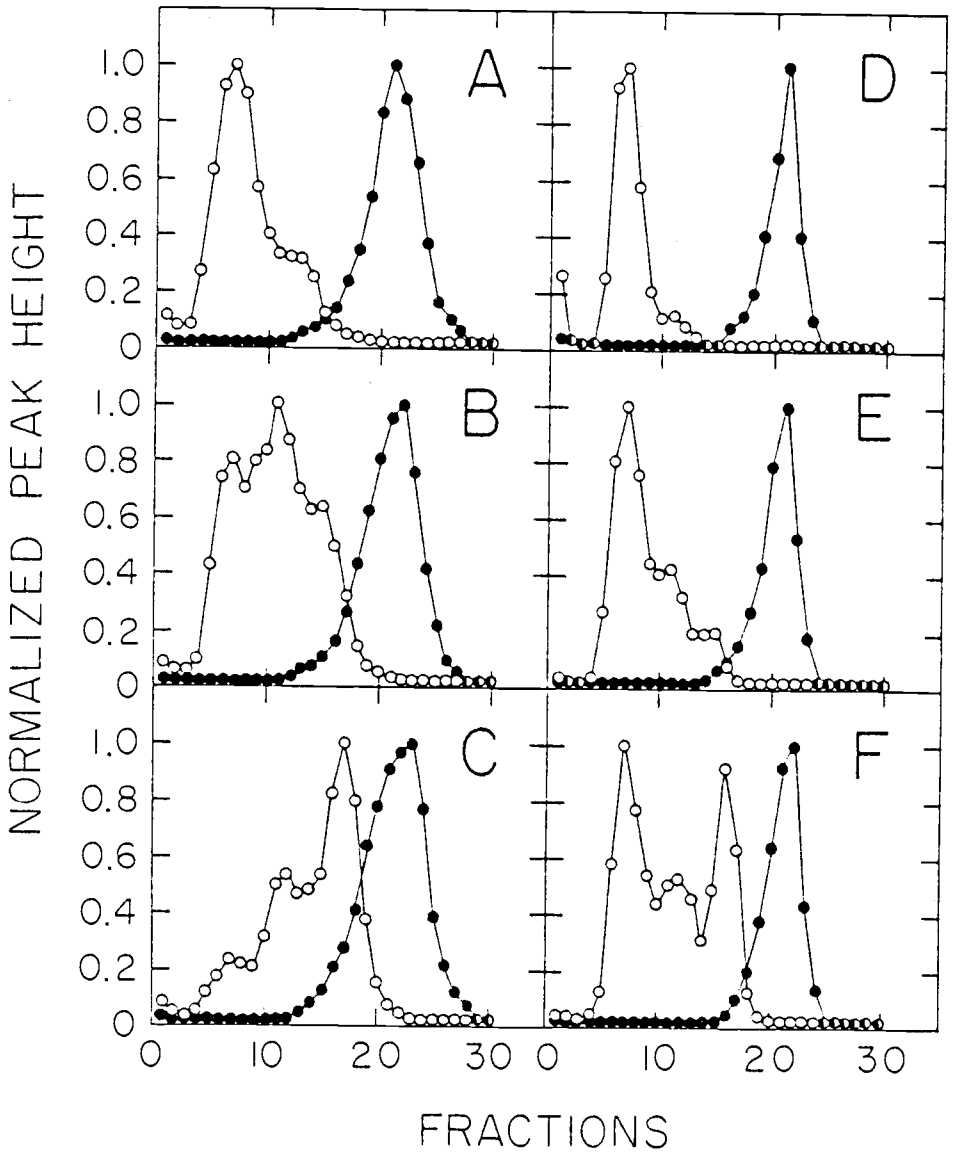
NORMALIZED PEAK HEIGHT
1.0
0.8
0.6
0.4
0.2
0
A
B
C
D
E
F
0
10
20
30
FRACTIONS

beginning of the chase in all cases except in the chase initiated at 14 hr after infection (see discussion above; Figure 3A), and (b) the total ^{32}P radioactivity in full heavy and hybrid DNA during the chase never exceeded twice the initial ^{32}P radioactivity in fully heavy DNA at the start of the chase (i.e., $[HH] + [HL] < 2[HH]_o$).

Since packaging of intracellular adenovirus DNA into virions begins at 18 hours (Green, 1962b) to 24 hours post infection (Strohl and Schlesinger, 1965; Rouse and Schlesinger, 1967) and only 20 percent of the total Ad2 DNA made during infection gets packaged into virus particles, our experiments are completed prior to significant addition of a pathway of DNA removal into virions.

The exact changes in the CsCl gradient profiles of adenovirus DNA during density-shift experiments depended on the time during infection at which the shifts occurred. For example, during the chase at 14 hr after infection, there was a shift from fully heavy (Figure 3A) to hybrid (Figure 3B) to fully light (Figure 3C) viral DNA. The almost complete loss of fully heavy DNA late in the chase (Figure 3C) indicated that all molecules had replicated at least once. In contrast, during the chases at 18 hr (Figures 3D through 3F) or at 22 hr (not shown) after infection, the persistence of fully heavy viral DNA suggested that only a fraction of the molecules had replicated at least once. Recently synthesized molecules, however, had a much greater chance to replicate again as shown by the

substantial accumulation of fully light DNA late in the chase (Figure 3F). These qualitative observations could be verified quantitatively by measuring the initiation rates i and i'. Figure 4 illustrates the measurement of the initiation rate of adenovirus DNA replication using the Fraction [HH] method described above. As predicted by Equation (10), a logarithmic plot of the fraction of ^{32}P radioactivity banding at the fully heavy density in each CsCl gradient versus the time after chase in light medium gave a straight line. The initiation rate was calculated in each case by using Equation (11): i = 0.0035, 0.0012, and 0.0005 initiations/min/end, respectively, for chases started at 14, 18, and 22 hr after infection.

The rate of initiation could also be measured by using the Fraction [HL] method described above. In Figure 5A the fraction of ^{32}P radioactivity banding at the hybrid density in each CsCl gradient was plotted against the time after chase in light medium. The plots passed through maxima at Fraction [HL] = 0.47, 0.325, and 0.225 where t_{max} = 50, 120, and 180 min, respectively, for chases started at 14, 18, and 22 hr after infection. Only the plot for the chase at 14 hr after infection approached the theoretical maximum of 0.5 predicted by Equation (12) where i = i'. The explanation can be seen in Figure 5B which displays theoretical curves generated by Equation (17) for various ratios of i'/i. The time coordinate has been normalized by using units of 1/i minutes.

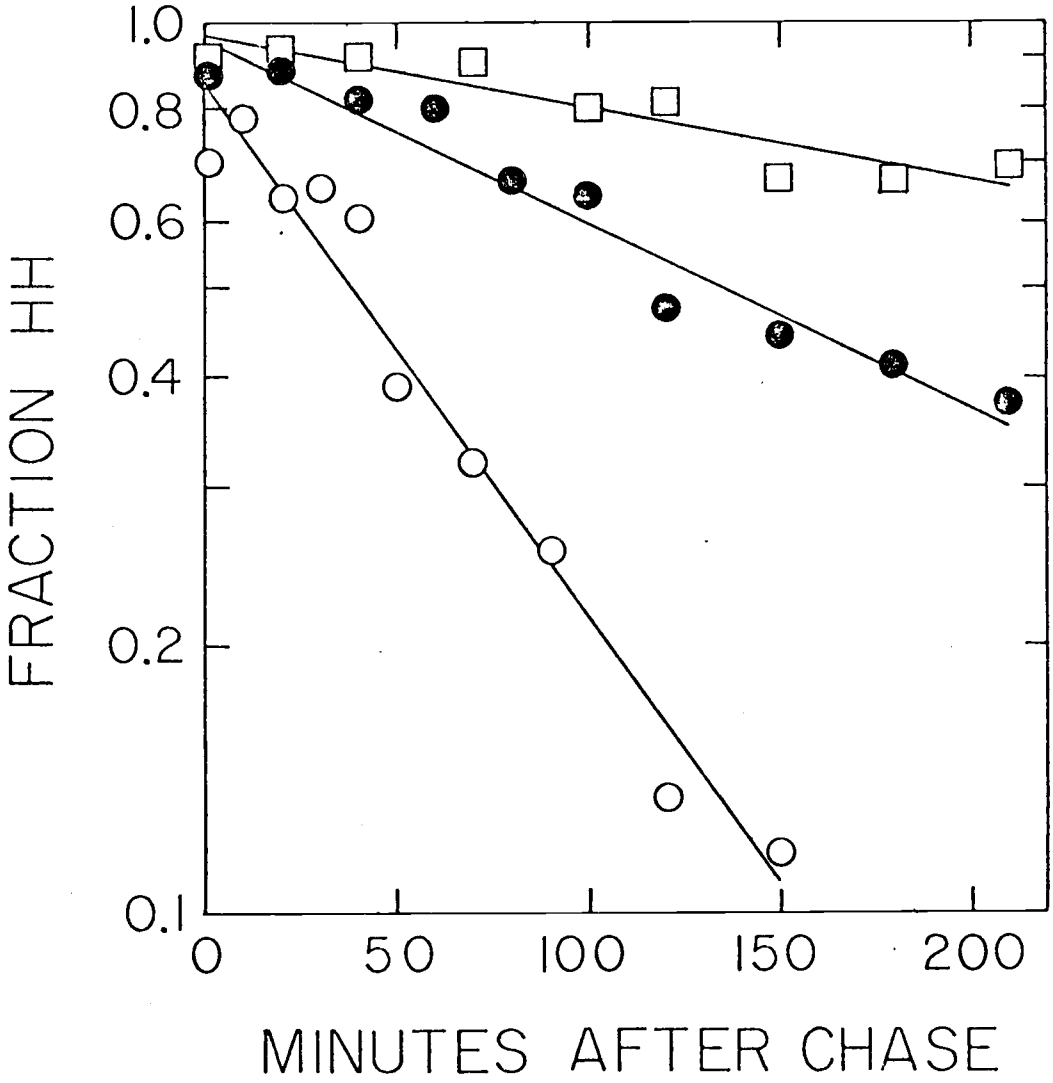

Figure 4. Measurement of the rate of initiation of adenovirus DNA replication using the Fraction [HH] method. The fraction of ^{32}P radioactivity banding at the fully heavy (HH) density in each CsCl gradient (see, for example, Figure 3) was plotted logarithmically against the time after chase in light medium. O , chase started at 14 hr after infection. ● , chase started at 18 hr after infection. □ , chase started at 22 hr after infection. In each plot, the solid line represents the least squares fit to the data. The initiation rate was calculated using Eq. (11): 0.0035, 0.0012, and 0.0005 initiations/min/end, respectively, for chases started at 14, 18, and 22 hr after infection.

Figure 5. Measurement of the rate of initiation of adenovirus DNA replication using the Fraction [HL] method. (A) The fraction of ^{32}P radioactivity banding at the hybrid (HL) density in each CsCl gradient (see, for example, Figure 3) was plotted against the time after chase in light medium. O , chase started at 14 hr after infection. The solid line was calculated using Equation (17) with $i = 0.0065$ and $i' = 0.0078$ initiations/min/end. ● , chase started at 18 hr after infection. The solid line was calculated using Equation (17) with $i = 0.0016$ and $i' = 0.0053$ initiations/min/end. □ , chase started at 22 hr after infection. The solid line was calculated by using Equation (17) with $i = 0.0006$ and $i' = 0.0042$ initiations/min/end. (B) Theoretical curves generated by Equation (17) plotted for various ratios of i'/i. The time coordinate is in units of $1/i$. Note that Equation (17) simplifies to Equation (12) when $i = i'$, and in that case $t_{max} = \ln 2/2i$ (Equation 14). The ratio of i'/i could be estimated by the intersection of the maximum experimental value of Fraction [HL] (dashed line) with the dotted line which connects the theoretical maxima. The abscissa (arrow) of the intersection yields the value of t_{max}. For example, during the chase at 14 hr after infection, Fraction [HL] = 0.47 at $t_{max} = 50$ min $= 0.325/i$ corresponding to $i'/i = 1.2$. Therefore, $i = 0.325/50 = 0.0065$ initiations/min/end and $i' = 1.2\ (0.0065) = 0.0078$ initiations/min/end. The values of i and i' at 18 hr and 22 hr after infection are given above.

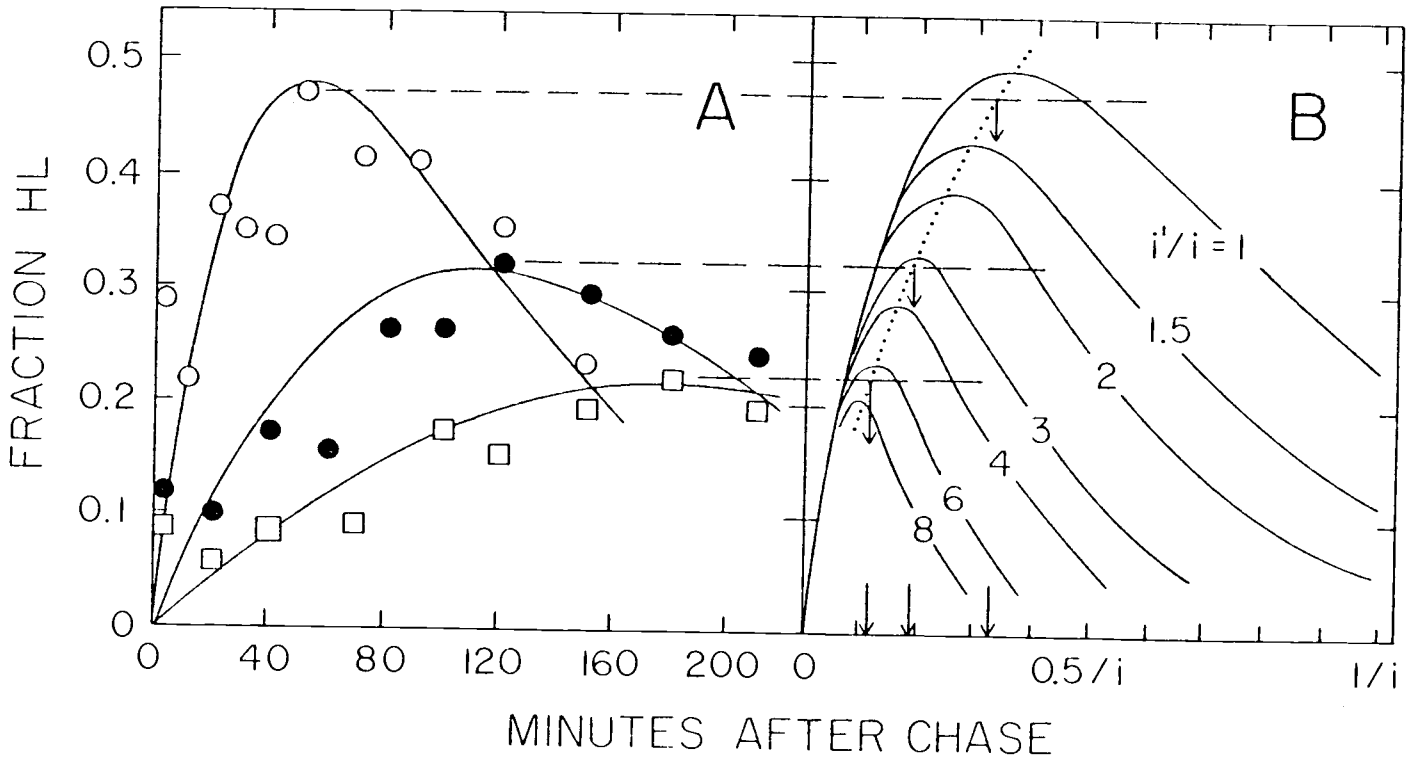
FRACTION HL
0.5
0.4
0.3
0.2
0.1
0
A
B
0
40
80
120
160
200
0
0.5/i
1/i
i'/i = 1
1.5
2
3
4
6
8
MINUTES AFTER CHASE

As the ratio of i'/i increases, the maximum value of Fraction [HL] decreases. It is clear, then, that the ratio of i'/i as well as t_{max} can be estimated by comparing maxima calculated with Equation (17) to the experimentally measured maximum of Fraction [HL] in each chase. This is shown graphically in Figure 5B as the intersection of the maximum experimental value of Fraction [HL] (dashed line) with the dotted line connecting the theoretical maxima. The abscissa of each intersection (arrows in Figure 5B) yields the values of $t_{max} = 0.325/i$, $0.190/i$, and $0.115/i$ min, respectively, at 14, 18, and 22 hr after infection. The values of i could then be calculated from the observed values of t_{max} in Figure 5A. For example, $t_{max} = 0.325/i = 50$ min or $i = 0.325/50 = 0.0065$ initiations/min/end at 14 hr after infection. Similarly, $i = 0.0016$ and 0.0006 initiations/min/end at 18 and 22 hr after infection. Table 1 compares the values of i measured by the Fraction [HH] and Fraction [HL] methods. The measured values of i agree very well except at 14 hr after infection where the presence of hybrid DNA at the start of the chase (Figure 3A) leads to a high estimate for i with the Fraction [HL] method.

The maximum value of Fraction [HL] determines the ratio of i'/i according to Equation (17) as discussed above. We estimated that $i'/i = 1.2$, 3.3, and 7.0, respectively, at 14, 18, and 22 hr after infection. Recently synthesized adenovirus DNA molecules

Table 1. Rate of initiation of adenovirus DNA replication.

Method	Hours After Infection	Initiations/min/end	
		i	i'
HH[a]	14	0.035	0.0042
	18	0.0012	0.0040
	22	0.0005	0.0035
HL[b]	14	(0.0065)	(0.0078)[c]
	18	0.0016	0.0053
	22	0.0006	0.0042
	Average		0.0042 $\pm$ 0.0007

[a] See Figure 4

[b] See Figure 5

[c] Not included in average

preferentially reinitiated replication since $i' > i$. This preference was slight at 14 hr after infection, but increased markedly later during infection. We interpret these results to mean that adenovirus DNA is partitioned into several pools, and at least one pool contains molecules destined for replication. The initiation rate in the replication pool, i', can be calculated from the ratios of i'/i estimated above. Table 1 shows that i' remained constant at all times after infection with an average value of 0.0042 ± 0.0007 initiations/min/end.

Calculation of the Rate of Initiation from Saturable Kinetics

Density-shift experiments provided physical (Figure 3) and kinetic (Table 1) evidence for a pool of replicating DNA molecules in adenovirus infected cells. We postulate that the size of the replicating pool limits the production of adenovirus DNA during infection. Figure 6 shows the production of adenovirus DNA during infection. The time course for synthesis of viral DNA shown in Figure 6 agrees generally with kinetics measured by several other methods (Green, 1962a; van der Eb, 1973; Flint *et al*, 1976; Fanning and Doerfler, 1977). The initial production of viral DNA was approximately logarithmic with a doubling time of 62 min (Figure 6, inset). However, the accumulation of viral DNA began

Figure 6. Production of adenovirus DNA during infection. HeLa cells were labeled for 24 hr with [^{3}H]thymidine, and then infected with adenovirus. Twelve hr after infection, cells were labeled with [^{32}P]orthophosphate. Total DNA was extracted from infected cells at the indicated times and analyzed by CsCl density gradient centrifugation. The number of viral molecules per cell was calculated at each time by assuming an average DNA content of 15×10^{-6} μg HeLa DNA per cell (Sober, 1970) and a molecular weight of 23×10^6 for adenovirus DNA. For example, the CsCl gradient prepared at 19 hr after infection contained 89,500 cpm ^{32}P of adenovirus DNA with a specific activity of 20,000 cpm ^{32}P per μg DNA and 82,800 cpm ^{3}H of HeLa DNA with a specific activity of 9,400 cpm ^{3}H per μg DNA, or

$$\frac{(89{,}500 \text{ cpm } ^{32}\text{P})\,(15 \times 10^{-6} \mu\text{g HeLa DNA/cell})\,(9{,}400 \text{ cpm } ^{3}\text{H}/\mu\text{g HeLa DNA})}{(20{,}000 \text{ cpm } ^{32}\text{P}/\mu\text{g Ad DNA})\,(3.8 \times 10^{-11} \mu\text{g Ad DNA/molecule})\,(82{,}800 \text{ cpm } ^{3}\text{H})}$$

$= 2 \times 10^5$ adenovirus molecules/cell. The solid line was calculated with an iterative program designed to model the production of adenovirus DNA (see Theory). The inset shows the same data with DNA concentration plotted logarithmically. The initiation rate was $i = V_{max}/(2K_M + 2[DNA])$ where V_{max} = 125,000 molecules/cell/hr, K_M = 143,000 molecules/cell, and [DNA] = 2,000 molecules/cell at 12 hr after infection.

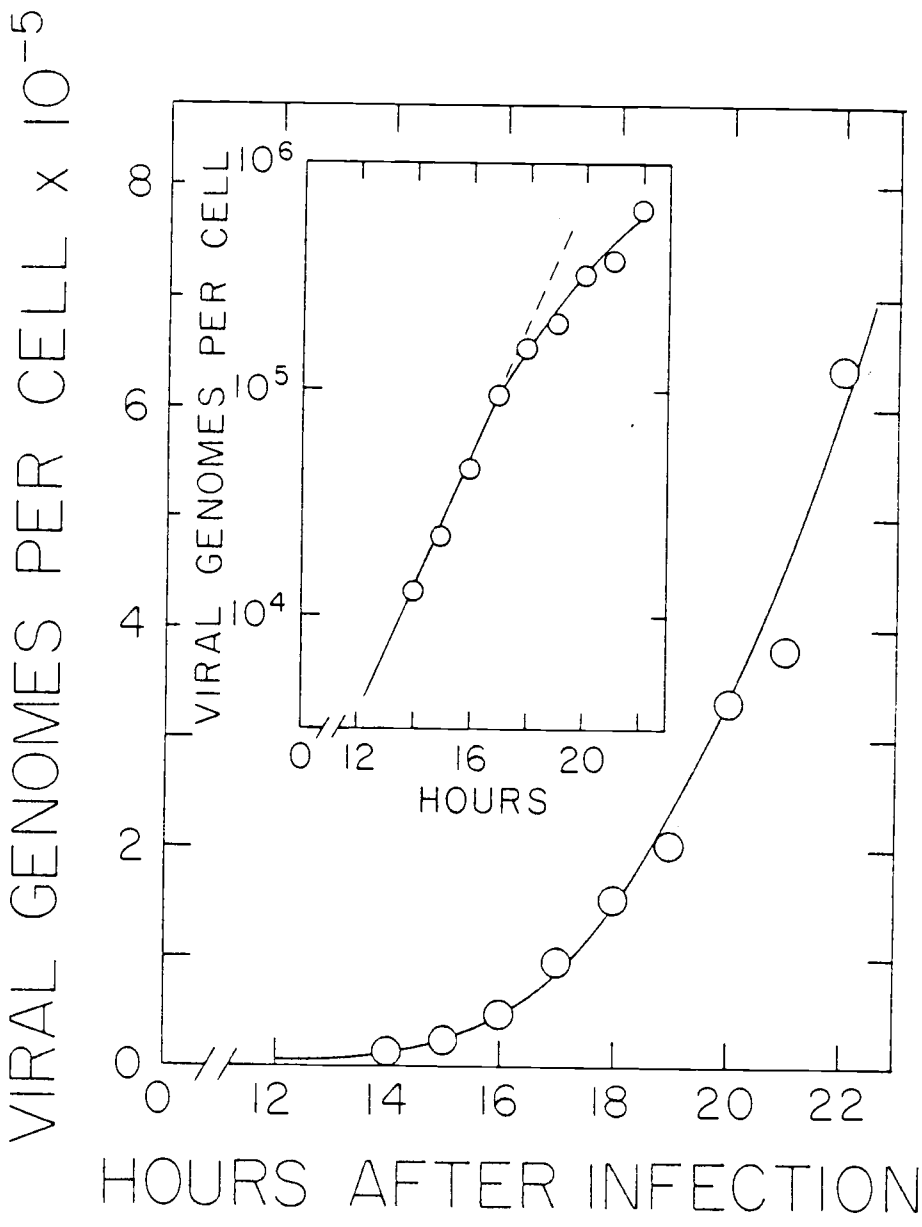
VIRAL GENOMES PER CELL x 10^{-5}
0
2
4
6
8
0
12
14
16
18
20
22
HOURS AFTER INFECTION
VIRAL GENOMES PER CELL
10^6
10^5
10^4
0
12
16
20
HOURS

to deviate significantly from logarithmic growth by 18 hr after infection, and thereafter the kinetics were roughly linear.

The rate of change of DNA concentration during infection, or velocity = d[DNA]/dt in units of viral genomes per cell per hr, was determined graphically as the tangent at any point on the curve in Figure 6. Figure 7 presents a double reciprocal, or Lineweaver-Burk plot (Segel, 1975), where 1/velocity was graphed against 1/[DNA]. The data points lie on a straight line which indicates that the production of adenovirus DNA during infection exhibits saturable kinetics. The intercept of the 1/velocity axis yields $1/V_{max}$ and the intercept of the 1/[DNA] axis yields $-1/K_M$ as indicated in Figure 7. In this experiment V_{max} = 125,000 genomes/cell/hr and K_M = 143,000 genomes/cell. The average values obtained in three independent experiments for Ad2, Ad5, and Ad7 were V_{max} = 118,000 $\pm$ 11,500 genomes/cell/hr and K_M = 177,000 $\pm$ 49,000 genomes/cell. In the formalism of Michaelis-Menten kinetics (Segel, 1975), we can write:

$$\text{velocity} = 2i\,[\text{DNA}] = V_{max}\,[\text{DNA}]/(K_M + [\text{DNA}]) \qquad (18)$$

or

$$i = V_{max}/(2\,K_M + 2\,[\text{DNA}]) \qquad (19)$$

It is important to realize that although the Michaelis-Menten

Figure 7. Determination of V_{max} and K_M for adenovirus DNA replication. The velocity of replication (in units of molecules/cell/hr) was estimated graphically as the tangent at any given point on the curve in Figure 6. The reciprocal of the velocity was plotted against the reciprocal of the concentration (in units of DNA molecules/cell). The solid line represents the least squares fit to the data. The intersection of the fitted line with the ordinate gives $1/V_{max}$ and the intersection with the abscissa gives $-1/K_M$. In this case, V_{max} = 125,000 molecules/cell/hr and K_M = 143,000 molecules/cell.

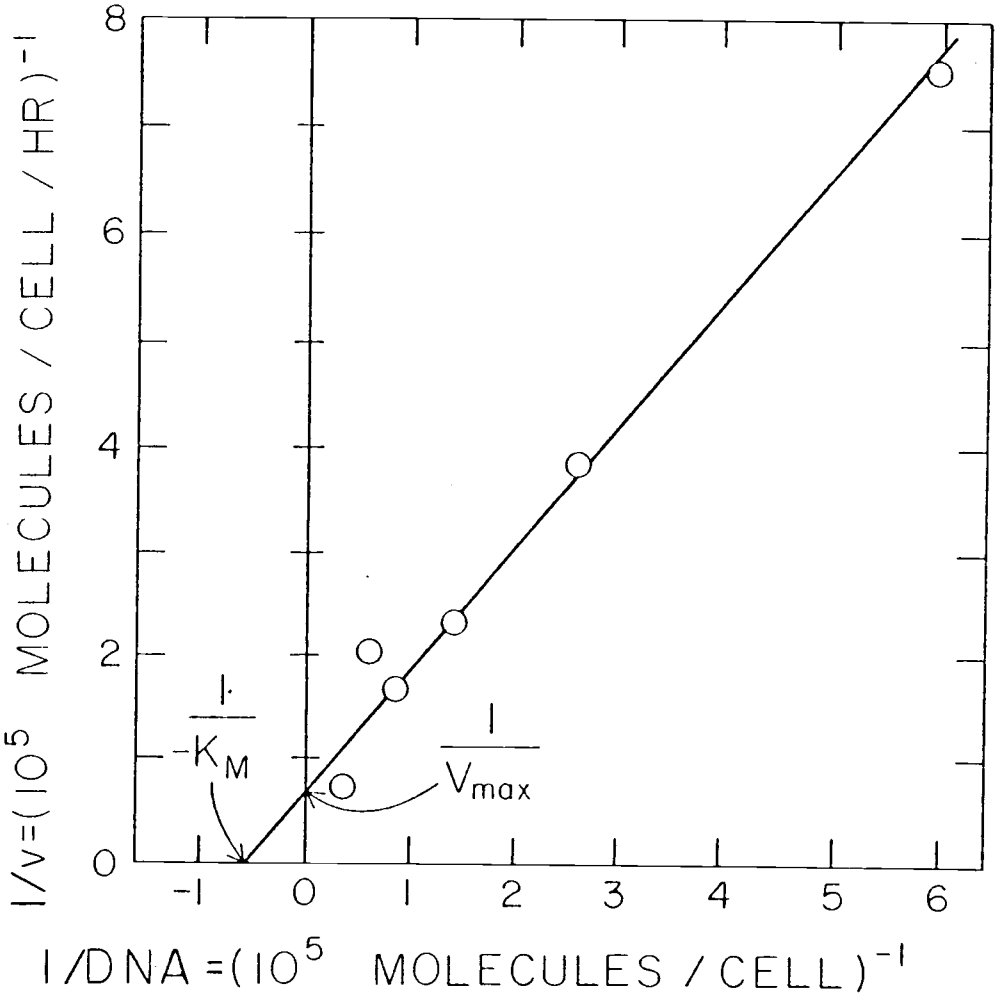
8
6
4
2
0
-1
0
1
2
3
4
5
6
1/v=(10^5 MOLECULES / CELL / HR)^-1
1/DNA =(10^5 MOLECULES / CELL)^-1
1/-K_M
1/V_max

equation has usually been derived by assuming either steady-state or equilibrium conditions, it can also be derived by considering that the overall reaction, in this case the production of viral DNA, occurs in irreversible steps (Segel, 1975). K_M is then a ratio of forward rate constants while V_{max} remains the maximum velocity of the reaction. Equation (19) adequately predicts the initiation rate as shown in Figure 10 below.

The average rate of adenovirus DNA replication is constant throughout the course of infection at 0.046 fractional lengths/min or 1600 nucleotides/min (Bodnar and Pearson, 1980a). The average time required to synthesize a molecule is 21.7 min or 0.362 hr. Thus we can estimate the size of the replication pool as

$$[DNA]_{pool} = V_{max} \text{ (time to synthesize a single molecule)}$$

$$= (118,000 \text{ molecules/cell/hr}) (0.326 \text{ hr})$$

$$= 43,000 \text{ molecules/cell.}$$

Alternatively, we can use Equation (19) in the form:

$$[DNA]_{pool} = (V_{max}/2i') - K_M \qquad (20)$$

where i' = (0.0042 initiations/min/end) (60 min) = 0.252 initiations/hr/end (Table 1). In this case, $[DNA]_{pool}$ = 57,000 molecules/cell, in excellent agreement with the value calculated above. The

average value for the size of the replication pool is 50,000 ± 7,000 molecules/cell, a concentration attained at 16 hr after infection (Figure 6) when the shift from logarithmic to linear kinetics begins.

We can further check the consistency of these results by comparison with previously reported growth parameters. By extrapolation of the DNA accumulation curve (Figure 6) we estimate that there will be approximately 1.5×10^6 Ad5 genomes per cell at 30 hours post infection. It has been shown that at 30 hours post infection there are about 10^4 Ad PFU per cell (Green, 1962b), that for Ad5 there are about 10 to 20 particles per PFU (Green et al, 1967) and about 10 to 20 percent of the Ad DNA is packaged (Green, 1962a). These data indicate that there are about 5×10^5 to 2×10^6 Ad5 genomes per cell at 30 hours post infection.

Calculation of the Rate of Initiation from Steady-state Kinetics

A detailed model for adenovirus replication has already been discussed thoroughly (Lechner and Kelly, 1977; Winnacker, 1978; Robinson et al, 1979). Figure 8 diagrams the relationship between each type of replicating adenovirus molecule. The types of molecules presented in Figure 8 account for more than 90% of the molecules scored by electron microscopy in the study of Lechner and Kelly (1977). We define the following terms: i' = rate of initiation on

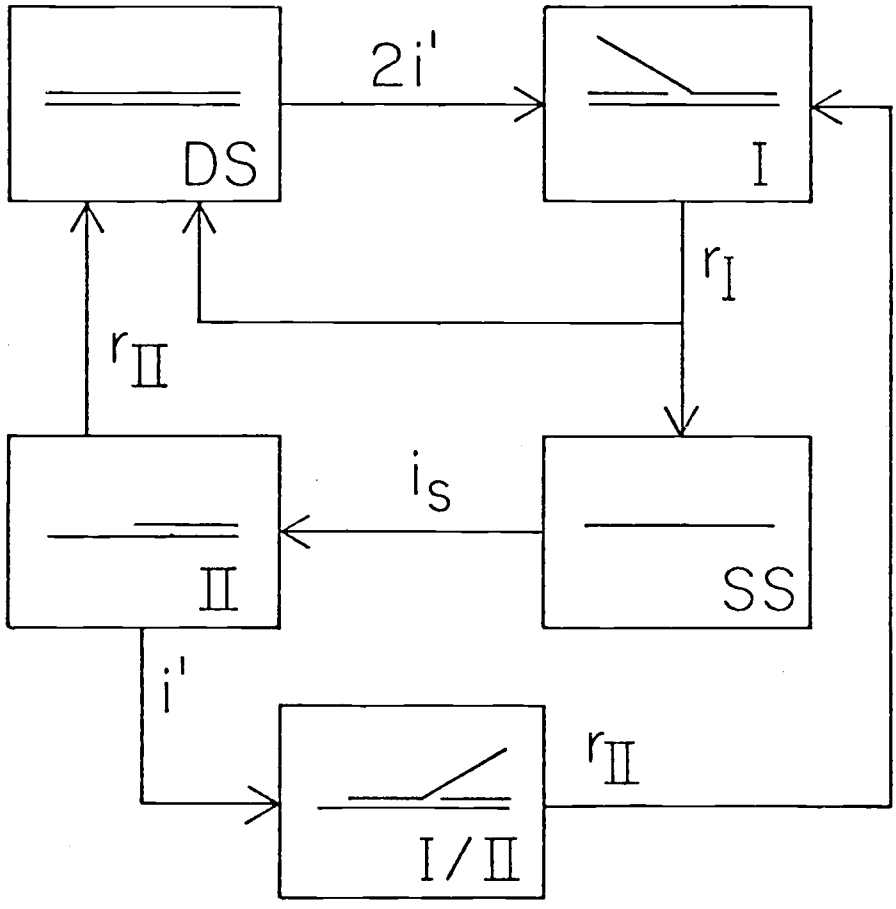

Figure 8. Model of adenovirus DNA replication. DS = double stranded molecules, SS = single stranded molecules, I = type I molecules, II = type II molecules, and I/II = type I/II molecules. The designations type I, type II, and type I/II for replicating adenovirus DNA molecules have been proposed by Lechner and Kelly (1977). i' = rate of initiation on double-stranded molecules in the replicating pool. i_S = rate of initiation on single stranded molecules. r_I = rate of replication on a type I molecule (displacement synthesis). r_{II} = rate of replication on a type II molecule (complementary synthesis).

double stranded molecules in the replicating pool, i_S = rate of initiation on single stranded molecules, r_I = rate of displacement synthesis, and r_{II} = rate of complementary synthesis. The units for initiation have been defined above as initiation events per minute per molecular end. The units for replication rate are fractional lengths per minute (Robinson et al, 1979; Bodnar and Pearson, 1980a; Part I). Since we do not know all the events leading to the initiation of complementary synthesis on displaced single strands, we assume $i_S \neq i'$. We also assume $r_I \neq r_{II}$, but $r_I + r_{II} = 2\ r$ where r = average rate of replication (Bodnar and Pearson, 1980a; Part I). This last point is supported by the data of Lechner and Kelly (1977) which show 95 (47%) type I growing points and 109 (53%) type II growing points in all replicating molecules analyzed by electron microscopy. We can describe the rate of change of each species in Figure 8 by a system of differential equations:

$$d[DS]/dt = -2i'[DS] + r_{II}[II] + r_I[I] \tag{21}$$

$$d[I/II]/dt = -r_{II}[I/II] + i'[II] \simeq 0 \tag{22}$$

$$d[II]/dt = -(i' + r_{II})[II] + i_S[SS] \simeq 0 \tag{23}$$

$$d[SS]/dt = -i_S[SS] + r_I[I] \simeq 0 \tag{24}$$

$$d[I]/dt = 2i'[DS] + r_{II}[I/II] - r_I[SS] \simeq 0 \tag{25}$$

The equations describe the rates of formation and decay of each species in terms of rate constants (i', r_I, etc.) and concentrations of each species (brackets). Mature, double stranded molecules increase with time, but we assume steady-state conditions for all other species (this is equivalent to a constant pool of replicating molecules as discussed above). Using appropriate algebra, we can show:

$$r_{II}[I/II] = i'[II] \tag{26}$$

$$(i' + r_{II})[II] = i_S[SS] = r_I[I] \tag{27}$$

$$d[DS]/[DS] = (2i'(i' + r_{II})/r_{II})dt \tag{28}$$

Equation (28) can be integrated to give:

$$[DS] = [DS]_o \exp(2i'(i' + r_{II})(t-t_o)/r_{II}) \tag{29}$$

where $[DS]_o$ is the concentration of double stranded molecules at time t_o. From Equation (29), we can calculate the doubling-time, t_d, for the production of double stranded molecules:

$$t_d = r_{II} \ln 2/(2i'(i' + r_{II})) \tag{30}$$

We can solve for the rate constants using Equations (26), (27), and (28) and the data from Lechner and Kelly (1977). We can use the number of molecules since we are interested only in the relative

concentrations: [I/II] = 18, [II] = 89, and [I] = 41. In the same study, the number of unit length single strands, [SS], was less than 10 (R. L. Lechner and T. J. Kelly, Jr., personal communication). Then

$$i' = r_{II}[I/II]/[II] = r_{II}(18/89) = 0.20\ r_{II} \text{ and}$$

$$r_I = (i' + r_{II})[II]/[I] = 1.20\ r_{II}(89/41) = 2.6\ r_{II}.$$

We have previously assumed $r_I + r_{II} = 2\ r$ where $r = 0.046$ fractional lengths/min (Bodnar and Pearson, 1980a; Part I). Substituting we get:

$$r_{II} = 2(0.046)/3.6 = 0.026 \text{ fractional lengths/min},$$

$$r_I = 2.6(0.026) = 0.068 \text{ fractional lengths/min},$$

$$i' = 0.20(0.026) = 0.0052 \text{ initiations/min/end},$$

$$i_S \geq 0.068(41/10) \geq 0.28 \text{ initiations/min/end},$$

and $$t_d = (0.026)(0.693)/((0.01)(0.031)) = 58 \text{ min}.$$

The calculated value of $i' = 0.0052$ initiations/min/end agrees remarkably well with the measured value of 0.0042 ± 0.0007 initiations/min/end (Table 1). Likewise, the calculated value of $t_d = 58$ min agrees very well with the value of 66 min measured in

the density-shift experiment (Figure 3A) and the value of 62 min measured in Figure 6. However, the calculations led to two surprising results. First, the initiation rate on single stranded molecules, i_S, was more than 50 times greater than the initiation rate on double stranded molecules. Secondly, displacement synthesis, r_I, was 2.6-times faster than complementary synthesis, r_{II}. No experimental procedure presently allows the independent measurement of the individual rates of replication, but we can test our conclusions in the following ways. Figure 8 shows that type I/II molecules arise from type II molecules by an initiation event. The average number of initiation events during the "lifetime" of type II molecules is $n = i'/r_{II}$. Using the values of i' and r_{II} derived from steady-state kinetics, $n = 0.0052/0.0026 = 0.2$. Table 2 presents the distribution of single stranded branches in type II and type I/II replicating molecules calculated from the Poisson relation $f_x = n^x e^{-n}/x!$ where $x = 0, 1, 2, \ldots,$ = number of single stranded branches. The calculated frequencies agree remarkably well with the frequencies observed by Lechner and Kelly (1977). The fraction of type II molecules which complete a round of replication <u>without</u> reinitiating to type I/II molecules is

$$f_o = [II]/([II] + [I/II]_{tot}) = e^{-i'/r_{II}} \qquad (31)$$

where $[I/II]_{tot}$ is the concentration of type I/II molecules with one or more single stranded branches. We can use the experimentally observed value of $f_o = 0.817$ (Table 2) and the value of $i' = 0.0042 \pm 0.0007$ initiations/min/end (Table 1) derived from density-shift experiments to estimate r_{II} which cannot be measured directly. Equation (31) predicts $r_{II} = 0.021 \pm 0.003$ fractional lengths/min which is significantly slower than the average rate of $r = 0.046$ fractional lengths/min (Bodnar and Pearson, 1980a; Part I).

We can estimate the value for the single stranded initiation rate (i_s) from biophysical data also. At 17 hours post infection approximately 35 percent of the Ad5 DNA is actively replicating (see Part III), and only 4 percent of the Ad DNA is in the form of completely displaced strands (Kedinger et al, 1978). Therefore $[DS]/[SS] \approx (0.65)/(0.04) = 16$. From equations (21) through (25) we can solve to find:

$$\frac{i_s}{i} = \left\{\frac{2(i + r_{II})}{r_{II}}\right\} \frac{[DS]}{[SS]} \approx 2\,[DS]/[SS] \qquad (32)$$

Substituting from above we find $i_s/i = 32$ supporting the hypothesis that single stranded DNA reinitiates much faster than mature double stranded DNA.

Table 2. Distribution of single stranded branches in type II and type I / II replicating molecules.

Molecules	Observed Frequency[a]	Calculated Frequency[b]
Type II (no branches)	0.817	0.819
Type I/II, one branch	0.165	0.164
Type I/II, two branches	0.009	0.016
Type I/II, three or more branches	0.009	0.001

[a] From Lechner and Kelly (1977).

[b] Calculated from the Poisson relation $f_x = n^x e^{-n}/x!$ where

$x = 0, 1, 2, \ldots,$ = number of single stranded branches,

$n = i'/r_{II}$ = average number of initiation events during the "lifetime" of a type II molecule, $i' = 0.0052$ initiations/min/end, and $r_{II} = 0.026$ fractional lengths/min.

Determination of the Initiation Rate by
Accumulation Curves for Mature Adenovirus DNA

As we saw in the preceding section steady-state kinetics derivation of the accumulation rate for mature (double stranded) adenovirus DNA can be expressed by the relationship (equation (29)):

$$\ln ([DS]/[DS]_o) = 2i(r_{II} + i)/r_{II} \quad (t - t_o) \qquad (33)$$

Since r_{II} is much larger than i, this equation can be approximated by:

$$\ln ([DS]/[DS]_o) = 2i\,(t - t_o) \qquad (34)$$

Therefore, we can measure the value of the initiation rate in still another way by plotting the logarithm of the concentration of mature DNA versus time and determining the slope which is equal to 2i.

The concentration of mature DNA was measured by using the previously mentioned protocol. Briefly, cells prelabeled for 24 hours with [^{3}H]thymidine were infected with Ad2 or Ad5, at 11 hours post infection [^{32}P]orthophosphate was added, and aliquots were harvested hourly from 13 to 22 hours post infection. Total intracellular DNA was extracted and mature double stranded DNA was purified by BD-cellulose column chromatography. Recovery of ^{32}P activity in adenovirus was corrected by normalizing to the ^{3}H cell DNA marker.

The growth curves (Figure 9) were not linear as would be expected for a constant initiation rate, but showed the same characteristic drop below exponential growth as seen for the total DNA growth curves above. This again indicated that the initiation rate is decreasing during infection. The initiation rate was then determined by using the slope of the line in Figure 9 and calculating the value with equation (34). The calculated values for Ad2 and Ad5 were very similar, and the curve for Ad5 is plotted in Figure 10. We can see that this method for measuring the initiation rate agrees well with the density-shift experiments and total adenovirus DNA growth curves.

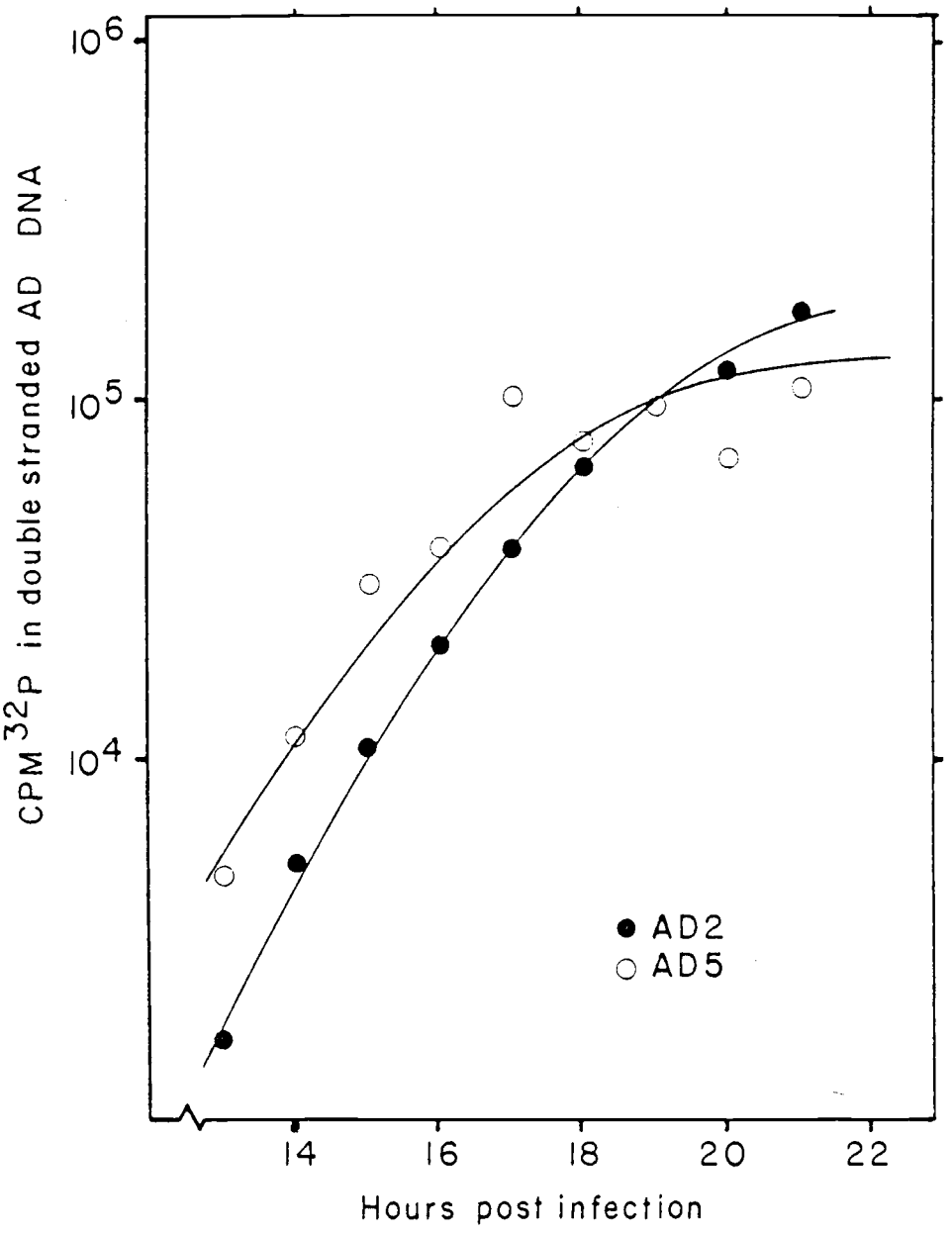

Figure 9. Accumulation of mature adenovirus DNA. Cells prelabeled with [^{3}H]thymidine for 24 hours were infected with Ad2 (●) or Ad5 (○), and labeled with [^{32}P] at 11 hours after infection. Aliquots were removed, and total intracellular DNA was extracted and separated by BD-cellulose chromatography. The double stranded DNA was counted corrected for recovery relative to ^{3}H cell DNA.

DISCUSSION

We have developed four methods to estimate the initiation rate of adenovirus DNA replication: (a) direct measurement during density-shift experiments, (b) calculation using the saturation kinetics of total viral DNA accumulation, (c) calculation using steady-state kinetics of viral DNA replication, and (d) calculation by exponential kinetics of double stranded viral DNA accumulation. As illustrated in Figure 10, the values for the rate of initiation estimated by each method agree quantitatively. Figure 10 shows that the value of i, the average initiation rate for all DNA molecules in the nucleus, decreased during the course of infection as measured during density-shift experiments by the Fraction [HH] method (open circles) or the Fraction [HL] method (closed circles). The value of i also decreased during the course of infection when calculated by equation (19) from the saturation kinetics of viral DNA accumulation (Figure 10, dashed line) and when calculated by equation (34) by using the exponential kinetics of mature viral DNA accumulation (Figure 10, dotted line). On the other hand, Figure 10 demonstrates that the value of i', the initiation rate for molecules that have replicated at least once during a density-shift, remained constant throughout infection (solid line) as measured during density-shift experiments by the Fraction [HH]

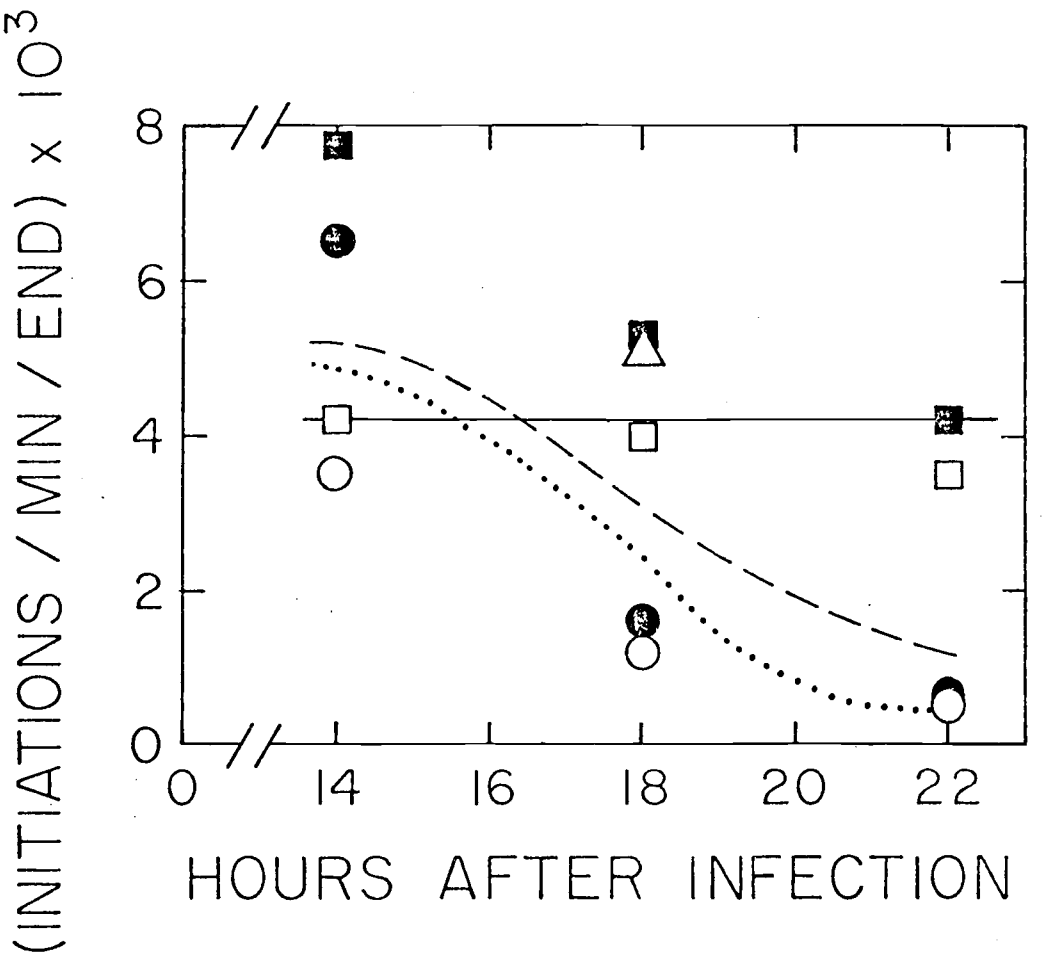

Figure 10. Rate of initiation of adenovirus DNA replication during infection. ○, i measured as described in Figure 4. ●, i measured as described in Figure 5. □, i' measured as described in Figures 4 and 5. ■, i' measured as described in Figure 5. △, i' measured from the data of Lechner and Kelly (1977). Solid line: the average value of i' = 0.0042 initiations/min/end (Table 1). Dashed line: i calculated from the relationship $i = V_{max}/(2KM + 2[DS]$ by using the data from Figure 6, and the average values V_{max} = 118,000 molecules/cell/hr and K_M = 177,000 molecules/cell. Dotted line: i calculated from the relationship $d(\ln [DS])/dt = 2i$ by using data for Ad5 from Figure 9.

method (open squares) or the Fraction [HL] method (closed squares). The value of i' calculated from the steady-state kinetics of adenovirus DNA replication agrees remarkably well (Figure 10, open triangle). Since $i' > i$ throughout infection, newly replicated viral DNA molecules were preferentially initiated. This preference was slight ($i'/i = 1.2$) at 14 hours after infection, but increased markedly ($i'/i = 7.0$) by 22 hours after infection. We interpret these results to mean that adenovirus DNA is partitioned into several pools, and at least one pool contains molecules destined for replication. The average rate of initiation in this pool was $i' = 0.0042 \pm 0.0007$ initiations/min/end (Table 1; Figure 9, solid line). The size of the replication pool was estimated to be $50,000 \pm 7,000$ molecules/cell. We do not yet know what factor limits the size of the pool. For example, the packaging of DNA into adenovirus particles apparently is not a limiting factor since assembly begins about 24 hours after infection under our experimental conditions (Robinson et al, 1979). Brison et al (1979) have recently shown that active replication and transcription complexes are physically distinct at 17 hr after infection; this provides additional evidence for the partitioning of adenovirus DNA into pools. Each of the methods to estimate the initiation rate can also be used to measure the doubling time for the production of viral DNA during the logarithmic phase of adenovirus replication. The doubling time measured during

density labeling was 66 min (Figure 3), the time measured for the production of viral DNA was 62 min (Figure 6), and the time calculated from steady-state kinetics was 58 min (Eq. (30)). The average doubling time was $t_d = 62 \pm 4$ min, 2.8-times longer than the average time to replicate an adenovirus DNA molecule (Bodnar and Pearson, 1980a). This confirms the postulate that initiation is the rate limiting step in adenovirus replication.

The single step growth curve for total intracellular adenovirus DNA accumulation shows that some factor required for initiation of replication is available at a constant concentration after the onset of DNA replication and is limiting. Early in infection this factor is in excess over the substrate adenovirus DNA, and the rate of DNA synthesis is dependent on the concentration of DNA. At about 17 hours post infection this factor is saturated with the substrate DNA, the rate of DNA synthesis reaches its maximum value, and DNA synthesis continues at a constant rate. Thus, the rate of adenovirus DNA replication shows the hyperbolic relationship to total adenovirus DNA concentration characteristic of saturable kinetics. This type of DNA accumulation curve has also been reported for DNA replication of SV40 (Manteuil et al, 1973) and polyoma (Roman, 1979).

The limiting factor in initiation could possibly be a cellular function as can be seen by comparing the characteristics of adenovirus and HeLa DNA replication. The average rate for adenovirus is

0.046 fractional genomes per minute (Part I) or 0.85 μm per minute, and this rate is constant over infection. We estimate that there are 50,000 replication sites per cell when adenovirus DNA replication reaches its maximum rate. For HeLa cells the DNA replication rate has been measured to be 0.5 to 1.4 μm per minute (Edenburg and Huberman, 1975; Painter and Schaefer, 1969) and there are approximately 10,000 to 100,000 replicons per cell (Painter and Schaefer, 1969; Hand and Tamm, 1974). The rate of replication is relatively constant during the cell cycle, and the rate of DNA synthesis depends on the number of replicons initiated during a given phase of the cycle (Painter and Schaefer, 1969; Wintersberger, 1978). No DNA polymerase has been identified that is coded by the adenovirus genome, and there is considerable evidence that the host DNA polymerases α and γ are involved in adenovirus DNA replication (Ito et al, 1975; van der Vliet and Kwant, 1978; Abboud and Horwitz, 1979; Longiaru et al, 1979; Habara et al, 1980). These data suggest that the limiting factor in adenovirus DNA replication might be a component of the cellular machinery required for replication (possibly the cellular DNA polymerase).

Density-shift experiments can be used to analyze the semiconservative DNA replication of any organism. Gustafsson et al, (1979) have independently derived equivalent, but not identical, equations

describing the relative amounts of density-labeled molecules during density-shift experiments with plasmid R1 DNA. Their equations will also give expressions for Fraction [HH] and Fraction [HL] identical to the relations derived here for the case $i = i'$ (except for a factor of 2 which enters our equations due to two origins of replication). Density-shift experiments have also been used to investigate the replication of polyoma DNA (Roman and Dulbecco, 1975; Roman, 1979) and SV40 DNA (Green and Brooks, 1978). These experiments clearly demonstrate that (a) newly synthesized viral DNA preferentially re-enters a subsequent round of replication, and (b) viral DNA is partitioned into replicating and non-replicating pools. We have modified the equations for Fraction [HH] and Fraction [HL] in order to measure the initiation rates of SV40 and polyoma DNA replication (see Part V). Although the density-labeling protocols of Green and Brooks (1978) and Roman (1979) differed significantly from ours, we estimated that $i' = 0.001$ initiations/min for SV40 and $i' = 0.004$ initiations/min for polyoma, both values in good agreement with the value of i' measured for adenovirus.

The development of the steady-state method to analyze adenovirus replication means that for the first time it is possible to determine rate constants for initiation, displacement synthesis, and complementary synthesis simply by counting specific types of replicating adenovirus DNA molecules by electron microscopy. We know

of no other replicating system that offers this advantage. As mentioned above, steady-state calculations of i' and t_d agree quantitatively with directly measured values. It is also important to emphasize that the rate constants calculated by this method quantitatively predict the frequencies of multiply initiated type I/II molecules (Table 2). However, the steady-state calculations led to two surprising conclusions: (a) the initiation rate on single stranded molecules, i_s, was more than 50-times greater than the initiation rate on double stranded molecules, i', and (b) displacement synthesis, r_I, was 2.6-times faster than complementary synthesis, r_{II}. Although we do not yet understand why $i_s >> i'$, at least two possibilities can be considered: (a) the mechanisms of initiation on single and double stranded molecules may differ fundamentally, or (b) the replication machinery may remain associated with the displaced single strand at the conclusion of displacement synthesis. Likewise, although we do not yet understand why $r_I > r_{II}$, we suggest below that the difference between the rates of displacement and complementary syntheses may provide a mechanism to generate defective adenovirus DNA molecules.

Adenovirus particles containing less than the normal amount of DNA have been characterized for Ad2 (Burlingham et al, 1974; Rosenwirth et al, 1974; Daniell, 1976), Ad3 (Prage et al, 1972;

Daniell, 1976), Ad7 (Tibbetts, 1977), Ad12 (Mak, 1971; Burlingham et al, 1974) and Ad16 (Wadell et al, 1973). These particles, which are non-infectious or show very low infectivity, are formed along with the infectious viruses and are not merely degradation products (Wadell et al, 1973; Rosenwirth et al, 1974). The defective viruses can be separated from the complete virus particles by CsCl equilibrium centrifugation since the defectives contain less than full length DNA and therefore band at lower buoyant densities. The DNA packaged in these defective particles is a linear duplex ranging from 15 percent of full size to full size in Ad2 and Ad3 (Daniell, 1976) or 12 to 80 percent of full size for Ad7 (Tibbetts, 1977). The distribution of lengths is heterogeneous although some discrete sized bands can be seen on agarose gels; for Ad2 most of the DNA is 30 to 40 percent of full size, but Ad3 shows major bands longer than 60 percent (Daniell, 1976).

The fraction of defective particles that are seen in a virus preparation is characteristic of a particular serotype. Usually 5 to 10 percent of all the virus particles are defectives in Ad2 infections (Rosenwirth et al, 1974; Burlingham et al, 1974; Daniell, 1976), but this fraction increases to 17 percent for Ad12 (Burlingham et al, 1974) and 30 percent for Ad3 (Prage et al, 1972; Daniell, 1976). These fractions seem to be independent of conditions of passage or MOI.

The fraction of defective DNA did not increase after multiple passages at high MOI for Ad2, Ad3, or Ad5 in HeLa and KB cells (Daniell and Mullenbach, 1978). Infection with Ad2 at 0.1 to 100 PFU per cell produces the same proportion of defective virions (Rosenwirth et al, 1974) while Ad3 infections at 0.5 to 50 PFU per cell produce the same fraction of defective intracellular DNA (Daniell and Mullenbach, 1978).

The structure of the DNA packaged in the defective virions has been studied by restriction endonuclease digestion and electron microscopy for Ad2, Ad3, and Ad7 (Daniell, 1976; Tibbetts, 1977). The restriction fragments from the left end of the genome are overrepresented in Ad2 and Ad3, and reanealling of defective DNA at low concentrations showed panhandle structures in the EM indicative of long inverted terminal repetitions from less than 150 base pairs to almost 50 percent of the total DNA length (Daniell, 1976). However, studies with Ad7 show less than 5 percent of the panhandle structures in the EM although the left end restriction fragments are still predominant (Tibbetts, 1977). DNA-protein complexes isolated from Ad2 and Ad3 defective virions show protease sensitive circles in the EM indicating that the terminal protein is present on both ends of the short DNA (Daniell, 1976).

When viral DNA is extracted from cell nuclei, the results are different. Here for Ad3 both ends of the genome are overrepresented

when cut by restriction enzymes (Daniell and Mullenbach, 1978). However, the fraction of defective DNA remains about the same (15 to 25 percent for Ad3), and the long terminal repetitions are still present. The differences in structures found in the virions probably are due to constraints in packaging. Defective DNA with either molecular end is made intracellularly, but only those with left ends are packaged since there is evidence for a sequence required for packaging present near the left end but outside the normal terminal repetition (C. Tibbetts, personal communication).

The adenovirus defective particles do not interfere with productive infection (Tibbetts, 1977). Cells infected with Ad2 at 1 PFU per cell produced the same yield of virus when coinfected with up to 1000 defective particles per cell (Daniell, 1976), and preinoculation with 100 defective particles per cell prior to Ad2 or Ad12 infection did not lessen the virus produced (Burlingham et al, 1974). The fraction of intracellular DNA that is less than full length is constant throughout the course of infection for Ad3 (Daniell, 1976); for Ad2 this fraction decreases early in infection, but becomes constant after about 20 hours into the infection (Rosenwirth et al, 1974). The fraction of defective virions is the same whether the virus is grown in HeLa or KB cells, in monolayer or suspension, or in 2 human fibroblast cell strains (Burlingham et al, 1974; Daniell and Mullehbach, 1978). However, when Ad2 or Ad5 are grown in monkey cells (where

DNA synthesis occurs but little packaging) the defective virions increase to 15 to 40 percent of the total virus (Daniell, Mullenbach and Fedor, EMBO Abstracts, 1978).

J. Sambrook (cited in Daniell, 1976) has proposed a mechanism to generate defective adenovirus DNA molecules. Parental single strands are released by displacement synthesis during replication. If a displaced single strand is broken endonucleolytically, the segment containing the 5' sequences may be able to form a hairpin by intramolecular base-pairing (Figure 11D). After repair synthesis, the molecule will have a normal double stranded end (Figure 11E) with an initiation site for replication. Complementary synthesis will then produce a defective genome (Figure 11F) with duplicated left ends in the form of a new, longer inverted terminal repetition, but lacking right end sequences. Since replication is symmetrical with respect to the ends, defective molecules with duplicated right ends, but lacking left ends, will also be generated (not shown). Although this mechanism accounts for the known structures of subgenomic molecules, it does not easily explain the differences in yields of defective genomes by various serotypes of adenovirus.

We propose an alternative route leading to the production of defective genomes. Figure 11A shows a type II molecule engaging in complementary synthesis. The growing point moves at a rate r_{II}.

Figure 11. A scheme for production of defective adenovirus DNA molecules. The open circles represent the 55,000-dalton protein covalently attached to the 5' end of each strand. (A) Type II molecule. The growing point moves at the rate r_{II}. The thin line represents the parental strand. The thick line represents the daughter strand synthesized by complementary replication. (B) Creation of a type I/II molecule. The displacement fork moves at the rate r_I where $r_I > r_{II}$. Thick and thin lines have been defined above. The thick, dashed line represents the daughter strand synthesized by displacement replication. (C) Premature displacement of a nascent strand when the type I growing point overtakes the type II growing point. The type I/II molecule is converted back to a type II molecule. (D) Hairpin formation by intramolecular base-pairing. (E) Regeneration of the terminal repetition by repair synthesis (thin line). (f) Complementary synthesis (thin dashed line) generates a defective adenovirus molecule. A new, longer inverted terminal repetition has been produced (T. R.). The defective molecule, in this case, is slightly smaller than the normal length and lacks sequences from the right-most 30% of the wild-type genome. Steps (D) through (F) have been proposed previously by J. Sambrook (Daniell, 1976).

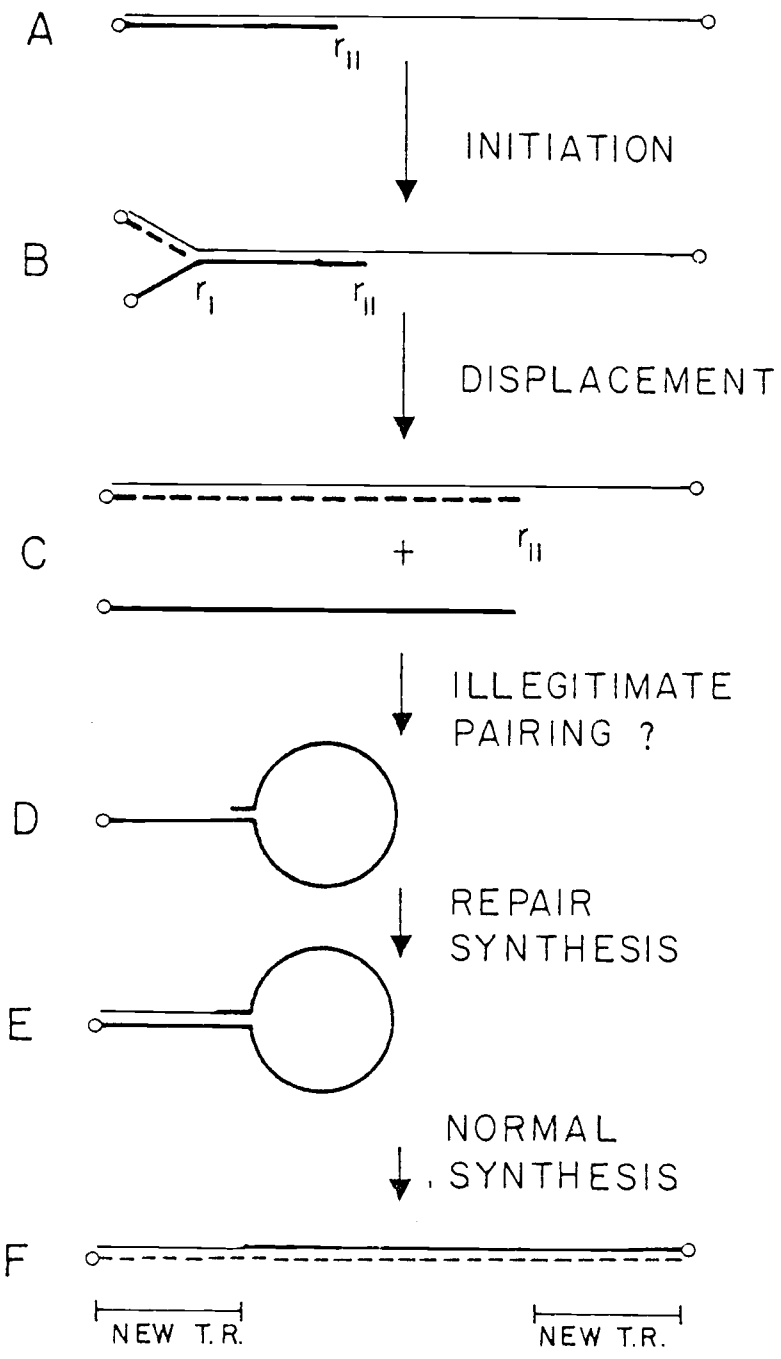
A
r_{II}
INITIATION
B
r_I
r_{II}
DISPLACEMENT
C
+
r_{II}
ILLEGITIMATE
PAIRING ?
D
REPAIR
SYNTHESIS
E
NORMAL
SYNTHESIS
F
NEW T.R.
NEW T.R.

An initiation event creates a type I/II molecule (Figure 11B) with a displacement fork moving at a rate r_I, where $r_I > r_{II}$. If initiation occurs before the growing point for complementary synthesis has traveled $1-(r_{II}/r_I)$ fractional lengths from the duplex end, the displacement fork will overtake the type II growing point. The simplest consequence is that a short nascent strand will be released prematurely (Figure 11C), and the type I/II molecule will revert back to a type II molecule. We call this process premature displacement synthesis, and we propose that this process provides the raw material for generating defective molecules. The displaced short strand (which has 5' sequences) can then be converted into a defective genome as described above (Figure 11, panels D through F).

This mechanism for formation of defective DNA precursors is consistent with available data accumulated on defective adenovirus DNA. The premature displacement synthesis mechanism predicts that single stranded DNA of random lengths extending from the 5' end will be displaced; the proposed mechanism of Sambrook postulates that the precursors are "broken" displaced strands of random lengths containing the 5' end sequences. We predict that both 5' ends would be overrepresented as is seen experimentally for intracellular DNA (Daniell and Mullenbach, 1978). The calculated fraction of type I/II molecules that would displace defective single strands is

$1 - (r_{II}/r_I)$ or about 60 percent of all type I/II molecules. Modeling replication to include this mechanism (derivation not shown) would lead to a quantity of defective single strands as seen below:

$$[\text{Defective SS DNA}] = \left(\frac{i'}{r_{II}}\right)\left(\frac{r_I - r_{II}}{r_I + i'}\right)[DS] \qquad (35)$$

Using the rate constants measured for Ad5 we calculate defective DNA precursors to be about 11 percent of the double stranded DNA concentration. Although several steps would then be necessary to form double stranded DNA, the concentration of precursors is approximately the right magnitude to account for the 5 to 10 percent defective virions seen in Ad2. Since i' in the above equation is constant over infection, one would expect the fraction of defective DNA to be constant over infection; this has been seen experimentally (Daniell and Mullenbach, 1978) although there is indication that this fraction decreases (Rosenwirth et al, 1974). Our model predicts that formation of defective DNA is an integral part of Ad DNA replication. This would lead to the following characteristics for the defective DNA (which are unusual for defective interfering particles) that are seen experimentally: (1) since formation of defectives is dependent on the ratios of rate constants, the number of defectives should be characteristic for a given type of adenovirus and host (Daniell, 1976) but should vary among types or among hosts for the same type (Daniell

et al, EMBO Abstract, 1978); and (2) the fraction of defectives should be independent of MOI (Rosenwirth et al, 1974; Daniell and Mullenbach, 1978). However, one would expect defectives up to twice full length Ad DNA if they are formed by premature strand displacement followed by repair synthesis as suggested by Sambrook; so far no defectives have been reported longer than full length Ad DNA.

Our model for generating defective adenovirus DNA molecules differs from the scheme of J. Sambrook (Daniell, 1976; Daniell and Mullehbach, 1978) in two important respects: (a) the short strands are newly-synthesized rather than parental, and (b) the process depends on the rate constants of replication which may explain the serotype-specific yield of defective molecules. The existence of premature displacement synthesis would suggest that the formation of defective DNA is a fundamental process in adenovirus replication. Although premature displacement synthesis only occurs when $r_I > r_{II}$, an increase in the average number of initiation events on type II molecules, $n = i'/r_{II}$ (Table 2), markedly increases the amount of prematurely released nascent strands.

THE KINETICS OF ADENOVIRUS DNA REPLICATION III:

Computer Simulation of DNA Growth

ABSTRACT

Simulation of adenovirus DNA replication is presented using the strand displacement model for replication (Lechner and Kelly, 1977) and rate parameters for DNA replication previously determined (Bodnar and Pearson, 1980a and 1980b; Part I and II). Calculated values are compared with biophysical determinations of DNA parameters for several experiments. An expanded method for determining rate constants from EM data which includes reinitiation of replicating molecules is presented. In all cases the mathematical model is quantitatively consistent with the experimental data.

INTRODUCTION

We have shown that the kinetics of adenovirus DNA replication can be explained by the completion of a single round of DNA replication in 22 minutes (Bodnar and Pearson, 1980a; Part I) and the buildup of total adenovirus DNA being controlled by a low probability of reinitiation of an adenovirus genome (Bodnar and Pearson, 1980b; Part II). We have measured or estimated the values for all the rate parameters required to describe adenovirus DNA replication: the rate of replication of a type I and type II molecule, r_I and r_{II}; the initiation rate for mature DNA and displaced single strands, i and i_s; and have shown that i can be expressed in terms of K_m, V_{max}, and DNA concentration. Knowing these parameters we can now describe the kinetics of DNA replication at any time after infection and in effect "grow" adenovirus on a computer. We have simulated DNA replication using an HP 9821A programmable calculator, determined pool sizes for all DNA forms as a function of time after infection, and used these simulations to look at various biophysical data determined throughout infection. In all cases the simulations were consistent with experimental data and often allowed better explanations for experimental characteristics than previously available.

We have also expanded the model for measuring rate constants from EM data to include reinitiation of already replicating molecules.

This model is consistent with previous data and shows that reinitiation of DNA replication is random on molecules already replicating.

THEORY

Calculation of Relative Activity of Various Replicating Pools

The iterative method for simulating Ad DNA growth presented in Part II gave results of pool sizes in terms of numbers of DNA molecules as a function of time post infection. Experimental results look at total radioactivity associated with different forms of the DNA, so we must convert numbers of molecules to relative activities.

1) Correction for sizes of the different replicating forms. Notice that a molecule that is completely single stranded will have half as many nucleotides as a mature double stranded DNA molecule and therefore, for uniformly labeled molecules the single stranded molecule will have half the activity. Similarly the pool of type I molecules will have on an average two complete strands plus a displaced strand about half genome length or will have about 1.25 times the activity of a mature DNA molecule. For type II molecules this ratio will be 0.75. Therefore, the number of molecules in each pool must be converted to an activity by these factors which we call correction factors (C. F.) below.

2) Correction for fraction of a molecule that is single stranded. Notice that a type I molecule will have on an average two full length DNA strands and a half genome length single stranded tail. Therefore,

the fraction of that molecule that is single stranded is (0.5)/(0.5+2) or 0.2. For type II molecules this will be 0.33, and for displaced single stranded DNA this will be 1.0. This will be called (fraction DNA_{ss}) below.

We can therefore calculate the fraction of DNA activities in various forms knowing the pool sizes from the iterative program and correcting them as shown below. In all cases the term [X] refers to the relative numbers of a given type of replicating form.

a) Percent of replicating DNA as single stranded DNA.

$$\left(\begin{matrix}\text{Fraction Rep.} \\ \text{Pool as } DNA_{ss}\end{matrix}\right) = \frac{100 \times \Sigma\ (\text{fraction } DNA_{ss})(\text{C. F.})\ [X]}{\Sigma\ (\text{C. F.})\ [X]}$$

b) Percent of total DNA in the replicating pool.

$$\left(\begin{matrix}\text{Percent total} \\ \text{DNA in Rep. Pool}\end{matrix}\right) = \frac{100 \times \Sigma\ (\text{C. F.})\ [X]}{[\text{Mature DNA}] + \Sigma\ (\text{C. F.})\ [X]}$$

c) Percent of total DNA that is single stranded.

$$\left(\begin{matrix}\text{Percent total} \\ \text{DNA as } DNA_{ss}\end{matrix}\right) = \frac{100 \times \Sigma(\text{C. F.})\ (\text{fraction } DNA_{ss})\ [X]}{[\text{Mature DNA}] + \Sigma\ (\text{C. F.})\ [X]}$$

d) Average growing points per replicating molecule.

$$\begin{matrix}\text{Avg. Forks} \\ \text{per molecule}\end{matrix} = \frac{\Sigma\ (\text{Growing points on X})\ [X]}{\Sigma\ [X]}$$

Calculation of the Number of Growing Points in Replicating Molecules

We define the following terms: t = time in min; x = position along the adenovirus genome in fractional length units where $0 \leq x \leq 1$; and r = average rate of replication expressed as fractional lengths per min. We also define subscript notations used in equations to follow: C = completed molecules; R = replicating molecules; T = total molecules (i.e. completed plus replicating molecules); r = r strand and l = l strand (strand designations are discussed in an article signed by 36 scientists: J. Virol. 22, 830-831, 1977); and i = 1, 2, ..., j for a restriction endonuclease that cleaves adenovirus DNA into j fragments. We assume adenovirus replicates by a strand displacement mechanism (Lechner and Kelly, 1977) with origins and termini of replication at both molecular ends (Figure 2B in Weingartner et al., 1976). We can write equations describing the relative accumulation of radioactive label at any point along either strand of adenovirus DNA molecules completed during a short time interval. We write for the r strand:

$$f_{Cr}(x,t) = rt-x; \quad 0 \leq x \leq rt \tag{1a}$$

$$f_{Cr}(x,t) = 0 \quad ; \quad x > rt \tag{1b}$$

Likewise, we write for the l strand:

$$f_{Cl}(x,t) = x-(1-rt) \quad ; \quad (1-rt) \leq x \leq 1 \tag{2a}$$

$$f_{Cl}(x,t) = 0 \quad ; \quad x < (1-rt) \tag{2b}$$

The boundary conditions for these equations must be strictly observed to avoid negative values. These equations are derived in detail in Part I. Now consider any interval along the genome, say restriction endonuclease fragment i with end coordinates x_1 and x_2. At any time, we can calculate the total relative radioactivity in either strand of fragment i by integrating expressions (1a), (1b), (2a), and (2b) at constant t and observing the boundary conditions for each equation:

$$F_{Cri} = \int_{x_1}^{x_2} f_{Cr}(x,t)\,dx = \frac{1}{2}\left([2rt-(x_2 + x_1)][x_2 - x_1] \right);$$

$$0 \leq x \leq rt \tag{3a}$$

$$F_{Cri} = 0 \quad ; \quad x > rt \tag{3b}$$

and

$$F_{Cli} = \int_{x_1}^{x_2} f_{Cl}(x,t)\,dx = \frac{1}{2}\left([(x_2 + x_1)-2(1-rt)][x_2 - x_1] \right);$$

$$(1-rt) \leq x \leq 1 \tag{4a}$$

$$F_{Cli} = 0 \quad ; \quad x < (1-rt) \tag{4b}$$

We define the average relative radioactivity as the total relative radioactivity uniformly distributed along the length of fragment i. Since the length of fragment i is $L_i = x_2 - x_1$, we obtain the average relative radioactivity in either strand of fragment i as:

$$\overline{F}_{Cri} = F_{Cri}/(x_2 - x_1) = \frac{1}{2}[2rt-(x_2 + x_1)] \; ;$$

$$0 \leq x \leq rt \tag{5a}$$

$$\overline{F}_{Cri} = 0 \; ; \; x > rt \tag{5b}$$

and

$$\overline{F}_{Cli} = F_{Cli}/(x_2 - x_1) = \frac{1}{2}[(x_2 + x_1)-2(1-rt)] \; ;$$

$$(1-rt) \leq x \leq 1 \tag{6a}$$

$$\overline{F}_{Cli} = 0 \; ; \; x < (1-rt) \tag{6b}$$

and, of course, the average relative radioactivity of the <u>double-stranded</u> fragment will be:

$$\overline{F}_{Ci} = \overline{F}_{Cri} + \overline{F}_{Cli} \tag{7}$$

For given values of r and t, equations (5a), (5b), (6a), (6b), and hence (7) can be evaluated readily for any restriction endonuclease fragment by using a program designed to account for the boundary conditions listed above (our program is written for the Hewlett

Packard 9821A calculator as listed in Appendix II).

If we now consider all molecules labeled during a short time interval (i.e., replicating molecules as well as newly completed molecules), the relative accumulation of radioactivity into both strands at any given point on the genome is:

$$f_T(x, t) = 2rt \tag{8}$$

The total relative radioactivity in fragment i of all the molecules is given by integrating at constant t:

$$F_{Ti} = \int_{x_1}^{x_2} f_T(x, t)dx = 2rt\,(x_2 - x_1) \tag{9}$$

and the average relative radioactivity in fragment i of all the molecules is:

$$\overline{F}_{Ti} = F_{Ti}/(x_2 - x_1) = 2rt \tag{10}$$

Therefore, we can calculate the average relative radioactivity in fragment i in replicating molecules from the expression:

$$\overline{F}_{Ri} = \overline{F}_{Ti} - \overline{F}_{Ci} \tag{11}$$

Now consider restriction endonuclease that cleaves adenovirus DNA into j fragments where the fragments are arbitrarily numbered

1, 2, . . . , j from left to right on the genome. Figure 4A shows that any internal restriction endonuclease fragment containing a growing point (either type I or type II) will be retained by the filter binding assay. Internal fragments lacking growing points will not be retained. Of course, terminal fragments (1 and j) will always be retained regardless of the presence of growing points. Let n = average number of growing points per molecule. The probability that a growing point will be located in fragment i between coordinates x_1 and x_2 is $n(x_2 - x_1)$ or nL_i. From the Poisson distribution, the fraction of all fragments i's containing at least one growing point is $1-\exp(-nL_i)$. Therefore, the fraction of radioactivity retained on filters after replacing molecules are cleaved by a restriction endonuclease is:

$$(\overline{F}_{R1} + \overline{F}_{Rj} + \sum_{i=2}^{j-1} \overline{F}_{Ri} [1-\exp(-nL_i)])/ \sum_{i=1}^{j} \overline{F}_{Ri} \qquad (12)$$

After S1 endonuclease digestion, shown diagramatically in Figure 4B, only the terminal fragments will bind to filters. In this case, equation (12) reduces to:

$$(\overline{F}_{R1} + \overline{F}_{Rj})/ \sum_{i=1}^{j} \overline{F}_{Ri} \qquad (13)$$

RESULTS

Simulation of Biophysical Data of Adenovirus DNA Replication

Determination of the rate constants allows simulation of adenovirus DNA replication over the course of an infection. Using the iterative model previously reported (Part II), we could simulate the pool sizes for the major replicating forms (neglecting reinitiation) on the HP 9821A programmable calculator, find the change in pool sizes for any minute, then numerically follow the accumulation of DNA during infection. The rate constants used for this simulation were: $r = 0.046$ fractional lengths/min (Bodnar and Pearson, 1980a; Part I); $r_I = 0.068$ fractional genome/min, $r_{II} = 0.026$ fractional genome/min, $i = V_{max}/2(K_m + [DS])$ where $V_{max} = 186,000$ genome/cell-hr, $K_m = 120,000$ genome/cell and $[DS] = 2000$ genome/cell at 11 hours post infection, and $i_s = 0.3$ initiations/molecule-min (Bodnar and Pearson 1980b; Part II). With appropriate corrections for the relative radioactivity per molecule for each replicating form due to differences in molecular weight and differing fractions of each molecule that is single stranded (as derived in the Theory), expected results for measurements of biophysical data can be calculated for any time after infection. Results of these calculations are shown in

Table 1 and compared with experimental determinations of equivalent data cited in the literature.

Measurement of the Fraction of Ad DNA that is Replicating and Fraction of DNA that is Single Stranded over Infection

Simulation of adenovirus DNA growth curves indicated that many characteristics of the DNA would change during the course of an infection. For example, since the initiation rate shows saturable kinetics (Bodnar and Pearson 1980b; Part II), one would expect the total number of replicating molecules to reach a maximum number at about 18 hours after infection and remain relatively constant afterwards. However, the total amount of DNA would continue to accumulate causing the percent of the DNA actively replicating to decrease over infection. Similarly, since the replicating molecules are partially single stranded, the fraction of DNA that is sensitive to single strand specific endonucleases such as S1 should also decrease during infection. Calculated curves for the percent of DNA replicating and percent of DNA that is S1 sensitive (as shown in Figure 1) indicated that changes in these parameters might be measurable.

Cells were prelabeled with [^{3}H]thymidine for a recovery marker for 24 hours, infected with Ad2 or Ad5, then labeled with ^{32}P starting at 11 hours post infection as previously described (Bodnar

Table 1. Computer simulation of biophysical data for adenovirus DNA replication.

Measurement	Hr.p.i.	Calculated	Experiment	Reference
Percent replicating DNA	17 hr	42	39	Kedinger et al, 1978
Percent ss DNA of total DNA	15 hr	14	19-24	Lavelle et al, 1975
Percent ss DNA of replicating DNA	14 hr	30	21-29	Pettersson, 1973
	15 hr	30	18-24	Tolun and Pettersson, 1975
Percent unit length ss DNA	17 hr	3	4	Kedinger et al, 1978

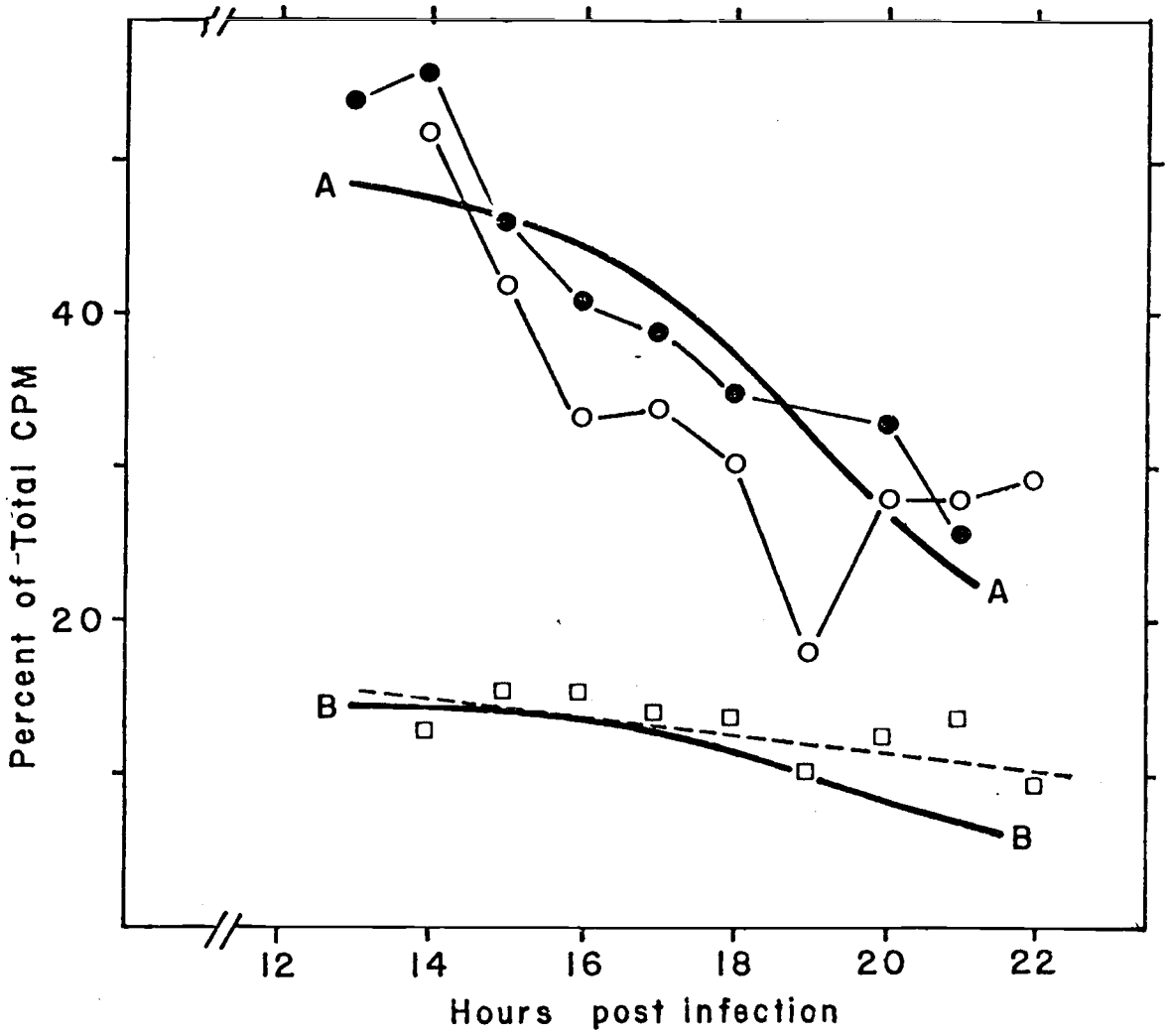

Figure 1. Comparison of calculated and experimental determinations of percent of activity in replicating and single stranded Ad DNA as a function of time post infection. Adenovirus DNA was labeled with ^{32}P from 11 hr post infection, isolated as described in the text, and separated by BD-cellulose column chromatography. The percent of activity associated with partially single stranded (replicating) molecules is shown for Ad2 (●) and Ad5 (○). The calculated curve derived from previously measured rate constants (Part I and II) for percent of activity in replicating molecules is curve A. Total Ad5 DNA labeled with ^{32}P was digested with S1 endonuclease as described in the text. The fraction S1 sensitive at times after infection is plotted (□) with a least squares fit of the data (- - - -). The calculated S1 sensitivity is shown as curve B.

and Pearson, 1980b; Part II). Aliquots were drawn hourly and fixed with NaCN (final concentration 0.01 M), digested with Pronase, total intracellular DNA phenol extracted, then treated with RNase. With this labeling procedure more than 90 percent of the ^{32}P TCA-precipitable activity is associated with adenovirus DNA (see Part II), so DNA was vortexed for 15 seconds to reduce viscosity, applied directly to BD-cellulose columns, and eluted as described before (Robinson, et al, 1979). The percent of ^{32}P activity associated with replicating molecules in the 1 M NaCl plus 2% caffeine wash compared with the total ^{32}P activity eluted in both the 1 M NaCl and 1 M NaCl plus 2% caffeine washes was calculated as shown in Figure 1. Other aliquots (50 μl) were digested with Hae III restriction endonuclease to reduce viscosity using conditions described before (Robinson et al, 1979). Samples were diluted to 200 μl, adjusted to 30 mM NaCl, 30 mM Na citrate (pH 4.5), and 10 mM $ZnSO_4$, and digested 15 minutes with 1 unit of S1 endonuclease. The samples were then precipitated with 2.5 ml 5 percent TCA, filtered, and counted. The percent of aliquots that was S1 sensitive was determined by comparison to equivalent samples treated identically without addition of S1. Controls were aliquots of the infected cells removed one minute after the ^{32}P addition (11 hours) with ^{32}P Ad2 virion added. Under conditions described above less than one percent of the intact virion DNA was digested, and if the control was heated in boiling

water for ten minutes prior to S1 treatment, 95 percent of the virion DNA was digested without Hae III treatment and 75 percent was digested with Hae III treatment (probably due to reannealing of the small fragments during S1 digestion). An average of three such experiments is shown in Figure 1. While there is considerable data scatter in this technique, the least squares fit of the data shows a decreasing trend in S1 sensitivity as predicted by calculations.

Pulse and Chase Experiment Simulation

Pulse and chase experiments have been reported to investigate the precursor product relationship between replicating and mature adenovirus DNA (Pearson, 1975; van der Eb, 1973). Infected cells were labeled with [^{3}H]thymidine then chased with unlabeled thymidine, and the kinetics of ^{3}H label in replicating and mature DNA was followed. We simulated these experiments to investigate if the rate parameters previously determined (Part II) could explain the rate of chase of label from replicating to mature DNA and the inability to completely chase the ^{3}H label from the replicating pool.

These experiments were simulated using an iterative method similar to that described in Part II. The adenovirus DNA was divided into pools of mature DNA, single stranded DNA, $(1/r_I)$ pools of type I molecules, and $(1/r_{II})$ pools of type II molecules as before. The

number of molecules in each pool was calculated as before (Part II). The total [^{3}H]thymidine pulse incorporated in each pool was calculated as in Figure 2. During one minute of replication of one molecule it was assumed that x CPM ^{3}H were incorporated. Therefore, each pool of replicating molecules will have CPM equivalent to x times the number of molecules in the previous pool due to incorporation during that minute. Note that since there is no activity incorporated in displaced single strands that all the activity from a completed type I molecule will go into mature DNA. To account for CPM in replicating molecules due to reinitiation it was assumed that a fraction of the total ^{3}H in mature and single stranded DNA equal to their respective initiation rates would enter the replicating pools each minute. Then the incorporation of [^{3}H] thymidine and movement of ^{3}H labeled DNA was simulated by following the flow from one pool to the next each minute. A pulse was simulated by letting x equal a constant and a chase was accomplished by setting x equal to zero.

Using this technique and the rate parameters listed above, we modeled pulse and chase experiments for times after infection where little segregation of replicating molecules is seen. Figure 3 shows a comparison of a simulated pulse and chase compared with experimental data (Pearson, 1975). This plot shows graphically why pulse labels are difficult to chase into mature DNA for adenovirus.

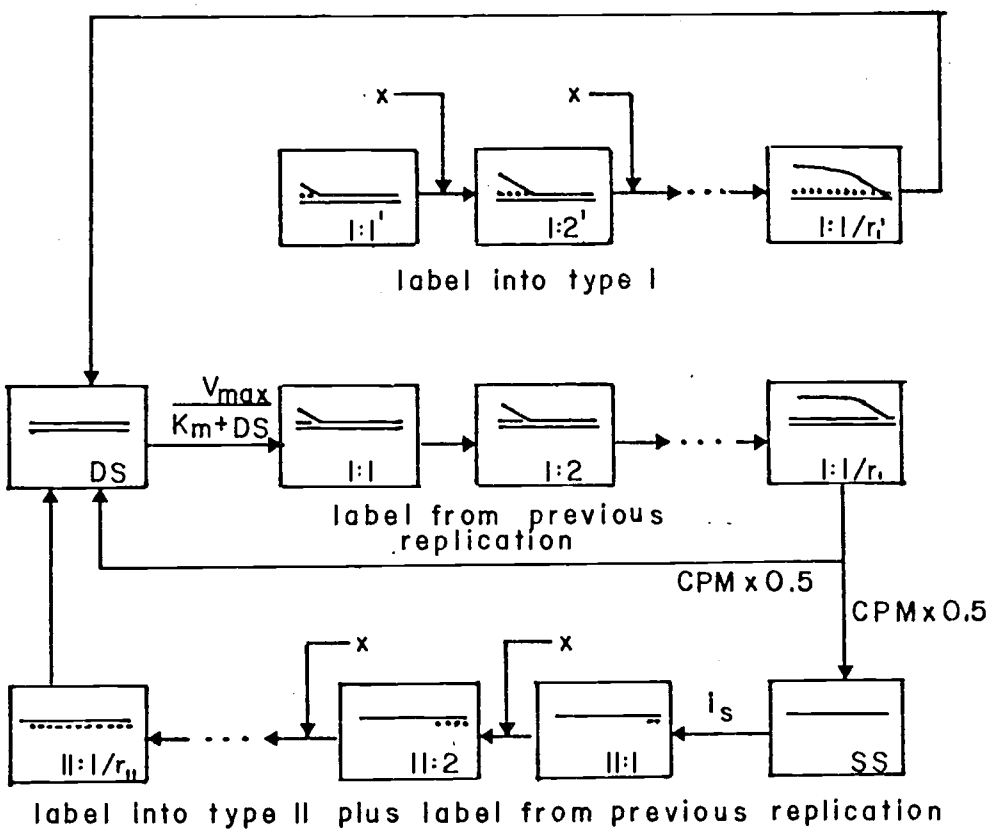

Figure 2. Method for simulation of pulse and chase experiments. Numbers of DNA molecules were calculated as in Part II, Theory. CPM in each pool were calculated for each minute using the change in CPM each minute as indicated, then calculating the changes in pool sizes for the next minute, etc. The CPM added to a replicating molecule in one minute is x. For a pulse x = constant; for a chase x = 0.

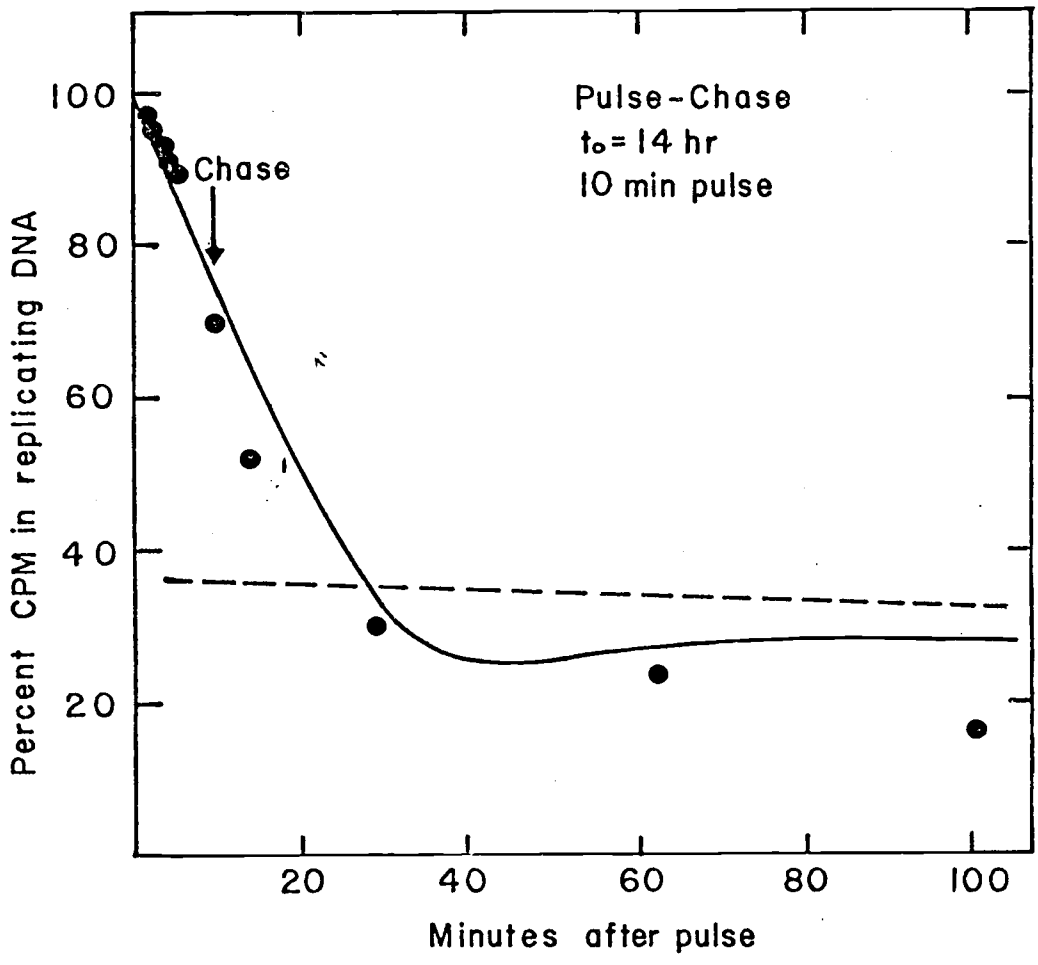

Figure 3. Simulation of pulse and chase experiment compared with data from Pearson, 1975 (●). Ad2 infected cells were pulsed with [^{3}H]thymidine for 10 minutes at 14 hours post infection, then chased with cold thymidine. Ad2 DNA was isolated and separated on CsCl/EtBr equilibrium gradients. Data were simulated as shown in Figure 2, with rate parameters as listed in the text: [^{3}H]thymidine pulse label (——); steady state value for percent of Ad2 DNA molecules replicating (- - - -).

There are two factors which affect that fraction of a pulse which remains in replicating DNA during a chase: 1) the time to complete a replicating molecule and 2) the re-entry of labeled molecules into the replicating pool. At the beginning of the chase the fraction of activity in replicating DNA drops rapidly as the label is chased into mature DNA by completion of the replicating molecules. This effect is complete in one replication time (22 minutes for adenovirus). The fraction will then rise toward a steady-state value as these labeled molecules reinitiate rounds of replication. Although the reinitiation rate for adenovirus is relatively slow at 14 hours post infection, it is still large enough that the fraction of activity in replicating molecules remains sizable throughout the chase. One would expect to chase the pulse from replicating molecules only as they are segregated into portions that replicate preferentially late in infection, and the labeled molecules enter the non-replicating portion. The other reported pulse and chase experiment (van der Eb, 1973) pulsed with [^{3}H]thymidine for 3 minutes at 14 hours post infection and chased for 60 minutes with unlabeled thymidine. At this time 20 to 25 percent of the activity was seen in replicating DNA; the calculated value for this experiment is 29 percent.

Calculation of the Average Number of Growing Points per Replicating Molecule

Adenovirus molecules completed during a short pulse of [^{3}H]-thymidine contain gradients of label decreasing from both molecular ends towards the center of the genome (Schilling, Weingartner and Winnacker, 1975; Tolun and Pettersson, 1975; Horwitz, 1976; Bourgaux, Delbecchi and Bourgaux-Ramoisy, 1976; Ariga and Shimojo, 1977). The label is asymmetrically located at the 3', but not 5', end of each strand (Weingartner et al., 1976; Sussenbach and Kuijk, 1977). Conversely, a short pulse of [^{3}H]thymidine preferentially labels newly initiated replicating molecules at the 5' end of each strand (B. Weingartner, T. Reiter and E. L. Winnacker, personal communication). Taking these patterns of labeling into account, we derived in detail equations describing the theoretical accumulation of label into completed and replicating molecules (see Part I). We also derive a relation (equation 12) between the average number of growing points per replicating molecule, n, and the fraction of radioactivity retained on filters after pulse-labeled replicating molecules are cleaved by a restriction endonuclease.

We propose that terminal protein molecules are linked to the 5' ends of all parental and daughter strands in type I and type II structures as diagrammed in Figure 4. Figure 4A shows that any

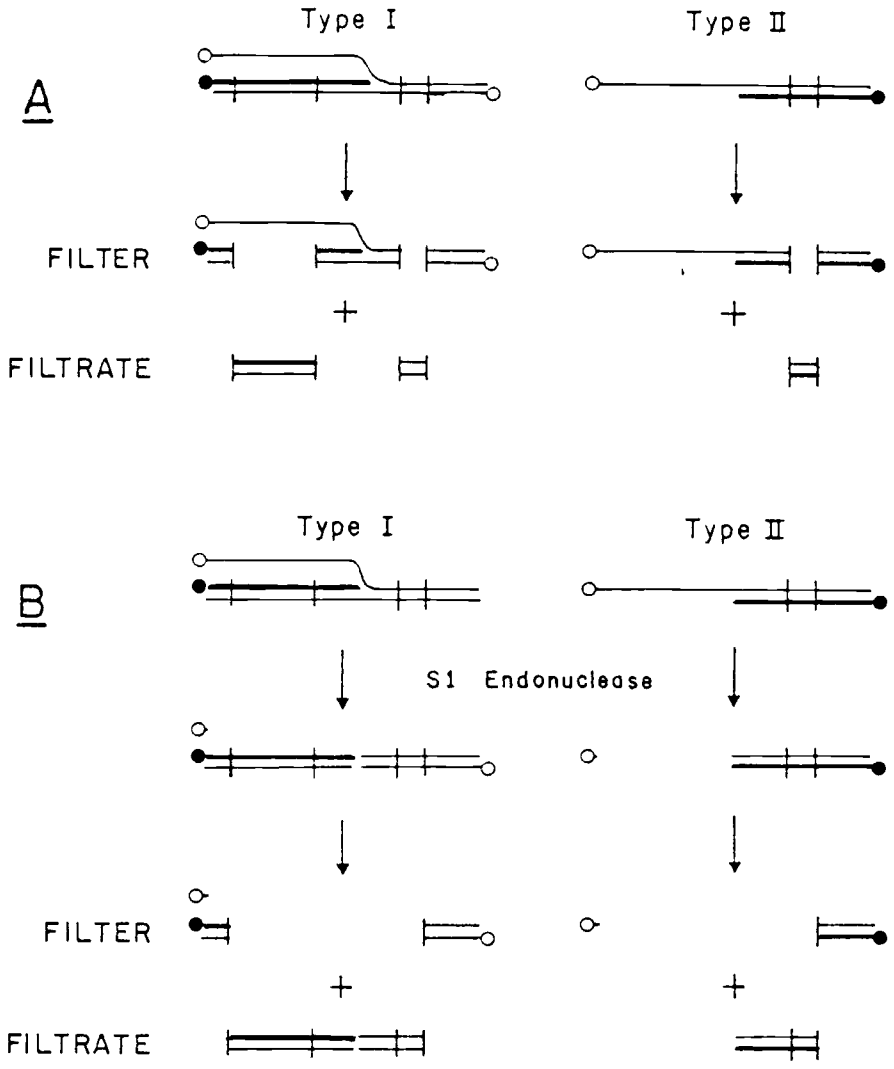

Figure 4. Diagramatic representation of replicating adenovirus DNA molecules containing terminal protein. The designations type I and type II for replicating molecules have been proposed by Lechner and Kelly (1977). Parental strands and newly replicated strands (i.e., radioactively labeled strands) are represented by thin and thick lines, respectively. Parental and new terminal protein molecules are indicated by open and closed circles, respectively. Vertical bars show sites cleaved by a restriction endonuclease. Since adenovirus replication is symmetrical with respect to the molecular ends, type I molecules replicating leftward and type II molecules replicating rightward are also possible (not shown). (A) After cleavage with a restriction endonuclease, only terminal fragments and internal fragments containing growing points are retained by filters. Internal fragments lacking growing points remain in the filtrate. (B) After cleavage with a restriction endonuclease plus digestion with S1 endonuclease, only terminal fragments bind to filters. All internal fragments remain in the filtrate.

internal restriction endonuclease fragment containing a growing point (either type I or type II) will be retained on GFC filters by the filter binding assay (Coombs, et al., 1979). Internal fragments lacking growing points will not be retained. Terminal fragments will always be retained regardless of the presence of growing points. After further digestion with the single strand specific Sl endonuclease, illustrated in Figure 4B, only the terminal fragments will bind to filters.

We can therefore estimate the average number of growing points on one replicating adenovirus genome by using equation (12) above and measuring the fraction of counts bound to a GFC filter of replicating Ad2 DNA. This experiment was described in detail previously (Robinson, et al., 1979). Briefly, Ad2 infected cells were pulsed with [^{3}H]thymidine at 17 hours post infection, harvested, and adenovirus chromatin extracted from nuclei by using ammonium sulfate (Wilhelm, et al., 1976, Robinson, et al., 1979). Replicating molecules were purified by glycerol gradient velocity centrifugation and Sepharose 2BCl column chromatography. The purified replicating molecules with terminal proteins still attached were then cut with Sma I, Hsu I, or Hpa I restriction enzymes or with one of these enzymes plus Sl endonuclease, and the fragments were assayed for binding to GFC filters under conditions where the terminal protein is retained but not the DNA.

In Figure 5 we plot the theoretical percent of radioactivity bound after cleavage with SmaI, Hsu I, or Hpa I endonucleases calculated in each case for n = 1.0, 1.5, and 2.0 growing points per molecule. The open circles indicate the measured values for each enzyme. The calculated values of n corresponding to each observed percent binding were: n = 1.75, 1.4, and 1.6 respectively for Sma I, Hsu I, and Hpa I or an average of 1.6 ± 0.2 growing points per molecule. By comparison, direct electron microscopic measurements give n = 1.25 growing points per replicating molecule (Lechner and Kelly, 1977). In Figure 5 we also plot the theoretical percent of radioactivity bound, calculated from equation (13), after cleavage with each restriction enzyme followed by digestion with Sl endonuclease. The open squares indicate the measured values which, except for Hpa I, agree closely with the theoretical calculations. We believe the higher binding in the case of Hpa I is due to partial digestion fragments.

It is clear that values for binding calculated from equation (12) depend primarily on the number and sizes of internal restriction endonuclease fragments whereas values calculated from equation (13) depend only on the sizes of terminal fragments. The calculated and observed values of binding after cleaving replicating molecules with Hsu I (11 restriction sites) or Sma I (12 sites) endonucleases did not differ markedly. But after further treatment with Sl endonuclease,

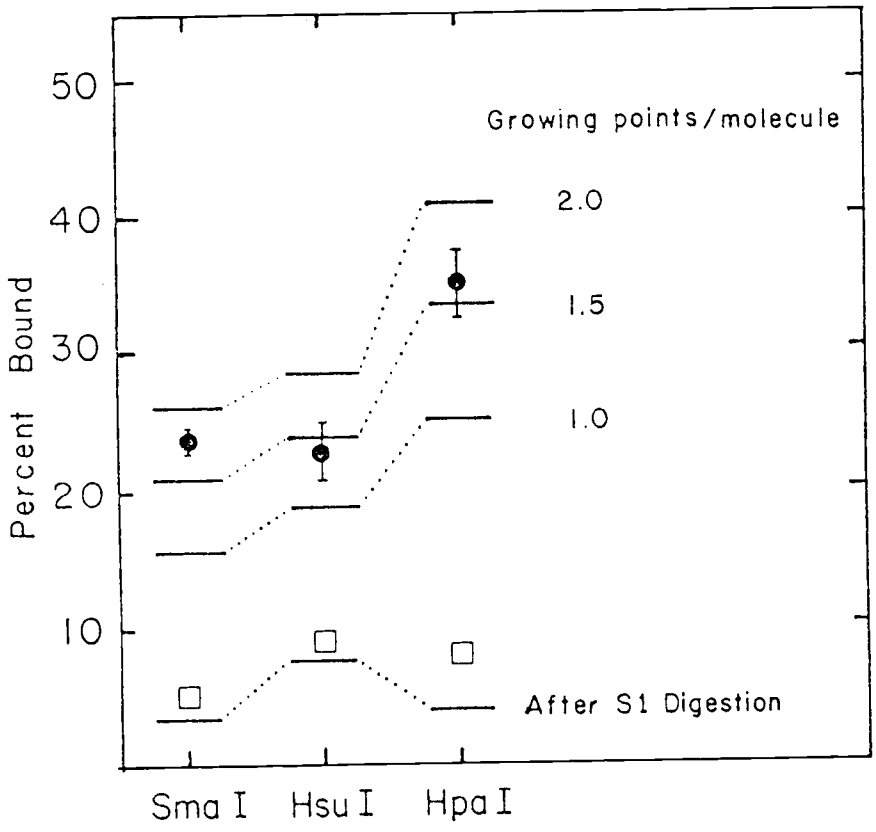

Figure 5. Determination of the number of growing points in replicating adenovirus DNA molecules. [^{3}H]DNA protein complex was purified as described previously (Robinson et al, 1979) cleaved with the indicated restriction endonuclease, and analyzed by the filter binding assay. The circles (●) indicate the average percent of radioactivity bound to filters after cleavage with each endonuclease: 23.7 ± 0.8, 22.9 ± 2.1, and 35.2 ± 2.4 for three independent measurements each with SmaI, HsuI, and HpaI respectively. The vertical bars represent the standard errors of the means in each case. The number of growing points per molecule were calculated with t = 10 min and r = 0.062 fraction lengths/min using equation (12) derived in Theory: 1.75, 1.4, and 1.6 respectively for SmaI, HsuI, and HpaI or an average of 1.6 ± 0.2 growing points per molecule. The horizontal bars correspond to the percent of radioactivity bound to filters after cleavage with each endonuclease calculated for 1.0, 1.5, and 2.0 growing points per molecule also with equation (12). The squares (□) indicate the average percent of radioactivity bound to filters after cleavage with the indicated restriction endonuclease plus digestion with S1 endonuclease: 5.1 ± 0.3, 9.0 ± 0.1, and 8.3 ± 0.2 respectively for SmaI, HsuI, and HpaI. The error limits are covered by each square. The horizontal bars labeled "after S1 endonuclease" represent the percent of radioactivity bound to filters calculated by equation (13).

the calculated and observed values for Hsu I were roughly twice as high as those for Sma I, in proportion to the sizes of terminal fragments. On the other hand, the calculated and observed values for binding after cleavage with Hpa I endonuclease (6 sites) were approximately 50% higher than those for Hsu I or Sma I.

Mathematical Model for Determination of Rate Constants for Adenovirus DNA Replication with Reinitiation Considered

We have previously developed a model to allow expression of concentrations of various adenovirus DNA pools as a function of the rate constants for replication (Bodnar and Pearson, 1980b; Part II). Without considering reinitiations of replicating molecules we derived relationships which relate the concentrations of the various replicating pools, and using the EM data of Lechner and Kelly (1977) we estimated that: $r_I = 2.0\ r_{II}$; $r_{II} = 4.4i$; $i_s > 48\ i$.

We desired to see if these relationships were valid considering reinitiation of replicating molecules prior to completion of a round of replication. Using the same assumptions as before we modeled the kinetics of DNA replication for all replicating forms up to those with three single-stranded branches as shown in Figure 6. The kinetic equations were derived as shown in matrix form in Figure 7. Since this matrix is too unwieldy to solve exactly, we assumed a steady state in all replicating intermediates as before

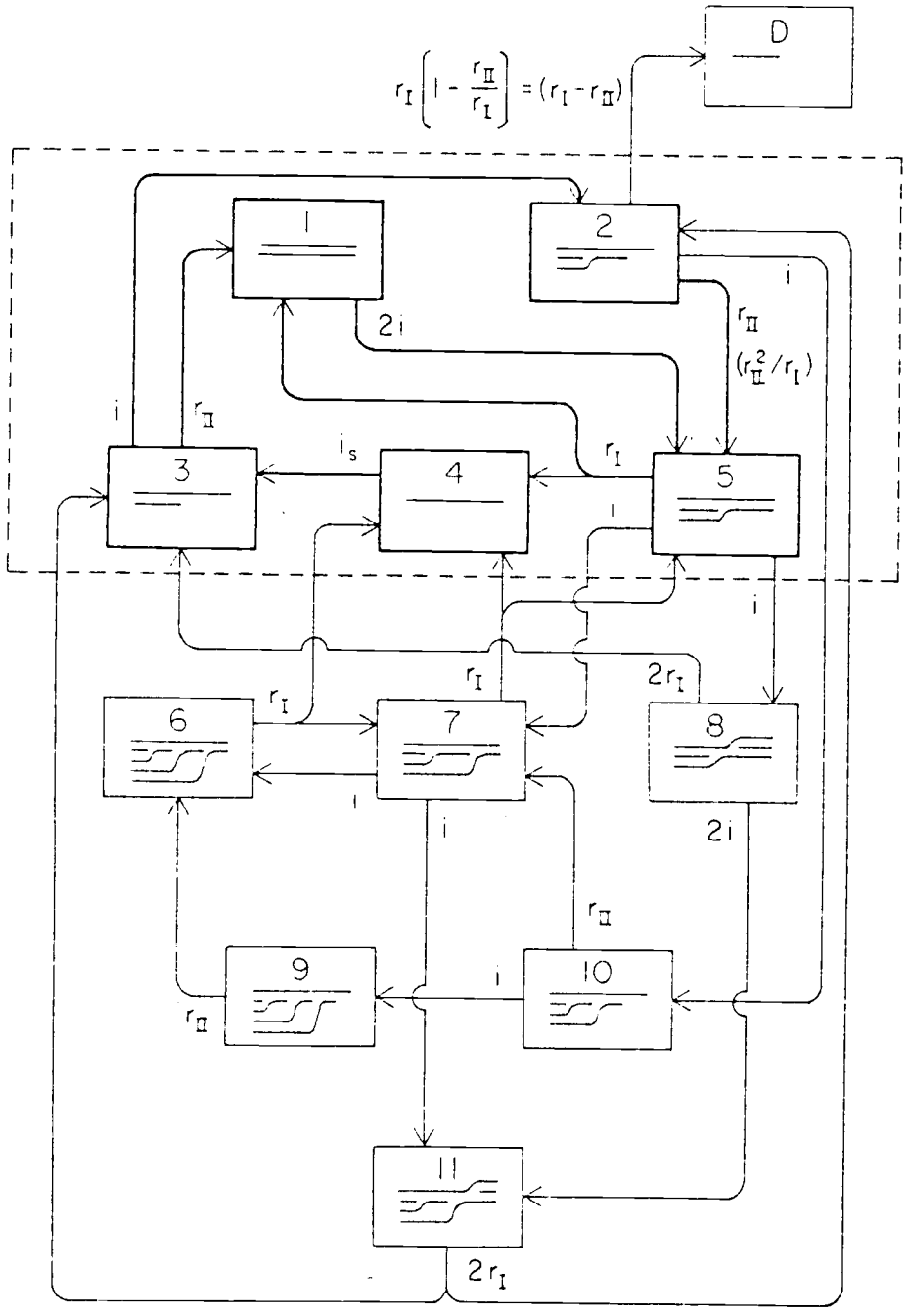

Figure 6. Model of adenovirus DNA replication. 1 = Double stranded mature molecule. 2 = Type I/II molecule with one branch. 3 = Type II molecule. 4 = Unit length single strand. 5 = Type I molecule with one branch. 6 = Type I molecule with three branches moving in the same direction. 7 = Type I molecule with two branches moving in the same direction. 8 = Type I molecule with two branches moving in opposite directions. 9 = Type I/II molecules with three branches. 10 = Type I/II molecule with two branches. 11 = Type I molecule with two branches moving in the same direction and one branch moving in the opposite direction. D = Defective single strands (shorter than unit length). r_I = rate of replication on a type I molecule. r_{II} = Rate of replication on a type II molecule. i = Rate of initiation on double stranded molecules. i_s = Rate of initiation on single stranded molecules. Lechner and Kelly (1977) first classified replicating adenovirus molecules as type I, type II, or type I/II molecules.

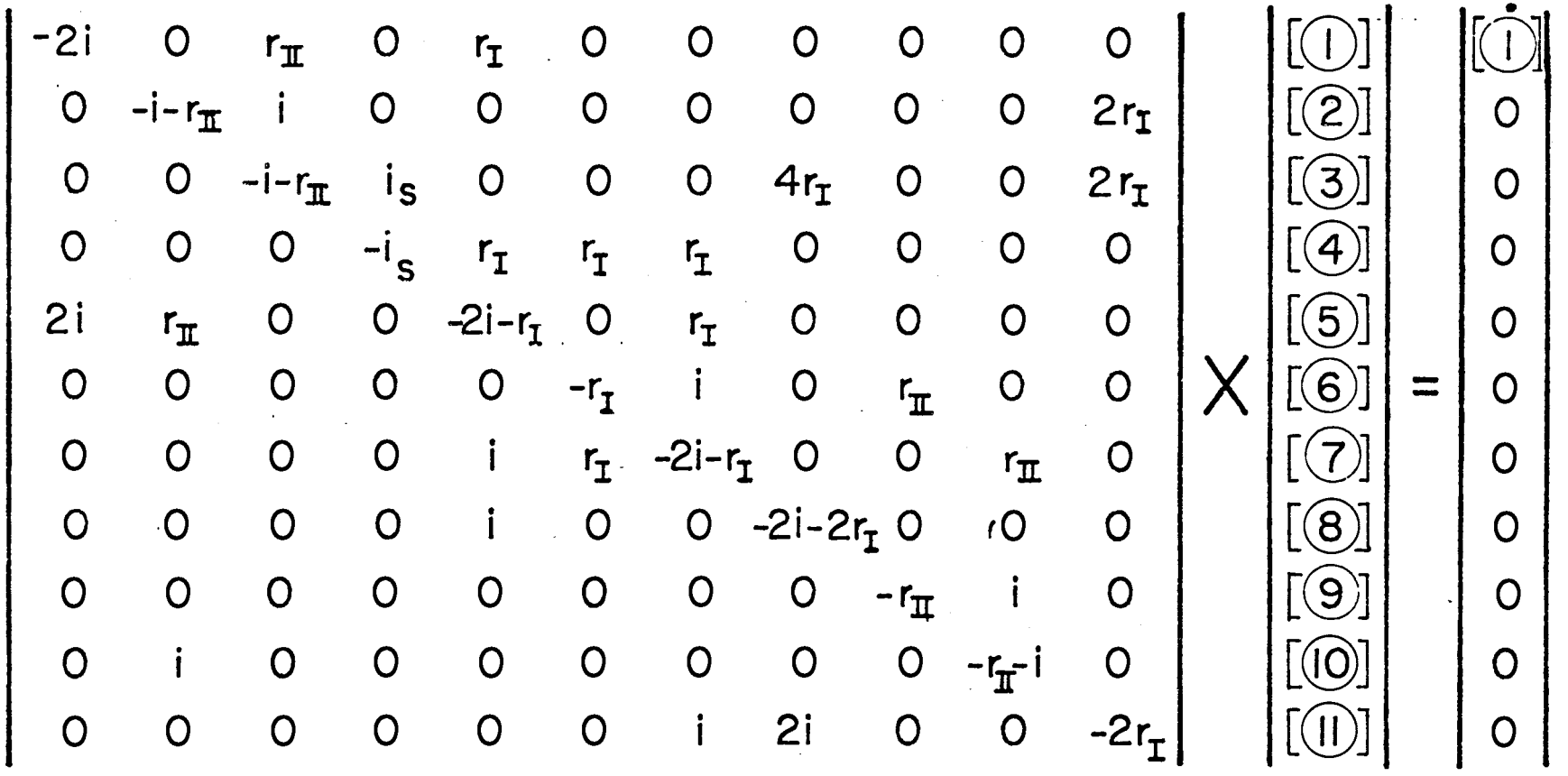

Figure 7. Rate equations for the replication scheme of Lechner and Kelly, (1977) as diagrammed in Figure 6. The equations are summarized in matrix form, the steady state approximation made for all replicating intermediates, and the rate of change of mature DNA (pool 1) is assumed constant. The data of Lechner and Kelly can then be fit by numerical solution of the matrix using the pivot method (Cullen, 1967) on the HP 9821A calculator.

and assumed that the rate of mature DNA accumulation is constant. These assumptions are valid since we have shown (Part II) that after 17 hours the size of the pool of replicating DNA is constant and DNA concentration increases linearly. These assumptions reduced the matrix to eleven linear equations in eleven unknowns. This was then solved numerically on the HP 9821A calculator by taking the relationships for the simplified model as above and obtaining a trial and error fit of the data by varying the rate constants in the solution of the larger matrix. The best fit of the Lechner and Kelly data was obtained with the relationships: $r_I = 1.67\ r_{II}$; $r_{II} = 5.6\ i$; $i_s > 21\ i$. The calculated pool sizes for these rate constants are shown in Table 2 along with the experimental values.

We can see the consistency of the calculated parameters in two ways. First, we see that the values obtained with and without reinitiations considered are almost the same. This is what we had expected since the molecule types we neglected in the simpler model account for less than ten percent of the total replicating forms. Therefore, the rate parameters derived by this method are also consistent with the biochemical data, and the conclusions reached in Part II apply. Secondly we can examine the relative predicted pool sizes calculated by this method. We used the <u>total</u> number of molecules of each type in the trial and error fit of the data, but in addition the ratios of the numbers of molecules of the same type with 1, 2, or 3

Table 2. Comparison of calculated with experimental results for data of Lechner and Kelly (1977). Replicating Ad2 DNA was spread on EM grids and the relative numbers of the various replicating forms were counted. The best fit of the data was obtained by trial and error fit of the matrix solutions (Figure 7) with the replicating forms as in Figure 6. The starred items were used in the fit; the other pool sizes are calculated using: $r_I = 1.67\, r_{II}$, $r_{II} = 5.6\, i$, and $i_s > 21\, i$.

Molecule Type	Lechner & Kelly Results	Calculated
Type 1		
Total	55	56*
1 ss DNA branch	41	47
2 ss DNA branches	11	8
>2 ss DNA branches	3	1
Type II		
Total	89	90*
Type I/II		
Total	20	18*
1 ss DNA branch	18	15.5
2 ss DNA branches	1	2
>2 ss DNA branches	1	0.5
Full Length SS DNA	<10	10*

branches are consistent with the experimental results. Physically this means that the system follows the assumption that any double stranded end in the replicating pool (regardless of whether that molecule is replicating or not) has the same probability of initiating another round of replication.

Also, we modeled the replication scheme with and without a pathway for generation of defective adenovirus DNA using the mechanism described in Part II. (The scheme with defectives is shown in Figure 6, and the scheme without defectives is listed in Figure 7). The numbers of defective DNA molecules calculated were consistent with the simple model presented in Part II, and the pool sizes for the other pools were essentially unchanged with the addition of a pathway to lead to defective DNA.

DISCUSSION

A large quantity of experimental data on DNA replication of adenovirus has been gathered in recent years. While the strand displacement mechanism of replication has been well supported, interpretations of results of individual experiments have often been unclear. In an effort to unravel one mechanism consistent quantitatively as well as qualitatively for all data we have modeled the strand displacement mechanism (Lechner and Kelly, 1977), estimated the rate constants for all component steps, and have compared the results that would be expected for computer simulations with those seen experimentally. In all cases modeled the results were consistent with the model calculations based on the strand displacement mechanism and rate constants measured previously (Bodnar and Pearson, 1980a and 1980b; Parts I and II). Simulations of biophysical determinations have shown that the model and rate parameters can predict the changes in characteristics of the adenovirus DNA pools over the course of an infection and that even though the initiation rate seems very low, it is still sufficiently large to prevent chasing of a [^{3}H]thymidine pulse from replicating to mature DNA, and it is also large enough to account for the number of multiply forked replicating intermediates.

In addition to the experiments discussed in detail above we also modeled data from several other experiments. For example, measurement of incorporation of a [^{3}H]thymidine pulse into Ad2$^+$ND$_I$ SV40-adenovirus hybrid virus has been reported using a labeling scheme similar to that described in Part I for total relative activity in mature adenovirus DNA during a pulse (Horwitz, 1974). We modeled the total relative incorporation curves for the SV40 and adenovirus portions of the hybrid genome as a function of pulse time and found that the shapes are consistent with a 17 minute replication time (data not shown). Temperature shift experiments using Ad5 temperature sensitive mutant ts125 were also investigated (Sussenbach and Kuijk, 1978). This mutant is defective in DNA replication and will complete rounds of replication but not start new rounds of replication after a shift to the nonpermissive temperature. Therefore, following a shift up then a shift down in temperature the DNA molecules are aligned to begin rounds of replication upon downshift. By slight modifications to our model for pulse incorporation in Part I we derived that following such a downshift a) the curve for total ^{3}H incorporation into DNA will be parabolic for one replication time then become linear, b) the percent of ^{3}H activity in replicating molecules will remain at 100 percent for one replication time then c) drop linearly to 50 percent in a second replication time. The experimental data showed the expected shapes, but since the

downshift was to 32°, the values for replication time were a) 60 minutes, b) 50 minutes, and c) 55 minutes, indicating that the rate of replication is slowed by a factor of about 2.5 by the drop of 5 degrees in temperature (data not shown).

In our systematic search of the adenovirus DNA replication literature, we found only two kinds of kinetic experiments that we could not model adequately. The first type included experiments where DNA replication was blocked with hydroxyurea then released and the kinetic parameters of the DNA measured (Sussenbach, et al., 1973; Ellens, et al., 1974; Vlak, et al., 1975; Sussenbach and van der Vliet, 1973). However, since the effect of hydroxyurea in addition to depleting deoxynucleotide pools is to induce breaks in DNA template strands (Walker, et al., 1977) we realized that we could not adequately determine the state of the DNA at the time of unblocking and therefore any modeling of these experiments would have little relevance to the actual condition of the DNA. Also, experiments where the pulse labeling of replicating Ad2 DNA was investigated were difficult to interpret (Bourgaux, et al., 1976). In this case replicating Ad2 DNA was pulsed with [^{3}H]thymidine, isolated, cut with a restriction enzyme and S1 endonuclease, and analyzed on agarose gels. Here we noted that since the replicating molecules have growing points randomly distributed along the genome, treatment with restriction enzymes will give (in addition to the normal

fragments) fragments with single stranded tails of random lengths. Further treatment with S1 will definitely give many fragments of random length for type II molecules and will probably cut the type I molecules at the nick at the growing point generating more random length fragments. (This was our protocol for the forks per molecule determination where the randomness of the fragment size was immaterial; see Figure 4 above.) However, when these fragments were sized on a gel, the numbers of random fragments would tend to obscure any interpretation of the results. We did learn, however, that cutting and sizing of replicating molecules may give rise to many artifacts due to the nature of the structures of those forms, and any such experiment must be very carefully designed. Thus, in every case where modeling of experiments with our measured kinetic parameters was possible, the simulations were either in agreement with the experimental data or the experimental design made any quantitative interpretation of the results impossible.

We believe the most convincing argument for the use of kinetic techniques to study viral DNA replication is the ability to relate many diverse characteristics of the replication mechanism. It is not so impressive to estimate a particular rate constant from a particular experiment, but when a single mechanism with a single set of rate constants can adequately model so many types of experiments, it shows the power of the kinetic approach to studying

mechanism. In this section we have taken rate parameters determined by measuring the specific activity of pulse labeled restriction fragments, counting molecules spread on an EM grid, and following the rate of density shift of BUdR labeled DNA, and we have used these to predict the characteristics of physical parameters as they vary throughout infection and the results of pulse-chase experiments. The close agreement of the predictions to the results in vivo certainly shows how kinetics can help in understanding such a dynamic system.

THE KINETICS OF ADENOVIRUS DNA REPLICATION: IV

Adenovirus Type 7 Kinetics

ABSTRACT

The kinetic techniques previously developed (Part I and II) were applied to adenovirus type 7 growth to investigate which parameters are controlled by the cell and which by the virus. Pulse labeling of restriction fragments showed that the replication time for Ad7 is 20 minutes. Growth curves and density labeling experiments revealed that the initiation rate for Ad7 is comparable to Ad2 and Ad5, decreases over infection, andexhibits saturable kinetics with similar V_{max} and K_m.

INTRODUCTION

We have previously described methods to measure the kinetic parameters for DNA replication of adenovirus types 2 and 5 (Parts I and II, Bodnar and Pearson, 1980a and 1980b). We have seen that the replication rate is comparable to that of uninfected HeLa cells, and that when the infecting virus saturates the replication machinery, the number of replication sites per cell is the same as that measured for HeLa cell DNA replication. This suggests that the kinetic parameters of adenovirus DNA replication are mediated by cellular factors required for both chain elongation and initiation of replication. To investigate this hypothesis further we wished to see if the kinetic constants would vary if the virus serotype and/or host cell type were changed.

The system used was the same HeLa host with adenovirus type 7. Adenovirus type 7 (Ad7) is a weakly oncogenic virus of Subgroup B. While heteroduplex mapping indicates that Ad2 and Ad5 are 85 percent homologous, Ad2 and Ad7 are only 10 percent homologous (Philipson et al, 1975). Also, Ad 2 and Ad5 produce about 5 to 10 percent of their virions containing defective DNA that is shorter than genome length (Burlingham, et al, 1974; Rosenwirth et al, 1974), while Ad7 produces 25 to 30 percent defective virions and intracellular DNA (Daniell, 1976; Daniell and Mullenbach, 1978).

Since we have postulated that the amount of defective adenovirus DNA made during an infection depends on the ratios of the rate parameters (Part II). we chose Ad7 to investigate this possibility as well as the question of cell or virus mediation of the rate constants.

Using the same methods as before we found that replication rate, initiation rate, V_{max}, K_m, and saturable kinetics of viral DNA replication are approximately the same for adenovirus type 2, 5, and 7.

RESULTS

Measurement of Replication Rate

The replication rate of Ad7 was measured with the method of pulse labeling of restriction fragments previously described (Part I, Bodnar and Pearson, 1980a). To reiterate, 2×10^8 HeLa cells were infected with Ad7, treated with 10^{-6} M FUdR for 30 min, the FUdR washed out and [^{3}H] thymidine added at 18 hours post infection. Cells were removed into KCN at 6 and 12 minutes after the pulse, nuclei made, and adenovirus chromatin extracted with ammonium sulfate (Part I, Robinson et al, 1979). The DNA was purified by RNAse then Pronase treatment, phenol extraction, and BD-cellulose column chromatography after mixing with ^{32}P labeled Ad7 virions. The mature DNA was ethanol precipitated, cut with restriction enzyme Hind III, and the fragments separated on one percent agarose gels. The relative specific activities were then used to determine the replication rate as described above (Part I).

The restriction pattern seen for Hind III was not that reported in the literature (Tibbetts, 1977b; Sekikawa and Fujinaga, 1977) for Ad7. However, we became aware of differences in Ad7 strains (Wadell and Varsanyi, 1978). Comparison of the restriction patterns for our strain with those of Wadell and Varsanyi using Eco RI, HpaI,

SmaI, Hind III, and Bam HI showed that our virus was Ad7 strain S-1058 (designated Ad7a).

The pattern of specific activities gave a best fit for calculated curves where r = 0.05 fractional lengths per minute or a 20 minute replication time as shown in Figure 1.

Measurement of Initiation Rate by Ad7 Growth Curves

To investigate the dependence of initiation rates on viral serotype we measured the initiation rate of Ad2 and Ad7 using the DNA accumulation curve method previously described (Part II, Bodnar and Pearson, 1980b). Briefly, HeLa cells prelabeled with [^{3}H] thymidine for 26 hours were split and parallel cultures were infected with Ad2 and Ad7. At 10 hours post infection ^{32}P (4 μCi/ml) was added, and starting at 12 hours post infection 10^{7} cells were removed each hour until 22 hours and fixed in 0.01 M KCN. Total intracellular DNA was prepared by Pronase treatment, phenol extraction, RNase treatment, and CsCl gradient equilibrium centrifugation. Specific activities of HeLa DNA (^{3}H) and adenovirus DNA (^{32}P, from an ammonium sulfate extracted sample at 21 hours post infection) were determined as described in Part II. Using ^{32}P/^{3}H ratios, specific activities, and DNA molecular weights, we determined the Ad2 and Ad7 growth curves in terms of adenovirus genomes per infected cell as shown in Figure 2. Slopes of these

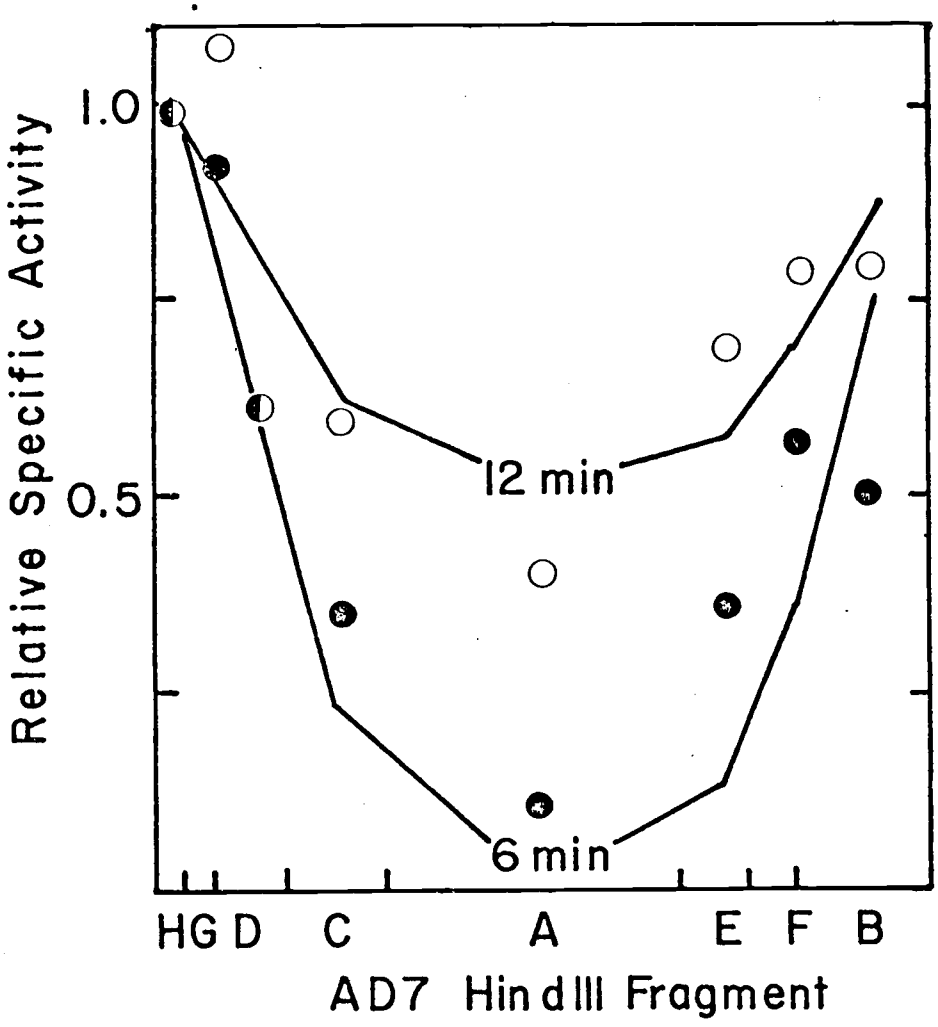

Figure 1. Replication rate of Ad7 determined by comparison of pulse labeled restriction fragment specific activities with calculated curves. Ad7 DNA pulse labeled with [^{3}H]thymidine for 6 (●) or 12 minutes (O) was mixed with ^{32}P labeled Ad7 virions, extracted and purified as previously described, cut with Hind III and the fragments separated on agarose gels. Theoretical curves are shown for r = 0.05 min^{-1} or a replication time of 20 minutes.

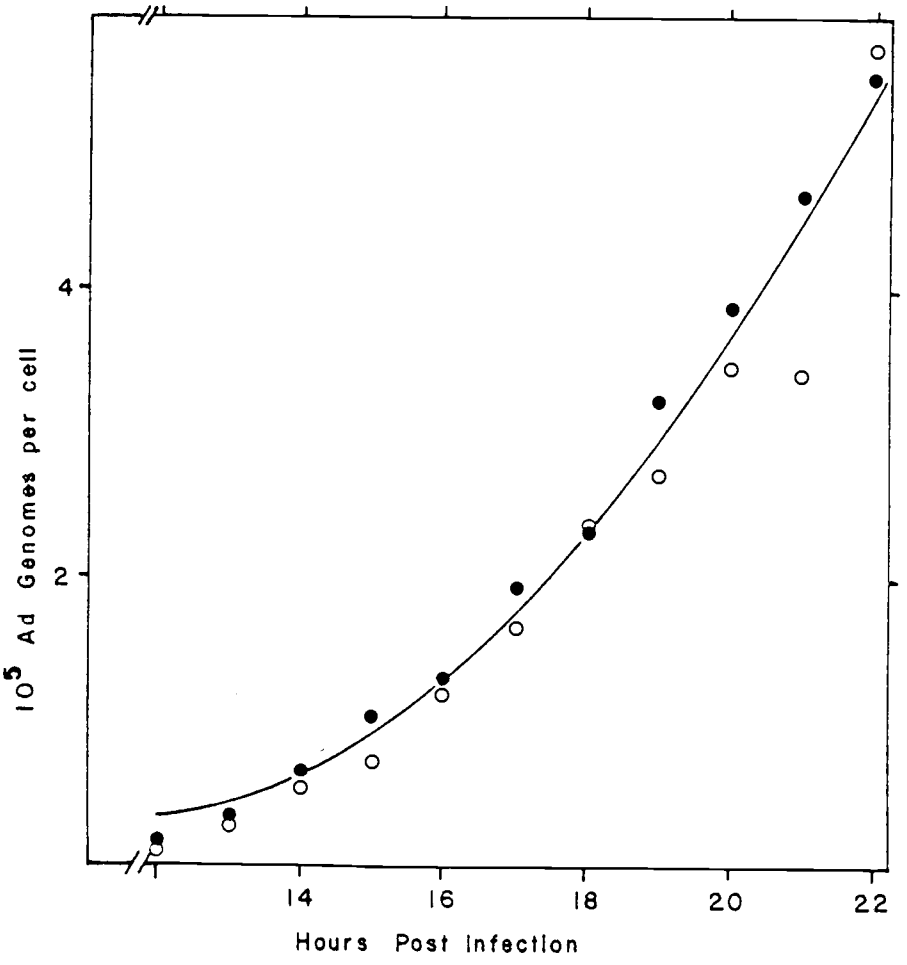

Figure 2. Total DNA accumulation for Ad2 (●) and Ad7 (○). Parallel cultures prelabeled with [^{3}H]thymidine were infected with Ad2 and Ad7, ^{32}P added at 10 hours post infection, aliquots removed and fixed in KCN, and total intracellular DNA prepared as previously described (Part II). Theoretical curve was calculated with $r = 0.046\ min^{-1}$, $i_s = 0.2$, $V_{max} = 120{,}000$ molecules/cell/hour, $K_m = 160{,}000$ molecules/cell.

curves were determined graphically, and V_{max} and K_m were determined with double reciprocal plots as described in Part II. Values were V_{max} = 125,000 Ad2 genomes per cell per hour and 105,000 Ad7 genomes per cell per hour, and K_m = 233,000 genomes per cell for Ad2 and 154,000 for Ad7.

The initiation rate for Ad7 DNA replication was determined with the relationship (equation 19, Part II):

$$i = V_{max}/(2\ K_m + 2\ [DNA])$$

Values for i were consistent with those for Ad2 and Ad5, and decreased over the course of infection as shown in Figure 4.

Measurement of Ad7 Initiation Rate
by Density-Shift Kinetics

The initiation rate for adenovirus type 7 DNA replication was determined with density-shift kinetics as previously described (Bodnar and Pearson, 1980b: Part II). As before, HeLa cells pre-labeled for 24 hours with [^{3}H]thymidine were infected with Ad7, shifted into medium containing BUdR and ^{32}P at 11 hours after infection, then shifted into medium containing ^{32}P but no BUdR at 14, 18, or 22 hours. Aliquots were removed following the chase of BUdR, total intracellular DNA was isolated and banded to equilibrium in CsCl. As shown in Part II the initiation rate can be then

determined from the slope of the line of Fraction [HH] versus time after the chase of BUdR with the relationship:

$$i = -(d \ln(\text{Fraction [HH]})/dt)/4$$

Results of these experiments are plotted in Figure 3.

Notice in Figure 3 that there was a substantial hybrid (HL) peak at zero time even at 22 hours post infection. Since this might be due to viral DNA produced prior to 11 hours, we varied the protocol to add BUdR at 4 hours, shift to BUdR plus ^{32}P medium at 11 hours, then continue as above to insure that all the Ad7 DNA was HH at the start of the density shift. However, there was still a large hybrid peak at the start of the chase, and the ^{3}H could be seen in the hybrid position also (data not shown) indicating that the ^{32}P in the hybrid peak was due to cellular DNA replication. Either Ad7 is much less effective in inhibiting cellular DNA replication or the titer of input virus did not insure that all cells were infected.

The presence of cellular DNA in the HL peak precludes determination of i and i' by the Fraction HL method (see Part II), but the Fraction HH method is sufficiently insensitive to the cellular contamination to allow estimation of the initiation rate by that method. Data as shown in Figure 3 were used to calculate the initiation rates plotted in Figure 4. The values obtained by this method agree well with the curve calculated by saturable kinetics of total viral

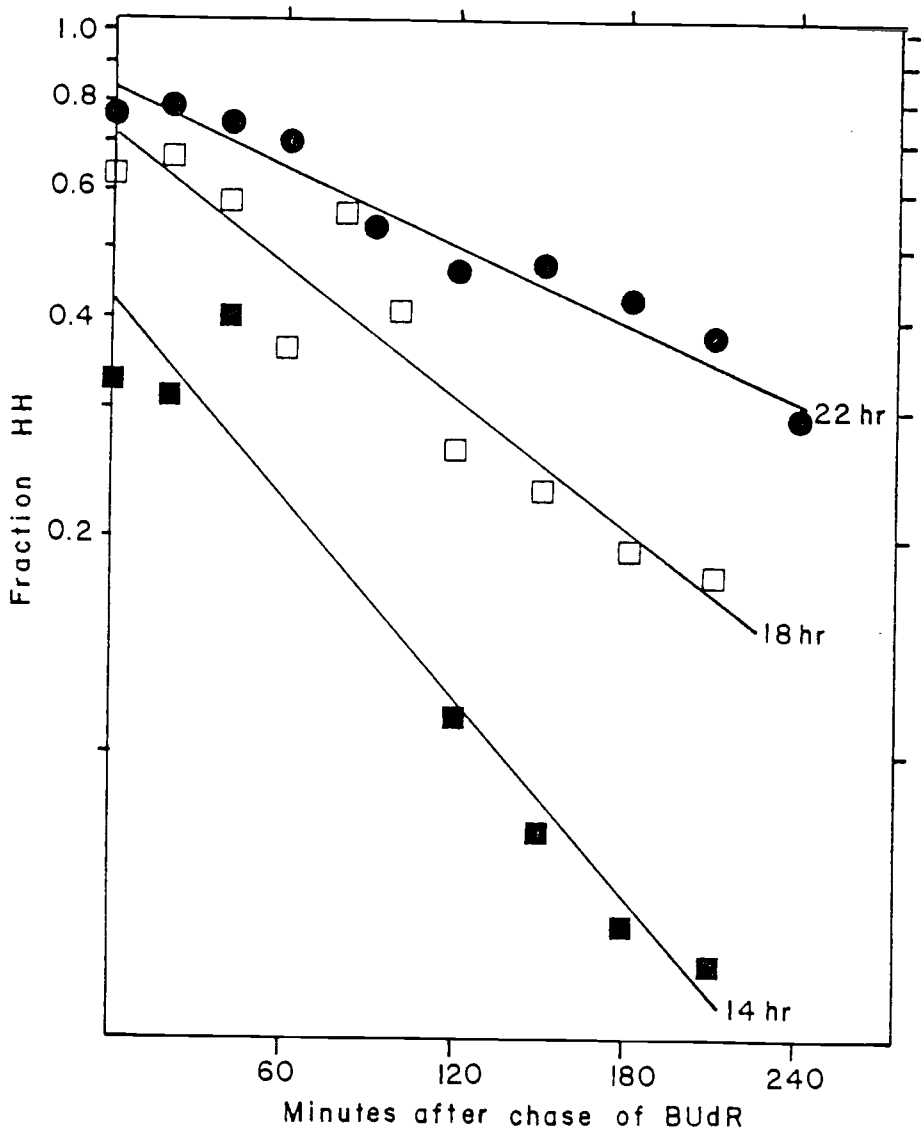

Figure 3. Measurement of the initial rate for Ad7 using Fraction HH method (see Part II). The fraction of ^{32}P radioactivity banding at the fully heavy (HH) density in each CsCl gradient was plotted logarithmically against the time after chase in light medium. Chases were started at 14 hr (■), 18 hr (□), and 22 hr (●) after infection. The solid lines are least squares fit to the data.

accumulation. The initiation rate for Ad7 decrease over infection and is comparable in magnitude to the initiation rate for Ad5 as can be seen by comparing Figure 4 with Figure 10 in Part II.

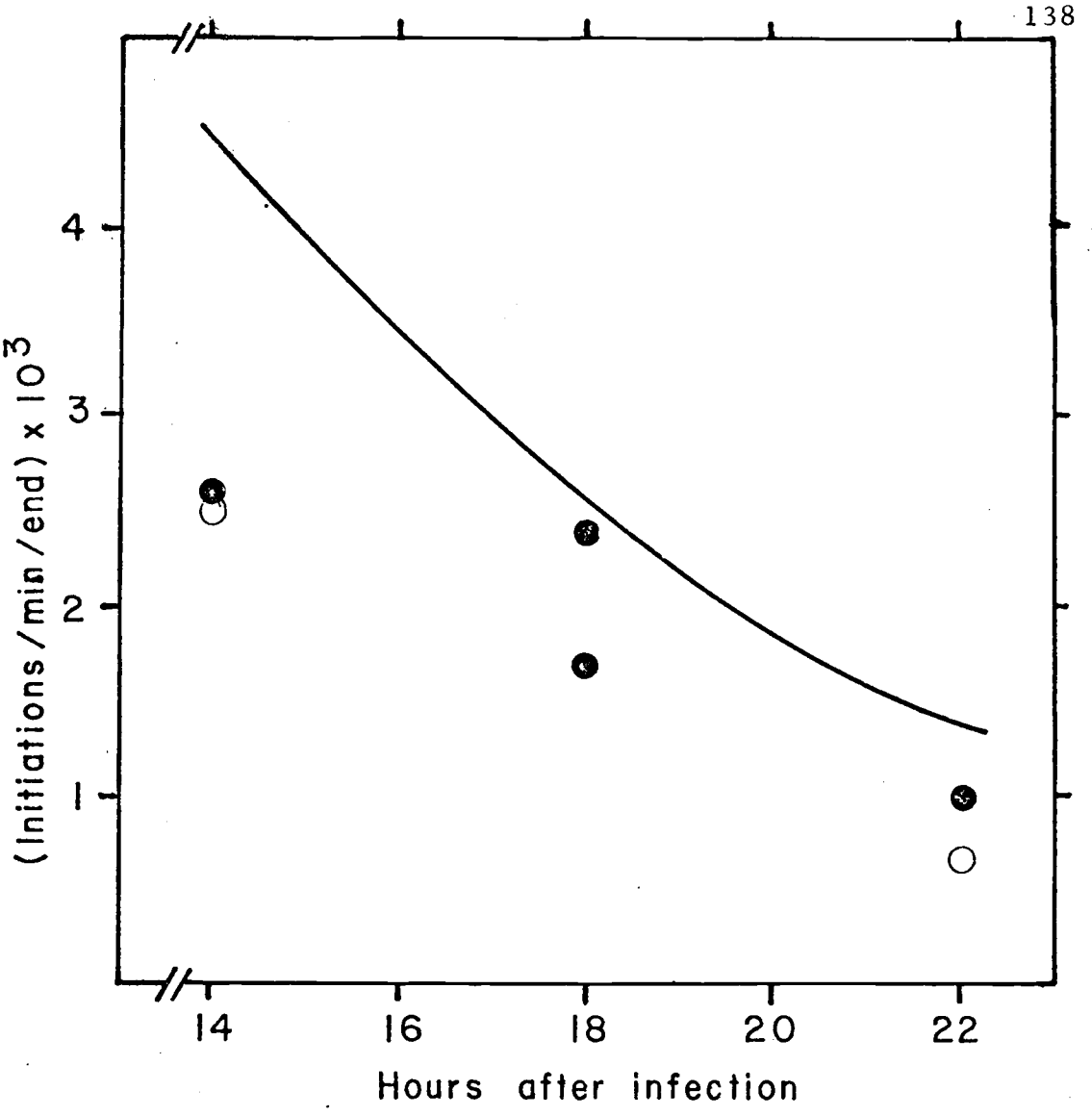

Figure 4. Rate of initiation of Ad7 DNA replication during infection. ● , i measured using the fraction HH method with BUdR and ^{32}P added at 11 hr after infection; ○ , i measured using the fraction HH method with BUdR added at 4 hours after and BUdR plus ^{32}P added at 11 hr; solid line, i calculated from the relationship $i = V_{max}/(2K_M + 2[DNA])$ using data from Figure 2.

DISCUSSION

We have measured the rate parameters of different adenovirus serotypes to investigate which steps in replication are mediated by viral gene products and which are limited by cellular factors. Since Ad2 and Ad7 are only 10 percent homologous, we expected that if viral gene products were the limiting factors in certain steps in replication that these serotypes should show differences in the rates of those steps. Rates measured here have shown that at least the following parameters are not dependent on the viral serotype: 1) the rate of replication, i. e. chain elongation, 2) the average initiation rate for all DNA molecules in the nucleus, and 3) the total number of replication sites per cell when the viral DNA saturates the replication machinery.

One might expect the replication rate to be the same for the different serotypes since no viral coded DNA polymerase has been identified. There is evidence that the host DNA polymerases α and γ are utilized by adenovirus for replication (Ito et al, 1975; van der Vliet and Kwant, 1978; Abboud and Horwitz, 1979; Longiaru et al, 1979; Habara et al, 1980). These results are consistent with our measurement that the rate of DNA polymerization is the same for Ad2, Ad5, Ad7, and uninfected HeLa cells.

The rate of total viral DNA accumulation is limited by the number of replication sites available, and this number is about 50,000 per HeLa cell for Ad2, Ad5, and Ad7. Since this is approximately the same as the maximum number of replicons found in an uninfected cell (Painter and Schaefer, 1969; Hand and Tamm, 1974), one might infer that the limiting factor for adenovirus DNA replication is a cellular factor required for initiation of replication. The limiting factor may also be an early viral protein; however, data on availability of early viral gene products is scanty. Only the 75K DNA binding protein has been quantitated during infection (Gilead et al, 1976). This protein binds single stranded DNA and is required for both initiation and elongation of DNA growing forks. Its synthesis begins early in infection and stops soon after onset of DNA replication with about 9×10^8 75K proteins synthesized per cell. Since one protein covers 7 nucleotides (van der Vliet, et al, 1978), this is about six times the number required to complex 50,000 replicating molecules.

In Part II we postulated that defective adenovirus DNA may be formed by a mechanism inherent in the normal DNA replication. We expected the fraction of DNA formed by this mechanism to be:

$$[\text{Defective SS DNA}] = (i/r_{II})\ \{(r_I - r_{II})/(r_I + i)\}[\text{DS DNA}]$$

Therefore, we expect the total number of defective molecules to be

determined by the ratios of the rate constants. Since Ad7 makes about three times as many defective DNA molecules as Ad2 or Ad5, we expected to see the difference in the rate parameters. The measured values for Ad7 show that the ratio of replication rate to initiation rate is the same as for Ad5. Therefore, if the proposed mechanism is valid, the difference between r_I and r_{II} must be larger. This difference has not been determined for Ad7; to do so will require an electron microscope study of the type reported by Lechner and Kelly, (1977) for Ad2.

THE KINETICS OF ADENOVIRUS DNA REPLICATION: V

Application of Kinetic Techniques to SV40 DNA Replication

ABSTRACT

Methods to measure kinetic parameters of viral DNA replication have been developed with the adenovirus system (Bodnar and Pearson, 1980a and 1980b; Part I and II). These techniques have been applied to SV40 DNA replication data available in the literature. These methods confirm that the time to complete one SV40 DNA molecule is 15 minutes, that initiation is the rate limiting step in replication exhibiting saturable kinetics, and that recently replicated molecules are preferentially reinitiated.

INTRODUCTION

We have previously investigated the kinetics of adenovirus DNA replication in terms of the time to complete one DNA molecule (Bodnar and Pearson, 1980a; Part I) and the time between rounds of replication (Bodnar and Pearson, 1980b; Part II), and we have modeled adenovirus DNA replication in terms of these measured rate parameters to simulate many types of experiments for studying DNA replication (Bodnar and Pearson, 1980c; Part III). Since there is a wealth of experimental data on the SV40 system concerning DNA replication, we decided to apply the techniques developed using adenovirus to SV40 DNA replication and compare the kinetics of the two systems.

We have previously derived several methods to determine the time required to complete replication of a single adenovirus DNA molecule. These derivations were modified to the mechanism of SV40 DNA replication and applied to the numerous [^{3}H]thymidine pulse experiments available for SV40 (Danna and Nathans, 1972; Nathans and Danna, 1972; Lai and Nathans, 1974; Shenk, 1978; Sebring et al, 1971; Fareed et al, 1973; Manteuil et al, 1973; Tapper and DePamphilis, 1978). These techniques confirm the previous estimate of replication time of an SV40 DNA molecule of 15 to 20 minutes (Nathans and Danna, 1972; Manteuil et al, 1973).

We have shown that initiation is the rate limiting step in adenovirus DNA replication and that this step shows saturable kinetics (Bodnar and Pearson, 1980b; Part II). Similar density shift experiments (Green and Brooks, 1978) and growth curves (Manteuil et al, 1973) have been reported for SV40. Kinetic analysis of these experiments shows that the rate of initiation of rounds of replication of SV40 is also very slow (10^{-4} to 10^{-3} initiations/molecule/minute) and that the growth curve shows saturable kinetics with a V_{max} of 600 molecules/cell/hr and a K_m that depends on the MOI.

Overall comparison of the kinetics of the two systems shows that control of DNA replication is remarkably similar between adenovirus and SV40. The notable exceptions are that there are about 50,000 replication sites per cell for adenovirus but only 150 per cell for SV40, and the replication rate for SV40 is about one eighth as fast as that for adenovirus.

THEORY

Calculation of Radioactive Label Incorporation into SV40 DNA during a Pulse

Assume a double stranded closed circular genome which replicates bidirectionally from a fixed origin to a fixed terminus. Define:

1) x = position on the genome, Genome coordinates are defined with the origin of replication as zero and terminus at $\pm$ 0.5. For SV40 this places the EcoRI site at +0.33 and the Hin A and C fragment junction at -0.15.

2) r = rate of DNA replication expressed as fractional genome lengths per minute.

3) t = time in minutes after the addition of [^{3}H]thymidine label.

4) $f_{1C}(x, t)$ = relative specific activity of pulse label at position x in a molecule completed during the pulse at time t for $0 < x < 0.5$, i.e. the half molecule that was completed by the clockwise growing fork.

4) $f_{2C}(x, t)$ = relative specific activity of pulse label at position x in a molecule completed during the pulse at time t for $-0.5 < x < 0$, i.e. the half molecule that was completed by the counterclockwise growing fork.

6) $F_{1C}(x_1, x_2, t)$ or $F_{2C}(x_1, x_2, t)$ = the total relative label in a frag-

ment between x_1 and x_2 at time t for each half molecule as above.

7) $\overline{F}_{1C}(x_1, x_2, t)$ or $\overline{F}_{2C}(x_1, x_2, t)$ = the average specific activity in a restriction fragment between x_1 and x_2 at time t for each half molecule as above.

8) $f_C(x, t) = f_{1C}(x, t) + f_{2C}(x, t)$, and similarly for $F_C(x_1, x_2, t)$ and $\overline{F}_C(x_1, x_2, t)$.

Assume:

1) Replication is bidirectional with both growing forks moving at the same rate and that rate is constant.

2) The probability of finding a growing fork is the same at any point on the genome.

3) The size of the replicating pool does not change during the pulse.

4) Reentry of labeled molecules into the replicating pool is negligible during the pulse.

Take a pulse of length t. During this period all molecules that have growing forks at (0.5 - rt) or closer to the terminus at the start of the pulse will be completed during the pulse. The least completed molecule at the pulse start that will be completed during the pulse will be the one with its growing forks at (0.5 - rt) and (rt - 0.5) at the start of the pulse, and molecules that are closer to completion will be equally likely. Therefore, if we define the specific activity at the terminus as 0.5 at one replication time (i.e. $f_{1C}(0.5, t) =$

$f_{2C}(-0.5, t) = 0.5$ at $rt = 0.5$), then the distribution of label will be as shown below.

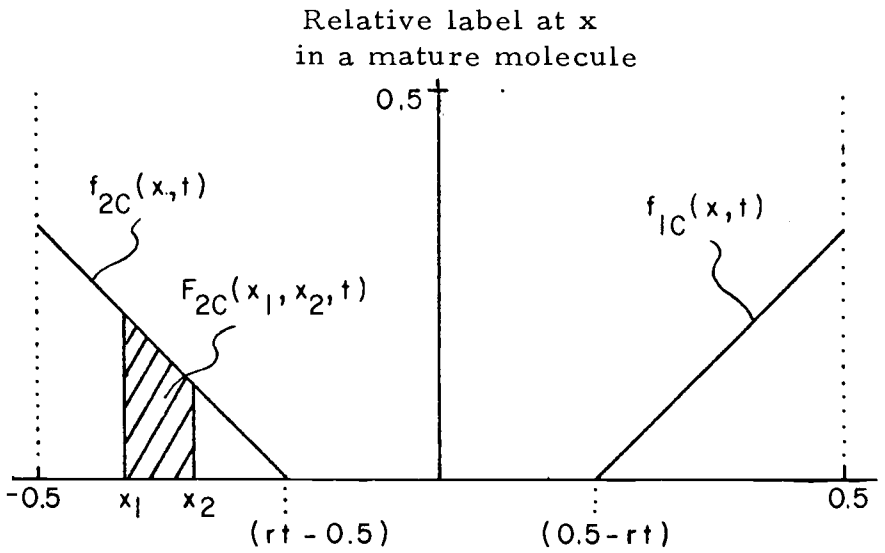

The specific activity on the right half-molecule will be given by:

$$f_{1C}(x, t) = rt + x - 0.5$$

where $rt - 0.5 < x < 0.5$

and $x > 0$

The total relative activity in a restriction fragment between x_1 and x_2 will be

$$F_{1C}(x_1, x_2, t) = \int_{x_1}^{x_2} f_{1C}(x, t)\, dx$$

$$= (x_2 - x_1)\,[0.5\,(x_1 + x_2) + rt - 0.5]$$

where $rt - 0.5 < x < 0.5$

and $x > 0$

The average activity in that fragment will be:

$$\overline{F}_{1C}(x_1, x_2, t) = F_{1C}(x_1, x_2, t)/(x_2-x_1)$$

$$= 0.5\,(x_1+x_2) + rt - 0.5$$

with boundary values as above.

For the left half-molecule these functions will be:

$$f_{2C}(x, t) = rt - x + 0.5$$

$$F_{2C}(x_1, x_2, t) = (x_2-x_1)\,[-0.5(x_1+x_2) + rt - 0.5]$$

$$\overline{F}_{2C}(x_1, x_2, t) = -0.5(x_1+x_2) + rt - 0.5$$

where $-0.5 < x < rt - 0.5$

and $x < 0$

The boundary values are very important to prevent meaningless negative values.

Define $F_T(x_1, x_2, t)$ as the total radioactive label incorporated into a given restriction fragment (x_1, x_2) at time t after the addition of label. Since there are two growing points per molecule incorporating label at a rate r, for the whole genome the total label will be incorporated at a rate rt, i.e. $F_T(-0.5, 0.5, t) = rt$. Then the total label incorporated into replicating molecules will be:

$$F_R(x_1, x_2, t) = F_T(x_1, x_2, t) - F_C(x_1, x_2, t)$$

Calculation of Total SV40
DNA Accumulation

Calculations of the total DNA buildup over an infection were done assuming that the initiation step shows saturable kinetics and that there is one type of replicating molecule that takes a constant time to complete a round of replication.

Assume:

1) The probability of initiation of replication is equal for all mature molecules, or that only an average initiation rate can be measured.

2) The concentration of Component II non-replicating molecules is very small.

3) The rate of initiation is limited by a component of the initiation complex other than the DNA, and that this component is constant in concentration throughout the infection.

4) A replicating molecule completes a round of replication in n minutes and this time is constant over infection. Also, replicating molecules cannot reinitiate rounds of replication.

Define:

1) [MAT] = concentration of mature DNA molecules (Component I).

2) $[REP_x]$ = concentration of replicating molecules that have completed x minutes of replication.

3) n = number of minutes required to complete a round of replication.

The total DNA was divided into n+1 pools, one for mature DNA and n for replicating molecules that have completed each minute of replication. The equations for changes in pool size are:

$$\Delta[MAT]/\Delta t = -\{V_{max}/(K_m+[MAT])\}[MAT] + [REP_n]$$

$$\Delta[REP_1]/\Delta t = \{V_{max}/(K_m+[MAT])\}[MAT] - [REP_1]$$

$$\Delta[REP_x]/\Delta t = [REP_{x-1}] - [REP_x]$$

The changes in pool size were approximated for each minute using Euler's method of taking the slope at time t and using that to get the value of time $t + \Delta t$, i.e. $[MAT] = [MAT] + \Delta[MAT]$, etc. The iterations were done on an HP 9821A programmable calculator using a Δt of 1 minute and a replication time of 14 minutes. The values for V_{max} and K_m were obtained from a Lineweaver-Burk plot of data of Manteuil et al, 1973 and adjusted to best fit of the data.

The value for V_{max} was corrected for MOI using the Poisson distribution for the number of cells infected (Manteuil et al, 1973).

$$V_{max} = V_{max}'(1 - e^{-MOI})$$

where V_{max}' is the value for V_{max} with 100 percent of the cells infected.

Calculation of Initiation Rate by Density-Shift Kinetics

We have previously shown a method to measure the initiation rate for semiconservative DNA replication where all forms (HH, HL, and LL) are radioactively labeled (Bodnar and Pearson, 1980b; Part II). The initiation rate can be also measured in experiments where uniformly labeled (^{32}P) or pulse labeled ($[^{3}H]$thymidine) DNA is chased with unlabeled bromodeoxyuridine (BUdR) (Green and Brooks, 1978; Roman and Dulbecco, 1975; Roman, 1979). In this case the form at time of chase (LL) is labeled and any new DNA strands made during the chase are unlabeled but heavy.

$$LL^{*} \xrightarrow{i} HL + HL^{*}$$

or

$$L^{*}L^{*} \xrightarrow{i} HL^{*} + HL^{*}$$

Note that no new label is made nor are any fully heavy molecules seen. From the differential equations similar to those previously described (Part II), we can derive for activity of the DNA that:

$$[LL] = [LL]_o \exp(-it)$$

$$[HL] = [LL]_o (1 - \exp(-it))$$

$$\text{Fraction } [LL] = [LL]/([LL] + [HL]) = \exp(-it)$$

or

$$\ln(\text{Fraction } [LL]) = -it$$

RESULTS AND DISCUSSION

Measurement of Replication Time

Pulse labeling experiments were modeled as shown in Theory, and the results were applied to three kinds of experiments that can be used to calculate the replication time of a DNA molecule. Briefly, the model assumes a Cairns model for replication with the growing forks moving at the same rate in either direction. The size of the replicating pool is assumed to be constant throughout the pulse with reinitiation of replicating molecules being negligible. Functions are derived which allow calculation of the change in specific activity of restriction fragments during the pulse and the relative incorporation of radioactive label into the replicating and mature molecules.

Calculations were done with the results of experiments of pulse labeling restriction fragments of the type developed by Danna and Nathans (1972). The relative specific activity of each fragment ($\overline{F}_C(x_1, x_2, t)$) was determined and normalized to the highest specific activity. The model showed that the replication rate can be determined from the experimental data by drawing a straight line through the values for specific activity to intercept the position of zero specific activity. The distance between that point and the terminus of replication is the distance that the replication fork has moved during

the pulse. Addition of values for both forks gives the value for the entire molecule, and the reciprocal of this gives the time to complete the entire genome. The average value for the replication rate can be used in the function ($\overline{F}_C(x_1, x_2, t)$) to obtain a calculated curve for the specific activities of the fragments as shown in Figure 1. This technique was applied to the following experiments of the Danna and Nathans type with the average replication time determined from each (corrected to full length SV40 for deletion and insertion mutants): Danna and Nathans, 1972, 9.4 minutes; Nathans and Danna, 1972, 12.6 minutes; Lai and Nathans, 1975, 18 minutes; and Shenk, 1978, 14 minutes. The average for all experiments was 14.1 minutes.

The relative incorporation of [^{3}H]thymidine label into the mature and replicating pools was calculated with the functions $F_C(-0.5, 0.5, t)$, $F_R(-0.5, 0.5, t)$, and $F_T(-0.5, 0.5, t)$ for the entire genome as defined in Theory. The results are plotted in Figure 2 and compared to Tapper and DePamphilis, 1978. From this plot one can see that ^{3}H incorporation into total DNA is linear and can be used to estimate the time needed for thymidine pools to equilibrate after [^{3}H]thymidine addition. From the experimental values for total activity we can see that this is about one minute for the data of Tapper and DePamphilis. The incorporation into mature DNA molecules begins parabolically and becomes linear after one replication time. The incorporation into replicating molecules builds up rapidly but reaches a plateau and

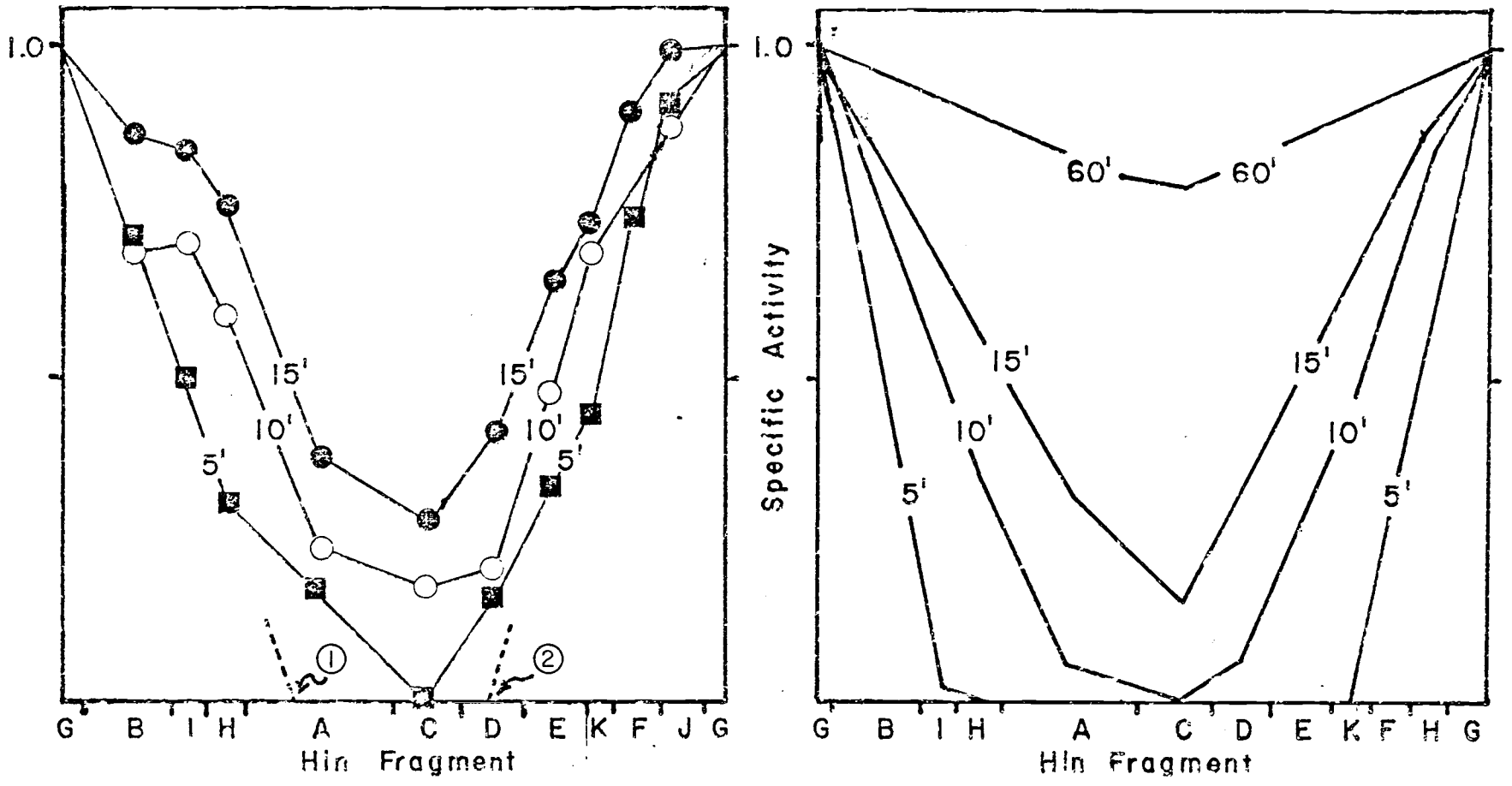

Figure 1. The relative specific activity of Hin restriction fragments of SV40 versus time after addition of a [^{3}H]thymidine pulse. A) experimental data of Danna and Nathans, (1972) and B) model calculations. The calculated curves use a value of r = 0.035 which corresponds to a replication time of 14 minutes. The dashed lines indicate the method that the replication rates were derived from experimental data. The distance between the terminus and the intercept of a straight line drawn through the 5 minute curves yields the distance moved by the growing fork during the pulse, i.e. ① = 0.36 genome/5 min = 0.072, ② = 0.33 genome/5 min = 0.066 giving a total of 0.136 genome/min per molecule or a replication time of 7.4 minutes.

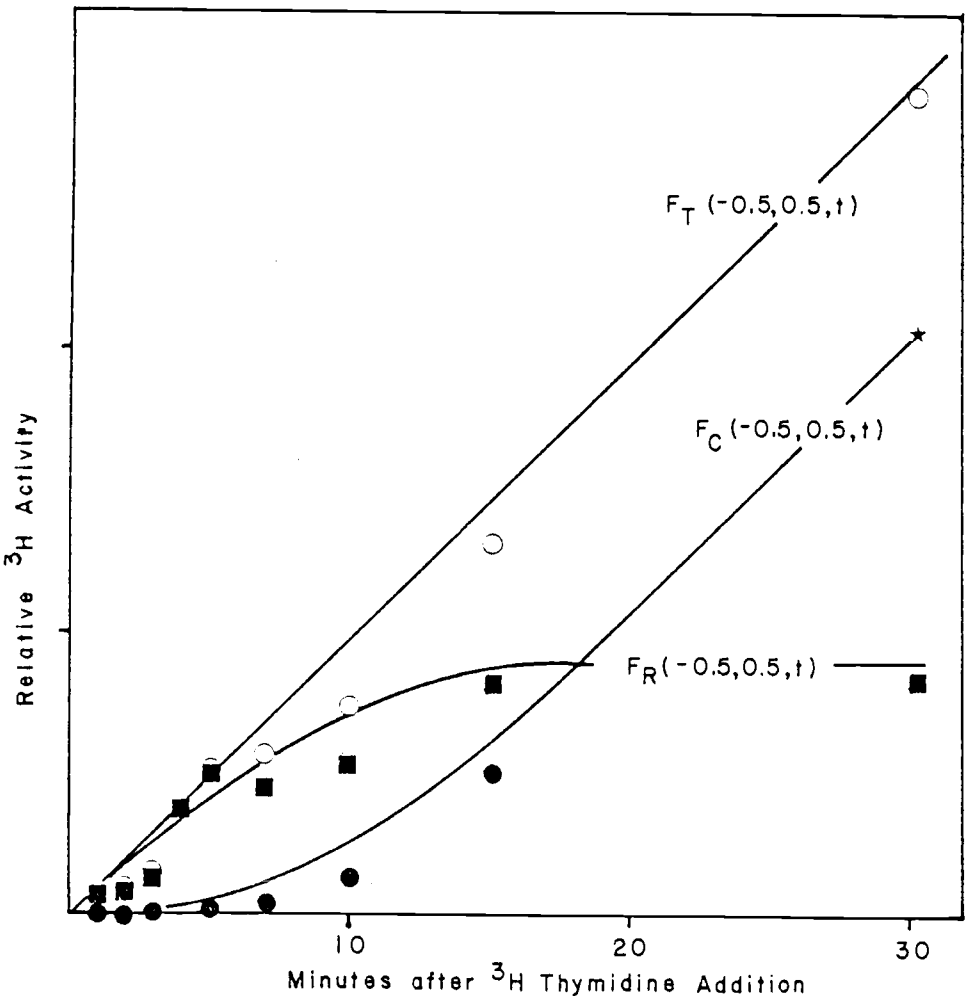

Figure 2. Theoretical curves for relative [^{3}H]thymidine incorporation into SV40 DNA during a pulse are compared with experimental data of Tapper and DePamphilis (1978). Curves are calculated for ^{3}H incorporation into total DNA, F_T; mature DNA, F_C; and replicating DNA, F_R using r = 0.028 genome/min or a replication time of 18 minutes. Data are for mature DNA (Comp. I), ● ; Replicating DNA, ■ ; and mature plus replicating DNA, ○ and are normalized to theoretical curves by setting the 30 minute values for mature DNA equal (★).

crosses the curve for mature molecules at one replication time. Using these criteria we calculate the replication time from the data of Tapper and DePamphilis as 18 minutes and the calculated curves for this replication time are shown in Figure 2. If there is significant reinitiation of labeled molecules during the pulse, the value for replicating molecules will continue to increase after one replication time and not plateau; this is not the case for SV40.

The usual method for estimation of replication time has been the time for the percent of [^{3}H]thymidine pulse label in the replicating molecules to decrease to less than fifty percent of the total activity (Dintzis, 1961; Manteuil, et al, 1973). Derivation of this ratio ($F_R(-0.5, 0.5, t)/F_T(-0.5, 0.5, t)$) confirms this method as shown in Figure 3. The calculations show that the percent of molecules replicating will drop linearly from 100 percent to 50 percent in one replication time then drop slowly toward zero. A least squares fit of results of five experiments (Levine et al, 1970; Sebring et al, 1971; Fareed et al, 1973; Manteuil et al, 1973) gives a line with an intercept at 101 percent, 50 percent replicating activity at 19.2 minutes and an r^2 (a measure of the linearity) of 0.85.

The time to complete replication of an SV 40 DNA molecule has been estimated to be 15 to 20 minutes (Nathans and Danna, 1972; Manteuil et al, 1973). Our model for DNA replication confirms this estimate and shows three methods by which this can be measured.

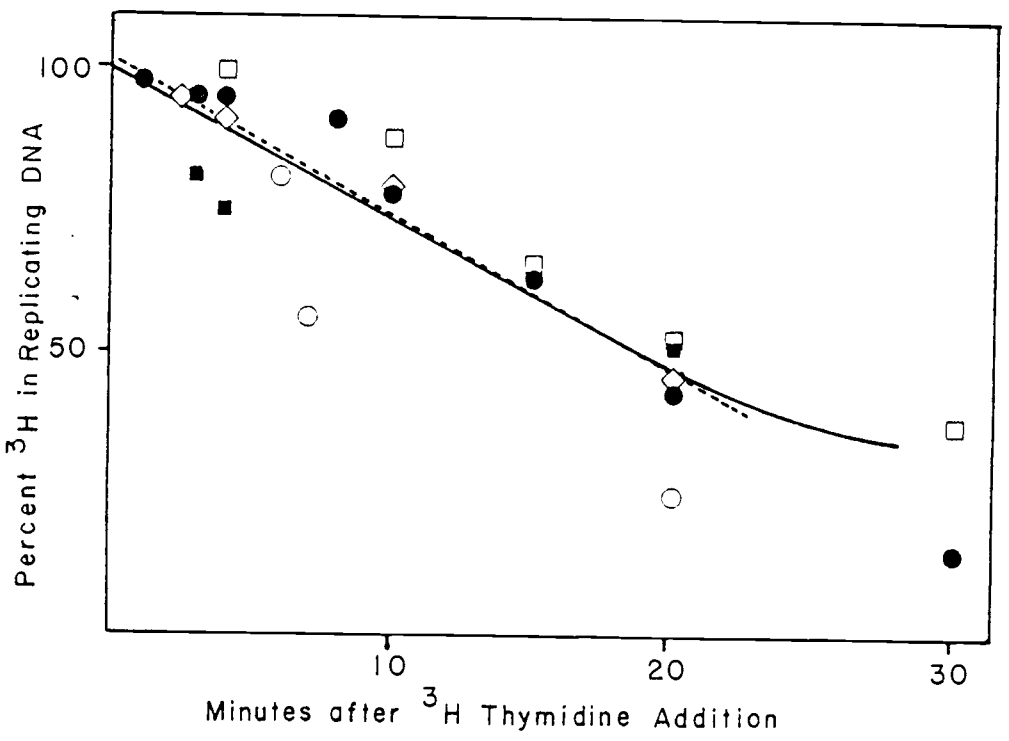

Figure 3. Replication time is estimated by noting the time required for the percent of [^{3}H] thymidine activity incorporated in replicating DNA during a pulse to drop to 50 percent. The theoretical curve (——) is for a replication time of 19 minutes. The dashed line is a least squares fit of the data points from the following experiments: Levine et al, Fig. 6 and 11, 1970 (● and ◇); Sebring et al, Fig. 1, 1971 (■); Fareed et al, Fig. 6, 1973, (○); Manteuil et al, Fig. 6, 1973 (□).

Measurement of Initiation Rate

We have previously shown that the average time between rounds of DNA replication can be measured by using density labeling experiments and total DNA accumulation curves (Bodnar and Pearson, 1980b; Part II). Experiments of these types are available for SV40, and these can be used to determine the initiation rate for SV40 with minor alterations to the derivations for adenovirus.

Density-shift experiments have been reported for SV40 where infected cells were pulse labeled with [^{3}H]thymidine for one hour, chased in cold medium for two hours, then labeled with cold BUdR, or labeled with ^{32}P from 19 to 40 hours postinfection, chased for 30 minutes in cold medium, then labeled with cold BUdR (Green and Brooks, 1978). This protocol can be used to measure the initiation rate, but since the density-shift is into unlabeled BUdR, the derivation is slightly different from that previously described (see Theory). The initiation rate can still be measured from the slope of the line of the ln (Fraction [LL]) versus time, but in this case the slope is -i. Applying this to the data of Green and Brooks (1978) (not shown) we find that the initiation rates are as follows:

^{3}H pulse for 1 hour

t_o = 23.5 hr	$i' = 8.5 \times 10^{-4}$ initiations/molecule/min
24 hr	$i' = 1.0 \times 10^{-3}$
40.5 hr	$i' = 8.7 \times 10^{-4}$
^{32}P long label	$i = 3.2 \times 10^{-4}$

Once again as for adenovirus the initiation rate for recently replicated molecules (i') is higher than that for the average DNA molecule, and the probability of reinitiation of the molecules in the replicating pool is approximately that for adenovirus (1×10^{-3} versus 5×10^{-3} min^{-1}). These hypotheses were reported qualitatively by Green and Brooks, 1978; our modeling techniques support their data quantitatively. Similar density shift experiments done with polyoma DNA (Roman and Dulbecco, 1975; Roman, 1979) show the same characteristics with $i' = 4 \times 10^{-3}$ min^{-1}.

Time course experiments of SV40 DNA accumulation have shown that the DNA concentration increases apparently exponentially until about 20 hours post infection and linearly thereafter (Manteuil et al, 1973; Levine et al, 1970). It has been suggested that this is due to a limited number of replicating sites per cell and that total DNA growth curves are dependent on the fraction of cells infected (Manteuil et al, 1973). We have modeled the data of Manteuil et al (1973) assuming

saturable kinetics as previously described (Part II). We assumed one type of replicating intermediate with a 14 minute replication time, an initiation rate equal to $V_{max}/(K_m + [DNA])$, and a V_{max} proportional to the number of cells infected. Using an iterative approach (see Theory) we fit the data of Manteuil et al (1973) as shown in Figure 4. From this model we can see that as for adenovirus the initiation step is the rate limiting step in SV40 DNA replication, and that this probability decreases as the replication machinery becomes saturated with DNA. The values for V_{max} and K_m were determined graphically for each curve using a double reciprocal plot. When corrected for the number of cells infected, V_{max} was essentially the same for all MOI, but K_m increased with increasing MOI. This is characteristic of a competitive inhibitor and may be due to the increasing numbers of noninfectious SV40 DNA molecules competing for the replication machinery at higher MOI's.

Calculations using the simulated growth curves show the consistency of this method with other data. The initiation rate by this method is 1×10^{-4} at 40 hours post infection compared with 3.2×10^{-4} from the density labeling experiments of Green and Brooks, (1978). Using the estimate of Manteuil et al (1973) that the maximum rate of SV40 DNA accumulation is about 600 molecules per cell per hour we can extrapolate our curves back to one DNA molecule per cell at about 9 hours compared to the estimate of 11 hours post infection for the

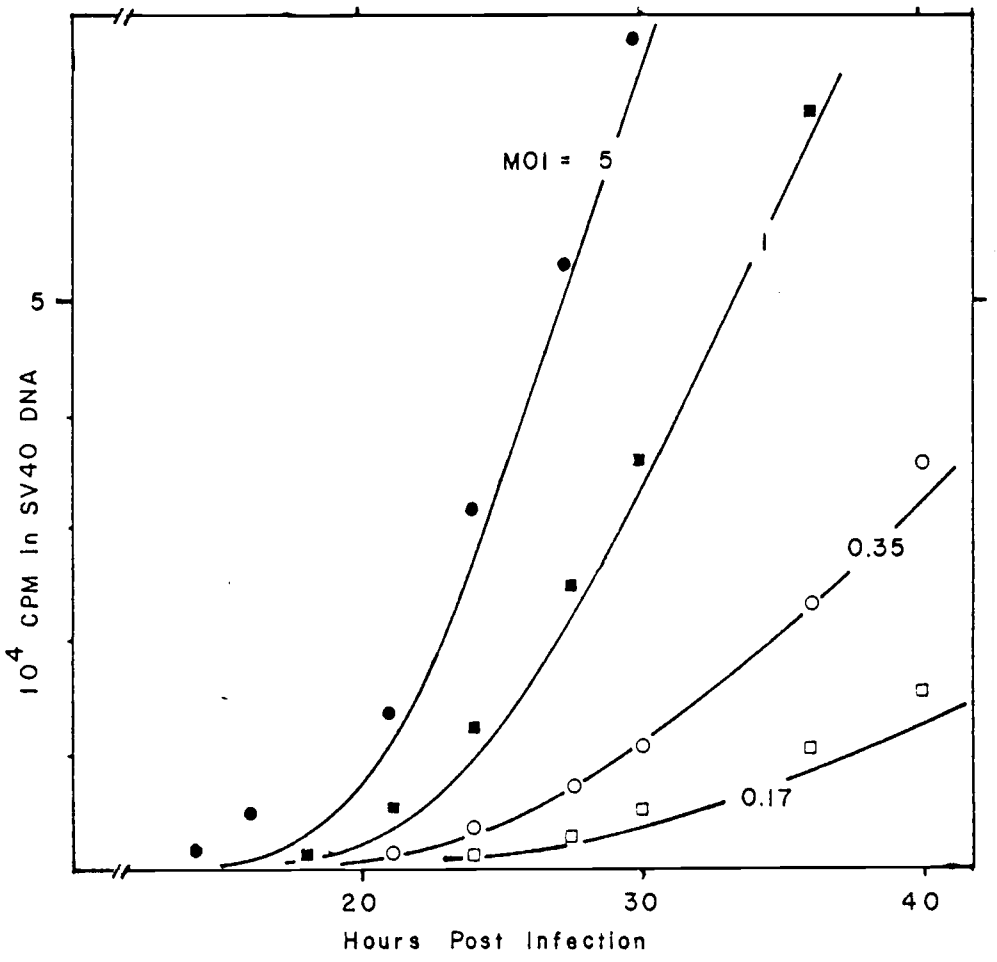

Figure 4. Theoretical curves for total SV40 DNA accumulation are compared with experimental data (Manteuil et al, 1973). ● MOI = 5, ■ MOI = 1, O MOI = 0.35, □ MOI= 0.17. Theoretical curves were calculated as follows: V_{max} and K_m were determined graphically from data, V_{max} corrected for MOI, points plotted by Euler's method as derived in the Theory. The t_o point was extrapolated where the curves crossed. The following values were used: V_{max} = 160 CPM/min x $(1 - e^{-MOI})$; CPM_o = 60CPM x $(1 - e^{-MOI})$ at 11 hours; K_m = 12,000 CPM/cell, (MOI = 5), 9,000 (MOI = 1), 6,000 (MOI = 0.35), 4,000 (MOI = 0.17).

onset of DNA replication (Manteuil et al, 1973). The model shows that only 3 to 4 percent of the DNA molecules are replicating at 30 hours post infection. Experimental values of 12 to 18 percent have been reported (Levine et al, 1970, Figure 4; Sebring et al, 1973, Figure 9; Fareed et al, 1973, Figure 2; Salzman et al, 1973, Figure 1) although a figure as low as 2.5 percent replicating molecules at 40 hours post infection has been reported (Green and Brooks, 1978).

Also, while many multiply initiated replicating DNA molecules are seen in adenovirus DNA, none have been reported for SV40. We can estimate the fraction expected by use of the Poisson distribution for an average lifetime for a replicative intermediate (1/2r) of 15 minutes and an initiation rate for the replication pool (i') of 1×10^{-3} min^{-1}. The fraction of singly initiated molecules is $P(1) = (i'/2r) \exp(-i'/2r) = .015$, and the fraction of doubly initiated molecules is $P(2) = (i'/2r)^2 \exp(-i'/2r)/2 = .0011$ or less than 1 percent of the replicating molecules will have initiated more than once. This is due to an initiation rate about one fifth of that for adenovirus.

Model calculations of SV40 and adenovirus DNA replication have shown many similarities that may be characteristic of eukaryotic DNA virus replication. The limiting step in replication in both cases is the initiation of a round of DNA replication which shows saturable kinetics for some component of the initiation complex that is approximately constant over infection. The growth curves therefore show

two distinct phases: an early pseudoexponential growth where the DNA concentration limits the DNA growth rate, and a later linear stage where the replication machinery is saturated with DNA, and DNA accumulation continues at a constant rate. Both SV40 and adenovirus show a segregation of DNA into replicating and non-replicating pools with preferential initiation of only certain DNA molecules.

However, there are two differences in the viruses. The replication rate in adenovirus is about 25 nucleotides per second but for SV40 it is only 3 nucleotides per second. Also, with a V_{max} of 600 DNA molecules per cell per hour and a replication time of 14 minutes, we can estimate that there are about 150 replication sites per cell for SV40. For adenovirus we have seen 50,000 sites per cell. The reasons for these differences is unclear and requires further investigation. Since most SV40 studies are done in CV-1 or African Green Monkey Kidney cell lines, the differences may be due to differences in the replication machinery of the host. Unfortunately there is currently no data available on the replication rates or numbers of replicons found in these cell types.

CONCLUSIONS AND GENERAL DISCUSSION

We have presented methods to measure the rate parameters for viral DNA replication in eukaryotic systems. The replication of DNA can be broken into two major steps: the initiation of a round of replication and the elongation of a DNA strand. Several methods to measure each have been presented and compared for the adenovirus/HeLa cell system. Since the replication rate is about an order of magnitude slower than nucleotide pool equilibration time and the initiation is still another order of magnitude slower, experiments can be designed where one of these can be measured and the others are either too fast or too slow to affect the data. This may not be possible in bacteriophage systems where the entire lytic cycle is over in the time to complete the pulse experiments presented here. However, in the slower eukaryotic systems the techniques developed here may be applied with other minor modification. We have extended these methods to available data on SV40 DNA replication and have seen that SV40 DNA replication exhibits similar characteristics to adenovirus and can be described by the same types of rate parameters.

The strand displacement mechanism of adenovirus DNA replication as suggested by Sussenbach (Ellens et al, 1974) and modified by Lechner and Kelly (1977) causes the adenovirus system to be somewhat more complex than other viral systems since it means that

there are at least two different replication rates, two initiation rates, and more than ten recognizable replicative intermediates. However, the greater number of replicating molecule types allows a very detailed (if rather tedious) analysis of the mechanism of adenovirus DNA replication. We have discussed the component rate parameters in detail in each of the previous parts, and we will therefore confine our discussion here to the application of our kinetic methods to the study of DNA replication in general. The kinetic approach has led to: 1) a greater understanding of the component steps in adenovirus DNA replication, 2) testable hypotheses for mechanisms in several stages of replication, and 3) a coherent dynamic picture for adenovirus DNA growth that allows a more intelligent interpretation of experimental data and the prediction of new experimental results.

The replication rate for adenovirus DNA is about 25 nucleotides per second and is constant over infection. Since this rate is independent of serotype (Ad2, Ad5, and Ad7) and is approximately equal to that of the uninfected cells (15 to 40 nucleotides per second; Edenberg and Huberman, 1975), the chain elongation step seems to be mediated by cellular factors. For viral DNA replication once a round of replication has started, completion of the DNA molecule is rapid and independent of the state of the infection.

The initiation of DNA replication has been shown to be the controlling step in replication in both prokaryotes (E. coli; c.f. Pierucci

and Helmstetter, 1969) and eukaryotes (HeLa; c.f. Painter and Schaefer, 1969; Hand and Tamm, 1974) where the total amount of DNA synthesized is modulated by the number of replicons operating at any time. We have shown that initiation is also the controlling step in adenovirus DNA replication, but in this case the control is much simpler. The required viral gene products are accumulated early in infection, and when DNA replication begins the kinetics of DNA accumulation indicate that the machinery for viral DNA replication is present roughly at a constant concentration. As infection proceeds, the rate of DNA accumulation increases as the DNA concentration increases, but at about 17 hours post infection the machinery is saturated with adenovirus DNA, and replication continues at a constant rate limited by some factor required for initiation of replication. Since the maximum rate of DNA accumulation is independent of serotype (Ad2, Ad5 and Ad7) and about the same as for uninfected HeLa cells, the limiting factor seems to be cellular.

Control of the initiation step in adenovirus type 5 infection is further modulated by a pooling of the intracellular viral DNA. Early in infection all Ad5 DNA molecules have about the same chance of replicating, but later in infection only certain molecules are destined for replication. This may be a spatial pooling due to a limited number of intranuclear sites that replicate the DNA (Simmons et al, 1974)

or due to pooling by function (i. e. the DNA that is transcribed is not replicated; Brison et al, 1979) or possibly by removal of DNA by a prepackaging step. The size of the replicating pool is relatively constant throughout infection. Analysis of SV40 DNA replication by the same techniques show that these characteristics of viral DNA replication rate, initiation rate, and preferential initiation of recently replicated DNA molecules also apply to SV40.

Measurement of the kinetic parameters for adenovirus DNA replication has suggested some modifications and additions to the strand displacement mechanism. The strand displacement model has been quantitatively consistent with all experiments performed or simulated during our studies, but the values of the rate constants obtained have led to proposals for the mechanism of Ad DNA replication which should be studied further. For example, the initiation rate for displaced single stranded DNA is much faster than that for mature DNA molecules. This suggests that initiation of the displaced strand is accomplished by a mechanism that maintains the ends of the strand and the replication machinery in close proximity throughout the displacement synthesis so that reinitiation of the displaced strand is very fast due to a high local concentration of the required factors. Also, the measured rate of replication for type II molecules is slower than that for type I molecules. As discussed in detail in Part II this difference in rates has suggested a mechanism for formation of

defective adenovirus DNA. This mechanism is interesting in that it suggests that formation of defective DNA is an integral part of the replication process and, at least for adenovirus, all virus preparations contain defective particles. The proposed mechanism for formation of the defective DNA depends on the ratios of the rate constants for replication. The rates for Ad7, which produces many defectives, should differ from Ad2, which produces few. Those measured thus far are the same, but using an electron microscope study similar to the Lechner and Kelly (1977) experiment one should be able to test the validity of this hypothesis.

When we began measuring rate parameters for replication, we had little idea that the results would not only support existing mechanisms but suggest new ones. Also they have allowed us to examine the adenovirus replication system in greater detail to plan experiments to test the hypotheses in a much more direct way than before. The protocol above to investigate formation of defectives is just one example. Another is our ability now to look realistically at the best procedure for labeling replicating intermediates. By examining the pulse labeling procedures in Part I we can see that to incorporate the most radioactivity into replicating DNA we should label for about 20 minutes; shorter pulses do not label all the replicating molecules, but longer pulses merely add to the label in

mature DNA which must then be separated from replicating DNA. The size of the total replicating pool increases until about 18 hours when the cellular replication machinery is saturated with adenovirus DNA, and afterwards the label in mature molecules increases without markedly increasing the number of replicating molecules. Therefore, the best time to harvest replicating molecules is about 18 hours post infection. Prior to our modeling of the adenovirus system, such estimates of the optimum time for such an experiment were crude at best.

These techniques also allow a better interpretation of experimental results. For example, there is now an in vitro system for initiation and replication of Ad2/5 DNA (Challberg and Kelly, 1979). These investigators purified a cell-free extract from HeLa cells infected in the presence of hydroxyurea. This extract allowed replication of exogenous template DNA-terminal protein complex with added ribo- and deoxyribonucleosides triphosphates. However, the reaction of extract prepared 21 hours after infection was linear for 1 hour and stopped after 2 hours with only 6 percent of the input DNA replicated. This corresponds to about 60 Ad2 DNA molecules synthesized per cell where we have seen that in vivo about 120,000 Ad5 molecules are made per cell per hour. We conclude that while the in vitro system looks promising, it does not fully reflect in vivo replication and that this system is still very inefficient in replicating adenovirus DNA.

The methods of chemical kinetics have been useful in many systems for elucidating mechanism of reactions. Our application of these techniques to an in vivo study of adenovirus DNA replication has demonstrated the power and utility of kinetics even in such a complex environment.

REFERENCES

Abboud, M. M., and Horwitz, M. S. 1979. The DNA polymerases associated with the adenovirus type 2 replication complex: effect of 2'-3'-dideoxythymidine-5'-triphosphate on viral DNA synthesis. Nuc. Acids Res. 6, 1025-1039.

Ariga, H. and Shimojo, H. 1977. Initiation and Termination Sites of Adenovirus 12 DNA Replication. Virol. 78, 415-424.

Bellett, A. J. D., and Younghusband, H. B. 1972. Replication of the DNA of Chick Embryo Lethal Orphan Virus. J. Mol. Bio. 72. 691-709.

Bodnar, J. W. and Pearson G. D. 1980a. Kinetics of Adenovirus DNA Replication. I. Rate of Adenovirus DNA Replication. Virol. 100. 208-211.

Bodnar, J. W. and Pearson, G. D. 1980b. Kinetics of Adenovirus DNA Replication. II. Initiation of Adenovirus DNA Replication. manuscript submitted.

Bodnar, J. W. and Pearson, G. D. 1980c. Kinetics of Adenovirus DNA Replication. III. Model for Adenovirus DNA Replication. manuscript in preparation.

Bourgaux, P., Delbecchi, L. and Bourgaux-Ramoisy, D. 1976. Initiation of Adenovirus Type 2 DNA Replication. Virol. 72. 89-98.

Brison, O., Kedinger, C., and Chambon, P. 1979. Adenovirus DNA Template for Late Transcription Is Not a Replicative Intermediate. J. Virol. 32, 91-97.

Burlingham, B. T., Brown, D. T., and Doerfler, W. 1974. Incomplete Particles of Adenovirus. I: Characteristics of DNA Associated with Incomplete Adenovirions of Types 2 and 12. Virol. 60, 419-430.

Challberg, M. D. and Kelly, T. J., Jr. 1979. Adenovirus DNA replication in vitro. Proc. Natl. Acad. Sci. USA. 76, 655-659.

Chardonnet, Y. and Dales, S. 1970. Early events in the interaction of adenovirus with HeLa cells. I. Penetration of type 5 and intracellular release of the DNA Genome. Virol. 40, 462-477.

Coombs, D. H. and Pearson, G. D. 1978. Filter-binding assay for covalent DNA-protein complexes: Adenovirus DNA-terminal protein complex. Proc. Natl. Acad. Sci. USA. 75, 5291-5295.

Coombs, D. H., Robinson, A. J., Bodnar, J. W., Jones, C. J., and Pearson, G. D. 1979. Detection of Covalent DNA-Protein Complexes: The Adenovirus DNA-Terminal Protein Complex and HeLa DNA-Protein Complexes. Cold Spr. Hbr. Symp. Quant. Bio., 43, 741-753.

Cullen, C. G. 1967. Matrices and Linear Transformations. Addison-Wesley Pub. Co., Reading, Mass.

Daniell, E. 1976. Genome Structure of Incomplete Particles of Adenovirus. J. Virol. 19, 685-708.

Daniell, E. and Mullenbach, T. 1978. Synthesis of Defective Viral DNA in HeLa Cells Infected with Adenovirus Type 3. J. Virol. 26, 61-70.

Danna, K. J., and Nathans, D. 1972. Bidirectional Replication of Simian Virus 40 DNA. Proc. Natl. Acad. Sci. USA. 69, 3097-3100.

Dintzis, H. M. 1961. Assembly of the Peptide Chains of Hemoglobin. Proc. Natl. Acad. Sci. USA, 47, 247-261.

Doerfler, W. 1969. Nonproductive Infection of Baby Hamster Kidney Cells (BHK 21) with Adenovirus Type 12. Virol. 38, 587-606.

Doerfler, W., Lundholm, U., Rensing, U., and Philipson, L. 1973. Intracellular forms of adenovirus DNA. II. Isolation in dye-buoyant density gradients of a DNA-RNA complex from KB cells infected with adenovirus type 2. J. Virol. 12, 793-807.

Edenberg, H. J., and Huberman, J. A. 1975. Eukaryotic Chromosome Replication. Ann. Rev. of Genetics. 9. 245-284.

Ellens, D. J., Sussenbach, J. S., and Jansz, H. S. 1974. Studies on the Mechanism of Replication of Adenovirus DNA. III. Electron Microscopy of Replicating DNA. Virol. 61, 427-442.

Fanning, E., and Doerfler, W. 1977. Intracellular Forms of Adenovirus DNA. VI. Quantitation and Characterization of the Four Size-Classes of Adenovirus Type 2 DNA in Human KB Cells. Virol. 81, 433-448.

Fareed, G. C., McKerlie, M. L., and Salzman, N. P. 1973. Characterization of Simian Virus 40 DNA Component II during Viral DNA Replication. J. Mol. Bio. 74, 95-111.

Flint, J. 1977. The Topography and Transcription of the Adenovirus Genome. Cell. 10, 153-166.

Flint, S. J., Berget, S. M., and Sharp, P. A. 1976. Characterization of Single Stranded Viral DNA Sequences Present during Replication of Adenovirus Types 2 and 5. Cell. 9, 559-571.

Fujinaga, K., and Green, M., Mechanism of viral carcinogenesis by DNA mammalian viruses: VII. Viral genes transcribed in adenovirus type 2 infected and transformed cells. Proc. Nat. Acad. Sci. USA, 65, 375-382.

Gilead, Z., Sugawara, K., Shanmugam, G., and Green, M. 1976. Synthesis of the Adenovirus-Coded DNA Binding Protein in Infected Cells. J. Virol. 18, 454-460.

Girard, M., Bouché, J.-P., Marty, L., Revet, B., and Berthelot, N. 1977. Circular Adenovirus DNA-Protein Complexes from Infected HeLa Cell Nuclei. Virol. 83, 34-55.

Green, M. 1962a. Biochemical Studies on Adenovirus Multiplication III. Requirement for DNA Synthesis. Virol. 18, 601-613.

Green, M. 1962b. Studies on the Biosynthesis of Viral DNA. Cold Spr. Hbr. Symp. Quant. Bio. 27, 219-235.

Green, M. and Daesch, G. E. 1961. Biochemical Studies on Adenovirus Multiplication II. Kinetics of Nucleic Acid and Protein Synthesis in Suspension Cultures. Virol. 13, 169-176.

Green, M., Mackey, J. K., Wold, W. S. M., and Rigden, P. 1979. Thirty-one Human Adenovirus Serotypes (Ad1-Ad31) Form Five Groups (A-E) Based upon DNA Genome Homologies. Virol. 93, 481-492.

Green, M., Piña, M., and Kimes, R. C. 1967. Biochemical Studies on Adenovirus Multiplication. XII. Plaquing Efficiencies of Purified Human Adenoviruses. Virol. 31, 562-565.

Green, M. H., and Brooks, T. L. 1978. Recently Replicated Simian Virus 40 DNA is a Preferential Template for Transcription and Replication. J. Virol. 26, 325-334.

Gustafsson, P., Dreisig, H., Molin, S., Nordström, K., and Uhlin, B. E. 1979. DNA replication control: Studies of plasmid R1. Cold Spring Harbor Symp. Quant. Biol. 43, 419-425.

Habara, A., Kano, K., Nagano, H., Mano, Y., Ikegami, S., and Yamashita, T. 1980. Inhibition of DNA Synthesis in the Adenovirus DNA Replication Complex by Aphicolidin and 2', 3'-Dideoxythymidine Triphosphate. Biochem. and Biophys. Res. Comm. 92, 8-12.

Hand, R. and Tamm, I. 1974. Initiation of DNA replication in mammalian cells and its inhibition by Reovirus infection. J. Mol. Bio. 82, 175-183.

Hodge, L. D., and Scharff, M. D. 1969. Effect of Adenovirus on Host Cell DNA Synthesis in Synchronized Cells. Virology 37, 554-564.

Horwitz, M. 1971. Intermediates in the Synthesis of Type 2 Adenovirus Deoxyribonucleic Acid. J. Virol. 8, 675-683.

Horwitz, M. S. 1974. Location of the Origin of DNA Replication in Adenovirus Type 2. J. Virol, 13, 1046-1054.

Horwitz, M. S. 1976. Bidirectional Replication of Adenovirus Type 2 DNA. J. Virol. 18, 307-315.

Ito, K., Arens, M., and Green, M. 1975. Isolation of DNA Polymerase γ from an Adenovirus 2 DNA Replication Complex. J. Virol. 15, 1507-1510.

Kedinger, C., Brison, O., Purrin, F. and Wilhelm, J. 1978. Structural Analysis of Viral Replicative Intermediates Isolated from Adenovirus Type 2 - Infected HeLa Cell Nuclei. J. Virol. 26, 364-379.

Kelly, T. J., Jr. and Lechner, R. L. 1979. The Structure of Replicating Adenovirus DNA Molecules: Characterization of DNA-Protein Complexes from Infected Cells. Cold Spr. Hbr. Symp. Quant. Biol. 43, 721-728.

Lai, C.-J., and Nathans, D. 1975. Non-specific Termination of Simian Virus 40 DNA Replication. J. Mol. Bio. 97, 113-118.

Lavelle, G., Patch, C., Khoury, G., and Rose, J. 1975. Isolation and Partial Characterization of a Single Stranded Adenoviral DNA Produced During Synthesis of Adenovirus Type 2 DNA. J. Virol. 16, 775-782.

Lechner, R. L. and Kelly, T. J., Jr. 1977. The Structure of Replicating Adenovirus 2 DNA Molecules. Cell 12, 1007-1020.

Levine, A. J., Kang, H. S., and Billheimer, F. E. 1970. DNA Replication in SV40 Infected Cells I: Analysis of Replicating SV40 DNA. J. Mol. Bio. 50, 549-568.

Lonberg-Holm, K., and Philipson, L. 1969. Early Events of Virus-Cell Interaction in an Adenovirus System. J. Virol. 4, 323-338.

Longiaru, M., Ikeda, J., Jarkovsky, Z., Horwitz, S. B., and Horwitz, M. S. 1979. The effect of aphicolidin on adenovirus DNA synthesis. Nuc. Acids Res. 6, 3369-3386.

Mak, S. 1971. Defective Virions in Human Adenovirus Type 12. J. Virol. 7, 426-433.

Manteuil, S., Pages, J., Stehelin, D. and Girard, M. 1973. Replication of Simian Virus 40 Deoxynucleic Acid: Analysis of the One-Step Growth Cycle. J. Virol. 11, 98-106.

Nathans, D., and Danna, K. J. 1972. Specific Origin in SV40 DNA Replication. Nature, New Biol. 236, 200-202.

Painter, R. B. and Schaefer, A. W. 1969. Rate of Synthesis along Replicons of Different Kinds of Mammalian Cells. J. Mol. Bio. 45, 467-479.

Pearson, G. D. 1975. Intermediate in Adenovirus Type 2 Replication. J. Virol. 16, 17-26.

Pearson, G. D. 1976. The Structure and Replication of the Adenovirus Genome. in The Biology of Tumor Viruses. Oregon State U. Press.

Pearson, G. D., and Hanawalt, P. C. 1971. Isolation of DNA Replication Complexes from Uninfected and Adenovirus-infected HeLa Cells. J. Mol. Bio. 62, 65-80.

Pettersson, U. 1973. Some Unusual Properties of Replicating Adenovirus Type 2 DNA. J. Mol. Bio. 81, 521-527.

Philipson, L., Pettersson, U. and Lindberg, U. 1975. Virology Monographs. Molecular Biology of Adenoviruses. Springer-Verlag, New York.

Pierucci, O., and Helmstetter, C. E. 1969. Chromosome replication, protein synthesis, and cell division in Escherichia coli. Fed. Proc. 28, 1755-1760.

Prage, L., Höglund, S., and Philipson, L. 1972. Structural Proteins of Adenoviruses. VIII. Characterization of Incomplete Particles of Adenovirus Type 3. Virol. 49, 745-757.

Raleigh, E. A. and Davis, R. W. 1976. Determination of DNA Concentration by Electron Microscopy. Anal. Biochem. 72, 460-467.

Rekosh, D. M. K., Russell, W. C., Bellett, A. J. D., and Robinson, A. J. 1977. Identification of a Protein Linked to the Ends of Adenovirus DNA. Cell. 11, 283-295.

Robinson, A. J., Younghusband, H. B., and Bellett, A. J. D. 1973. A Circular DNA-Protein Complex from Adenoviruses. Virol. 56, 54-69.

Robinson, A. J., Bodnar, J. W., Coombs, D. H., and Pearson, G. D. 1979. Replicating Adenovirus 2 DNA Molecules Contain Terminal Protein. Virol. 96, 143-158.

Roman, A. 1979. Kinetics of Reentry of Polyoma Progeny Form I DNA into Replication as a Function of Time Post Infection. Virol. 96, 660-663.

Roman, A. and Dulbecco, R. 1975. Fate of Polyoma Form I DNA During Replication. J. Virol. 16, 70-74.

Rosenwirth, B. Tjia, S., Westphal, M., and Doerfler, W. 1974. Incomplete Particles of Adenovirus. II. Kinetics of Formation and Polypeptide Composition of Adenovirus Type 2. Virol. 60, 431-437.

Rouse, H. C. and Schlesinger, R. W. 1967. An Arginine-Dependent Step in the Maturation of Type 2 Adenovirus. Virol. 33, 513-522.

Salzman, N. P., and Thoren, M. M. 1973. Inhibition in the Joining of DNA Intermediates to Growing Simian Virus 40 Chains. J. Virol. 11, 721-729.

Sebring, E. D., Kelly, T. J., Jr., Thoren, M. M., and Salzman, N. P. 1971. Structure of Replicating Simian Virus 40 Deoxyribonucleic Acid Molecules. J. Virol. 8, 478-490.

Schilling, R., Weingärtner, B., and Winnacker, E.-L. 1975. Adenovirus Type 2 DNA Replication. II. Termini of DNA Replication. J. Virol. 16, 767-774.

Segel, I. H. 1975. Enzyme Kinetics. Behavior and Analysis of Rapid Equilibrium and Steady-State Enzyme Systems. John Wiley and Sons, New York, N. Y., pp. 957.

Sekikawa, K., and Fujinaga, K. 1977. Cleavage Maps of Human Adenovirus Type 7 DNA by Restriction Endonuclease Hind III and Eco RI. Virol. 82, 509-512.

Shenk, T. 1978. Construction of a Viable SV40 Variant Containing Two Functional Origins of DNA Replication. Cell 13, 791-798.

Simmons, T., Heywood, P., and Hodge, L. D. 1974. Intranuclear Site of Replication of Adenovirus DNA. J. Mol. Bio. 89, 423-433.

Sober, H. A. (ed.) 1970. Handbook of Biochemistry. Selected Data for Molecular Biology. The Chemical Rubber Co., Cleveland, Ohio, p. H-113.

Stillman, B. W., and Bellett, A. J. D. 1979. An Adenovirus Protein Associated with the Ends of Replicating DNA Molecules. Virol. 93, 69-79.

Strau, S. E., Sergeant, A., Tigges, M. A., and Raskas, H. J. 1979. Parental Adenovirus Type 2 Genomes Recovered Early or Late in Infection Possess Terminal Proteins. J. Virol. 29, 828-832.

Strohl, W. A., and Schlesinger, R. W. 1965. Quantitative Studies of Natural and Experimental Adenovirus Infections in Human Cells. I. Characteristics of Viral Multiplication in Fibroblasts Derived by Long-Term Culture from Tonsils. Virol. 26, 199-207.

Sussenbach, J. S., Ellens, D. J., and Jansz, H. S. 1973. Studies on the Mechanism of Replication of Adenovirus DNA. II. The Nature of Single Stranded DNA in Replicative Intermediates. J. Virol. 12, 1131-1138.

Sussenbach, J. S. and Kuijk, M. G. 1977. Studies on the Mechanism of Replication of Adenovirus DNA. V. The Location of Termini of Replication. Virol. 77, 149-157.

Sussenbach, J. S. and Kuijk, M. G. 1978. The Mechanism of Replication of Adenovirus DNA. VI. Localization of the Origins of the Displacement Dynthesis. Virol. 84, 509-517.

Sussenbach, J. S., and van der Vliet, P. C. 1973. Studies on the Mechanism of Replication of Adenovirus DNA. I. The Effect of Hydroxyurea. Virol. 54, 299-303.

Sussenbach, J. S., van der Vliet, P. C., Ellens, D. J., and Jansz, H. S. 1972. Linear intermediates in the replication of adenovirus DNA. Nature,New Biol. 239, 47-49.

Tapper, D. P., and DePamphilis, M. L. 1978. Discontinuous DNA Replication: Accumulation of Simian Virus 40 DNA at Specific Stages in its Replication. J. Mol. Bio. 120, 401-422.

Tibbetts, C. 1977a. Viral DNA Sequences from Incomplete Particles of Human Adenovirus Type 7. Cell 12, 243-249.

Tibbetts, C. 1977b. Physical Organization of Subgroup B Human Adenovirus Genomes. J. Virol. 24, 564-579.

Tibbetts, C., Pettersson, U., Johansson, K., and Philipson, L. 1974. Relationship of mRNA from Productively Infected Cells to the Complementary Strands of Adenovirus Type 2 DNA. J. Virol. 13, 370-377.

Tolun, A., Aleström, P. C. and Pettersson, U. 1979. Sequence of Inverted Terminal Repetitions from Different Adenoviruses: Demonstration of Conserved Sequences and Homology between SA7 Termini and SV40 DNA. Cell. 17, 705-713.

Tolun, A. and Pettersson, U. 1975. Termination Sites for Adenovirus Type 2 DNA Replication. J. Virol. 16, 759-766.

van der Eb, A. J. 1973. Intermediates in Type 5 Adenovirus DNA Replication. Virol. 51, 11-23.

van der Vliet, P. C., Blanken, W. M., Zandberg, J., and Janz, H. S. 1978. In "NATO Advanced Study Institutes Series" (I. Molineux and M. Kohiyana, eds.), 17, 869-883.

van der Vliet, P. C. and Kwant, M. M. 1978. Role of DNA polymerase γ in adenovirus DNA replication. Nature. 276, 532-534.

van der Vliet, P. C., and Sussenbach, J. S. 1972. The Mechanism of Adenovirus-DNA Synthesis in Isolated Nuclei. Eur. J. Biochem. 30, 584-592.

Vlak, J. M., Rozijn, T. H., and Spies, F. 1976. Replication of Adenovirus Type 5 DNA in KB Cells: Localization and Fate of Parental DNA during Replication. Virol. 72, 99-109.

Vlak, J. M., Rozijn, T. H., and Sussenbach, J. S. 1975. Studies on the Mechanism of Replication of Adenovirus DNA. IV. Discontinuous DNA Chain Propagation. Virol. 63, 168-175.

Wadell, G., Hammarskjöld, M.-L., and Varsanyi, T. 1973. Incomplete Virus Particles of Adenovirus Type 16. J. Gen. Virol. 20, 287-302.

Wadell, G., and Varsanyi, T. M. 1978. Demonstration of Three Different Subtypes of Adenovirus Type 7 by DNA Restriction Site Mapping. Infect. and Imm. 21, 238-246.

Walker, I. G., Yatscoff, R. W., and Sridhar, R. 1977. Hydroxyurea: Introduction of breaks in template strands of replicating DNA. Biochem. and Biophys. Res. Comm. 77, 403-408.

Weingärtner, B., Winnacker, E.-L., Tolun, A. and Pettersson, U. 1976. Two Complementary Strand-Specific Termination Sites for Adenovirus DNA Replication. Cell. 9, 259-268.

Wilhelm, J., Brison, O., Kedinger, C., and Chambon, P. 1976. Characterization of Adenovirus Type 2 Transcriptional Complexes Isolated from Infected HeLa Cell Nuclei. J. Virol. 19, 61-81.

Winnacker, E.-L. 1978. Adenovirus DNA: Structure and Function of a Novel Replicon. Cell 14, 761-773.

Wintersberger, E. 1978. DNA replication in eukaryotes. Rev. Physiol. Biochem. and Pharmacol. 84, 93-142.

APPENDICES

APPENDIX I.

MATERIALS AND METHODS

Cells and Virus.

HeLa S_3 cells were grown in suspension culture at concentrations between 2.5×10^5 and 6×10^5 cells per ml using medium F-13 (Grand Island Biological Co.) supplemented with 7 percent fetal calf serum (v:v) (Sterile Systems or Grand Island Biological Co.). Adenovirus type 2 was obtained from Dr. Joseph Weber, Department of Microbiology, University of Sherbrooke, Quebec, Canada. Adenovirus types 5 and 7 were obtained from the American Type Culture Collection. Crude virus lysates were prepared at 48 hours after infection by resuspending infected cells in PBSd plus 10 percent glycerol (v:v, 15 ml per liter of infected cells), sonicating, and clearing the lysate by low speed contrifugation. For virus infections cells were concentrated 10 to 50 times in serum free medium and inoculated with crude virus lysate (1 to 2 ml per liter). After 20 minutes the cells were diluted to 4×10^5 cells per ml. Adenovirus used for preparation of DNA size markers was purified by twice CsCl banding according to Doerfler (1969).

Enzymes

Pronase (Grade B, Calbiochem) was self-digested at 37° for 2 hr at a concentration of 10 mg/ml before use. Pancreatic ribonuclease XA (Sigma Chemical Co.) at 5 mg/ml in combination with T1 ribonuclease (Sigma Chemical Co.) at 5000 units/ml were heated to 100° for 5 min before use to inactivate any contaminating DNase activity.

Radioactive Labeling

HeLa DNA was labeled by growing cells in medium containing [^{3}H]thymidine (0.5 μCi/ml, 70 Ci/mmol, New England Nuclear or ICN) or [^{14}C]thymidine (0.05 μCi/ml, 50 mCi/mmol, New England Nuclear). Adenovirus DNA was labeled by growing infected cells in phosphate-free medium F-13 (Grand Island Biological Co.) containing 2 percent dialyzed fetal calf serum (v:v) (Grand Island Biological Co.) and [^{32}P] orthophosphate (20 μCi/ml, carrier-free, New England Nuclear). Pulse labeling of adenovirus DNA proceeded by growing infected cells in 10^{-6} M FUdR for 20 to 30 min to deplete thymidine pools, concentrating the cells 10 to 20 times, then adding [^{3}H]thymidine to 250 μCi/ml. Incorporation was stopped by adjusting cultures to 0.01M NaCN or KCN. Samples were precipitated on Whitman GFC filters and counted with a Packard Model 3330 scintillation counter by using the following settings: ^{32}P and ^{3}H; ^{32}P, 1%, 50-1000 and ^{3}H, 60%, 50-500; ^{14}C and ^{3}H; ^{14}C, 25%, 200-1000 and ^{3}H, 60%, 50-500.

Restriction Enzyme Digestions

Digestions were performed in 50 μl Buffer I (10 mM Tris, 1mM EDTA, 0.1 M KCl, pH 7.2) with DNA at 0.1 to 1 μg/μl. After addition of 5 μl 0.1M $MgCl_2$ restriction enzyme (1 unit/μg DNA) was added and incubated at 37° for 1 hr. A second aliquot of enzyme was added, and the sample was incubated for 1 hr at 37°. The reaction was stopped by addition of 5 μl of 0.2M EDTA.

Proteolytic Extraction of DNA

Infected cells (10-20 ml at 3-6 x 10^5 cells/ml) were spun down and washed in 10 ml PBSd (135 mM NaCl, 2 mM KCl, 8 mM Na_2HPO_4 1.5 mM KH_2PO_4), then centrifuged 5 min at 5,000 rpm in an HB-4 rotor. The pellet was resuspended in 2 ml PBSd with 0.4 ml 0.1 M EDTA, 0.2 ml Pronase (10 mg/ml), and 0.4 ml 10 percent SDS (v:v) and incubated at 37° for 2 hr. The sample was extracted with 2 ml phenol and vortexed 15 seconds. (Note that if the sample is not vortexed to shear the cellular DNA, the increased viscosity will make column chromatography and ^3H counting irreproducible.) Two more extractions with IAC (1:24 isoamyl alcohol:chloroform) and three ether extractions followed. The DNA preparations were further digested for 2 hr with pancreatic ribonuclease (10 μg/ml) and T1 ribonuclease (10 units/ml). This sample was then used directly on

BD-cellulose columns, dialyzed into 10 mM Tris, 1 mM EDTA, 10 mM NaCl, pH 7.5 for CsCl density gradient centrifugation or precipitated with 5 ml ethanol and 0.1 ml 4 M NaOAc in preparation for restriction enzyme digestion.

Ammonium Sulfate Extraction of Adenovirus DNA

Concentrated infected cells (10 ml at 5×10^6 to 10^7 cells/ml) were spun down then washed with PBSd as above. The cell pellet was resuspended in 2.5 ml TITE (0.1 M NaCl, 20 mM Tris, 10 mM EDTA, 0.02% Triton X100 (v:v), pH 7.9) on ice for 10 min then the cells were broken with 5 strokes in a Dounce homogenizer (B pestle). The sample was centrifuged 10 min at 2500 rpm in an HB-4 rotor, and the pellet was resuspended in 2.5 ml TEAD (50 mM ammonium sulfate, 20 mM Tris, 10 mM EDTA, 1 mM DTT, pH 7.9). Ammonium sulfate (0.3 ml, 2M) was added dropwise while swirling (final concentration = 200 mM). As the last drops were added the nuclei began to aggregate. After heating at 37° for 2 min the preparation was centrifuged 15 min at 10,000 rpm in an HB-4 rotor. The pellet was white and fluffy at this point for effective extraction of the adenovirus chromatin. The supernatent was saved, and PMSF was added to 0.1 mM if adenovirus DNA-protein complex was to be prepared by glycerol gradient centrifugation.

Glycerol Gradient Separation of Replicating and Mature Adenovirus DNA

Ammonium sulfate extracted adenovirus chromatin (about 2 ml) was layered on a 10 percent to 40 percent glycerol gradient in an SW 27.1 tube (7 ml 80 percent glycerol cushion (v:v) in 200 mM ammonium sulfate, 2 mM EDTA, 10 mM Tris, 0.1 mM PMSF, pH 7.9 under a 10 to 40 percent glycerol gradient in the same buffer). The gradients were centrifuged 5 hr at 24,000 rpm at 4°C in an SW 27 rotor. About 30 x 0.3 ml fractions were collected through a pin-hole in the bottom of the tube after discarding the cushion. Fractionation patterns are shown in Robinson et al, 1980.

Column Chromatography

Benzoylated-DEAE-cellulose (Sigma Chemical Co.) was poured into columns (0.5 ml in 3 ml syringes with a Whatman GFC filter for support) in buffer containing 0.25 M NaCl, 10 mM Tris-HCl (pH 8.0), and 5 mM EDTA. After samples were applied, the columns were washed 4 times with 1 ml of the buffer above, four times with 1 ml of 1 M NaCl, 10 mM Tris-HCl (pH 8.0), and 5 mM EDTA to elute the completely double stranded DNA, then finally four times with 1 ml of 1 M NaCl, 10 mM Tris-HCl (pH 8.0), 5 mM EDTA, and 2% caffeine to elute any partially single stranded DNA.

CsCl Density Gradient Centrifugation

CsCl gradients were constructed with 7.9 g CsCl plus 6.0 g liquid. The buffer contained 10 mM Tris-HCl (pH 7.6), 10 mM NaCl, and 1 mM EDTA. Centrifugation was for at least 36 hours (usually 42-48 hours) at 37,000 rpm at 20° in a 50-Ti angle rotor. Gradients were collected volumetrically from the bottom of the centrifuge tube as previously described (Pearson and Hanawalt, 1971).

Filter Binding Assay

The filter binding assay for adenovirus DNA containing terminal protein is described in detail in Coombs and Pearson (1978) and Robinson et al (1980).

Agarose Gel Electrophoresis

Adenovirus restriction fragments were separated on one percent agarose gels made in buffer containing 40 mM Tris, 1 mM EDTA, 20 mM sodium citrate, and 1 μg/ml ethidium bromide (pH 7.2). The gels were run at 50 volts using the same buffer for a running buffer. Bands were visualized with a short wave ultraviolet light, cut out, and counted after autoclaving in 0.5 ml water and mixing with 2 ml Handifluor.

APPENDIX II

Computer Programs

Programs were written for the Hewlett-Packard 9821A programmable calculator. Explanatory steps not in the actual programs are added here to define variables and describe sections of the program. These have the step number "R" for REMARK as written in the appendix.

Pulse Labeled Specific Activities

This program evaluates the average relative radioactivity ($\bar{F}_T(x_1, x_2, t)$) at any time following addition of a [^{3}H]thymidine pulse using the relationships and boundary conditions derived in Part I. The flow chart for boundary conditions is as below (with program steps circled (x)).

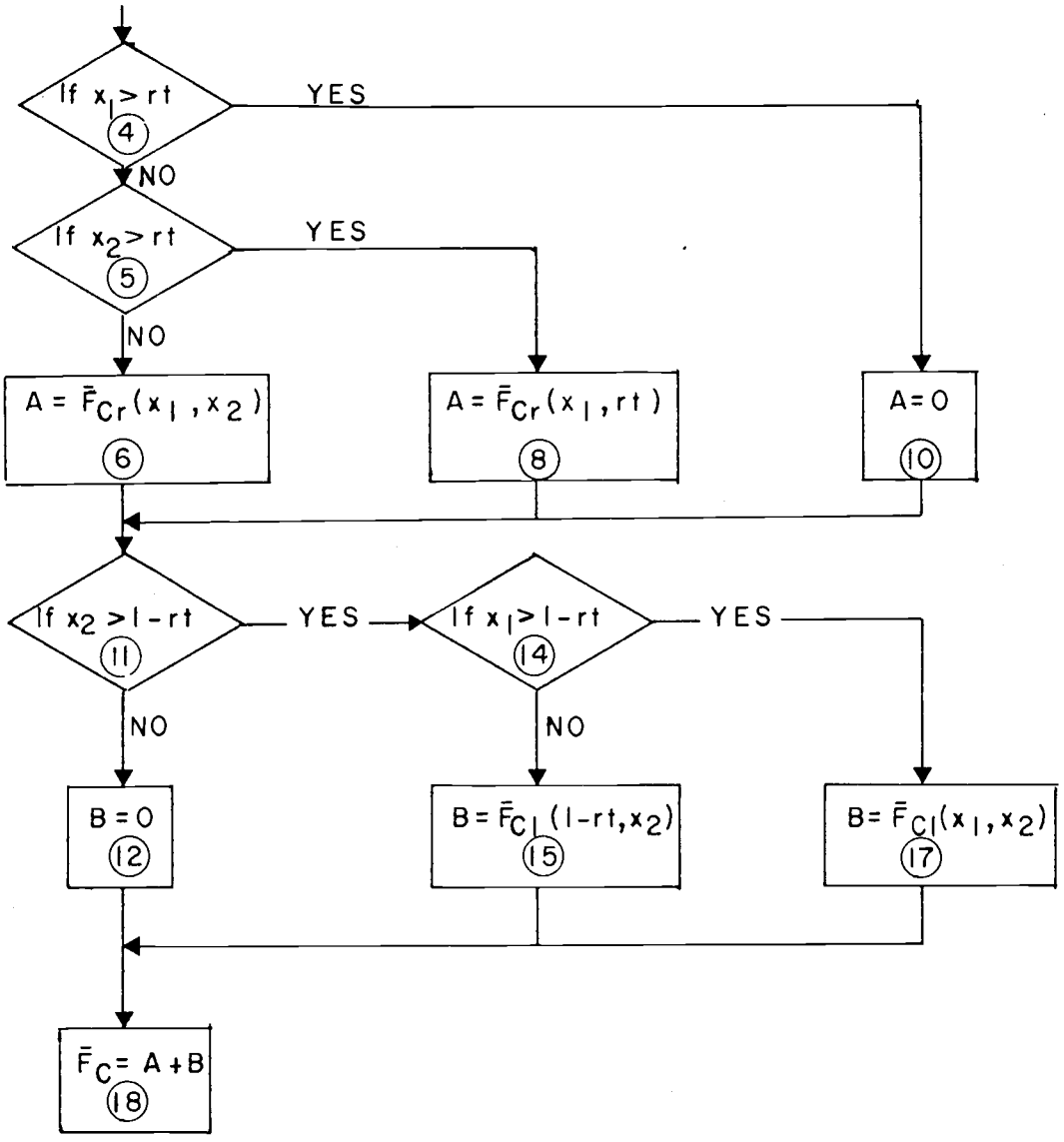

The following variables are used:

A = $\overline{F}_{Cr}$

B = $\overline{F}_{Cl}$

R1 = x_1 = left end of restriction fragment

R2 = x_2 = right end of restriction fragment

R3 = r = replication rate

R4 = t = pulse length

R10 = normalization factor (used to relate specific activity of a fragment to the fragment with the highest specific activity).

```
 0    ENT "RATE", R3
 1    ENT "PULSE TIME", R4, "NORM FACTOR", R1Ø
 3    ENT "RIGHT END", R2; FXD 4; Ø →A; Ø →B
 4    IF R1 > R3*R4; GTO 1Ø
 5    IF R2 > R3*R4; GTO 8
 6    Ø.5 (2*R3*R4 - (R1 + R2)) → A
 7    GTO 11
 8    Ø.5 (2*R3*R4 - (R1 + R3*R4)) →A
 9    GTO 11
10    Ø →A
11    IF R2 > 1 - R3*R4; GTO 14
12    Ø →B
13    GTO 18
14    IF R1 > 1 - R3*R4; GTO 17
15    Ø.5 (1 - R3*R4 + R2 - 2* (1 - R3*R4)) →B
16    GTO 18
17    Ø.5 (R1 + R2 - 2* (1 - R3*R4)) →B
18    (A + B) * R1Ø →C
19    SPC 1; PRT "ENDS", R1, R2, "REL ACT", C
20    GTO 2
21    END
```

Density Shift Kinetics

This program calculates the relative [HH], [HL], and [LL] for the chase of a BUdR density label as shown in Part II. The shape of the percent [HL] curve as a function of i'/i can be calculated as shown in Part II, Figure 5.

```
 R    R1 = i (for HH); R1Ø = i' (for HL and LL)
 0    ENT "I1", R1, "I1", R1Ø; FXD 3
 1    Ø →R2; Ø →R3; Ø →R4; Ø →R5; Ø →R7
 R    T MAX is the length of the chase.
 2    ENT "T MAX", R6
 3    PRT "I1 = ", R1, "I2 = ", R1Ø
 4    EXP (-2*R1*R5) →R2
 5    2* (1 - EXP (-2*R1*R5)) →R3
 6    2/(R1 + R1Ø)*(R1*EXP(2*R1Ø*R5) + R1Ø*EXP(-2*R1*R5))-2 →R4
 7    R3/(R2 + R3 + R4) →R7
 8    PRT "TIME", R5; SPC 1
 9    PRT "HH, HL, LL", R2, R3, R4, "FRACTION HL", R7
10    SPC 3
11    R5 + 5 →R5
 R    R5 = time counter (5 min intervals)
12    IF R5 ≤ R6; GTO 4
13    END
```

Iterative Growth Simulation
Using Saturable Kinetics

This program simulates growth of adenovirus DNA by an iterative method as described in Part II (see Figure 6). It computes physical parameters versus time post infection as shown in Part III (Table 1 and Figure 1).

```
 R   R1 = r_I; R2 = r_II; R3 = V_max; R7 = K_m; R4 = i_s. Enter rate
     parameters.
 0   ENT "RATE 1", R1, "RATE 2", R2
 1   ENT "V MAX", R3, "K M", R7, "I(S)", R4; FXD 4
 R   R101 = CPM(Ø) = Initial Value for [DS]
 2   Ø →R151; Ø →C; ENT "CPM(Ø), R101
 3   1/R1 →R5; 1/R2 →R6; 1 →X; 1 →Y; Ø →R5Ø
 R   R101 = [DS]; R(2ØØ + X) = [I]_x where each pool represents type I
     molecules 1/xth complete; R(3ØØ + Y) = [II]_y for type II molecules;
     R401 = [SS]; R151 = Δ[DS]; R(25Ø + X) = Δ[I]_x; R(35Ø + Y) =
     Δ[II]_y; R451 = Δ[SS]. Set all pools equal to zero.
 4   Ø →R(2ØØ + X); Ø →R(25Ø + X).
 5   X + 1 →X; IF X ≤ R5 + 1; GTO 4
 6   Ø →R(3ØØ + Y); Ø →R(35Ø + Y)
 7   Y + 1 →Y; IF Y ≤ R6 + 1; GTO 6
 8   Ø →R 401; Ø →R451
 9   PRT "RATE 1", R1, "RATE 2", R2
10   PRT "V MAX", R3, "K M", R7, "I(S)", R4
11   SPC 2
 R   Calculate changes in pool sizes in one minute.
12   R(3ØØ + R6) + R(2ØØ + R5) - R3/(R7 + R101) * R101 →R151
13   R3/(R7 + R101) * R101 - R201 →R251
14   2 →X
15   R(199 + X) - R(2ØØ + X) →R(25Ø + X)
16   X + 1 →X; IF X ≤ R5 + 1; GTO 15
17   R4 * R401 - R301 →R351
18   2 →Y
19   R(299 + Y) - R(3ØØ + Y) →R(35Ø + Y)
20   Y + 1 →Y; IF Y ≤ R6 + 1; GTO 19
21   R(2ØØ + R5) - R4 * R401 →R451
 R   Increment each pool as [X] = [X] + Δ[X].
```

```
22    R1Ø1 + R151 →R1Ø1
23    1 →X
24    R (2ØØ + X) + R (25Ø + X) →R (2ØØ + X)
25    X + 1 →X; IF X ≤ R5 + 1; GTO 24
26    1→ Y
27    R (3ØØ + Y) + R (35Ø + Y →R (3ØØ + Y)
28    Y + 1 →Y; IF Y ≤ R6 + 1; GTO 27
 R    R5Ø = time counter (in minutes); C = loop time increment (min).
29    1 + R5Ø →R5Ø; R4Ø1 + R451 →R4Ø1
30    C + 1 →C; IF C ≤ 29; GTO 12
31    Ø →C; R5Ø/6Ø →Z; FXD 2
32    PRT "TIME (HR)", Z; SPC 1; FLT 3
33    Ø →Z; 1 →X; Ø →R2Ø; Ø →R21
 R    Z = [I]total; A = [II]total; R2Ø = CPM [I]total; R3Ø = CPM [II]total
      R21 = CPM SS in [I]; R31 = CPM SS in [II].
 R    Total all pool of type I and II correcting for relative CPM in
      each molecule.
34    Z + R (2ØØ + X) →Z; R2Ø + (X*R1*2)/2*R(2ØØ + X) →R2Ø; Ø.5 *
      (X*R1) * R (2ØØ + X) →R22
35    R22 + R21 →R21; X + 1 →X; IF X≤ R5 + 1; GTO 34
36    PRT R1Ø1, Z
37    Ø →A; 1 →Y; Ø →R3Ø; Ø →R31
38    A + R (3ØØ + Y) →A; R3Ø + (Y*R2+1)/2*R(3ØØ + Y) →R3Ø; Ø.5
      (1 - Y*R2) *R (3ØØ + Y) →R32
39    Y + 1 →Y; R31 + R32 →R31; IF Y ≤ R6 + 1; GTO 38
40    PRT A, R4Ø1
 R    B = total [DNA], R23 = total CPM [DNA]
41    R1Ø1 + A + Z + R4Ø1 →B; R1Ø1 + R2Ø + R3Ø + Ø.5 * R4Ø1 →R23
42    PRT "TOTAL DNA - NR, CPM", B, R23
43    (R23 - R1Ø1)/R23*1ØØ →B; PRT "PCT REP", B
44    (R21 + R31 + Ø.5*R4Ø1)/R23*1ØØ - B; PRT "PCT SS", B
45    Ø.5*R3/(R7 + R1Ø1) →B; PRT "I = ", B
46    GTO 11
47    END
 R    Program is an endless loop; stop when enough data has been
      obtained.
```

Average Growing Points per
Replicating Molecule Calculation

This program calculates the fraction of CPM that will bind a glass fiber filter for a given average number of growing points per molecule when pulse labeled replicating molecules are assayed with the filter binding assay as shown in Part III, Figure 4. The number and right end coordinates of the fragments of the desired restriction enzyme are the input variables as shown below:

Average growing points per molecule = R25

Number of restriction fragments = R6 (up to 13 can be used)

r_I = R3 ; r_{II} = R5

t = R4 = pulse time

```
0:
FXD 3;ENT "AVG F
ORKS",R25;ENT "N
R FRAG",R6;PRT "
AVG FORKS/DNA",R
25⊢
1:
PRT "NR FRAG",R6
;ENT "RT END 1",
R11⊢
2:
IF R6=1;GTO "AA"
⊢
3:
ENT "RT END 2",R
12⊢
4:
IF R6=2;GTO "AA"
⊢
5:
ENT "RT END 3",R
13⊢
6:
IF R6=3;GTO "AA"
⊢
7:
ENT "RT END 4",R
14⊢
8:
IF R6=4;GTO "AA"
⊢
9:
ENT "RT END 5",R
15;IF R6=5;GTO "
AA"⊢
10:
ENT "RT END 6",R
16;IF R6=6;GTO "
AA"⊢
11:
ENT "RT END 7",R
17;IF R6=7;GTO "
AA"⊢
12:
ENT "RT END 8",R
18;IF R6=8;GTO "
AA"⊢
13:
ENT "RT END 9",R
19;IF R6=9;GTO "
AA"⊢
```

```
14:
ENT "RT END 10",
R20;IF R6=10;
GTO "AA"⊢
15:
ENT "RT END 11",
R21;IF R6=11;
GTO "AA"⊢
16:
ENT "RT END 12",
R22;IF R6=12;
GTO "AA"⊢
17:
ENT "RT END 13",
R23⊢
18:
"AA";PRT "RT END
S"⊢
19:
1→X⊢
20:
PRT R(10+X)⊢
21:
1+X→X;IF X≤R6;
GTO 20⊢
22:
ENT "RATE 1",R3;
0→R10⊢
23:
ENT "RATE 2",R5;
PRT "RATE 1",R3,
"RATE 2",R5⊢
24:
ENT "PULSE TIME"
,R4;PRT "PULSE T
IME",R4⊢
25:
1→R8;0→R50;0→R7;
0→R9⊢
26:
0→A;0→B;0→X;0→Y;
R(9.+R8)→R1;R(10
+R8)→R2⊢
27:
FXD 2⊢
28:
IF R1>R3*R4;GTO
34⊢
29:
IF R2>R3*R4;GTO
32⊢
30:
.25(2*R3*R4-(R1+
R2))→A⊢
31:
GTO 35⊢
32:
.25(2*R3*R4-(R1+
R3*R4))→A⊢
33:
GTO 35⊢
34:
0→A⊢
35:
IF R2>1-R3*R4;
GTO 38⊢
36:
0→B⊢
37:
GTO 42⊢
38:
IF R1>1-R3*R4;
GTO 41⊢
39:
.25(1-R3*R4+R2-2
(1-R3*R4))→B⊢
40:
GTO 42⊢
41:
.25(R1+R2-2(1-R3
*R4))→B⊢
42:
IF R1>R4*R5;GTO
48⊢
43:
IF R2>R4*R5;GTO
46⊢
44:
.25(2*R4*R5-(R1+
R2))→X⊢
45:
GTO 49⊢
46:
.25(2*R4*R5-(R1+
R4*R5))→X⊢
47:
GTO 49⊢
48:
0→X⊢
49:
IF R2>1-R4*R5;
GTO 52⊢
```

```
50:
0→Y⊢
51:
GTO 56⊢
52:
IF R1>1-R4*R5;
GTO 55⊢
53:
.25(1-R4*R5+R2-2
(1-R4*R5))→Y⊢
54:
GTO 56⊢
55:
.25(R1+R2-2(1-R4
*R5))→Y⊢
56:
(R5*R4*2-(A+B)*R
5/R3-(X+Y))*(R2-
R1)→C⊢
57:
IF R8=1;GTO "AB"
⊢
58:
IF R8=R6;GTO "AB
"⊢
59:
C*(1-EXP (-R25*(
R2-R1)))+R9→R9;R
50+C→R50⊢
60:
GTO "AC"⊢
61:
"AB";C+R7→R7;R50
+C→R50⊢
62:
"AC";R8+1→R8;IF
R8≤R6;GTO 26⊢
63:
(R7+R9)*100/R50→
X;R7*100/R50→Y⊢
64:
PRT "PCT ON FILT
ER";X⊢
65:
PRT "PCT ON FILT
ER","AFTER S1";Y
;SPC 14⊢
66:
GTO 0⊢
67:
END ⊢
Σ17355
R979
```

Pulse and Chase Simulation

This program simulates a pulse and chase experiment for adenovirus DNA as described in Part III. The variables used are:

r_I = R1

r_{II} = R2

V_{max} = R3

K_m = R7

i_s = R4

x = CPM incorp per rep molecule = R51

t_o = pulse start time = R53

t_1 = chase start time = R54

CPM ^{3}H = R55

Pools of numbers of DNA molecules as described in Iterative Growth Simulation Program

Pools for ^{3}H pulse activity:

DS = R102, ΔDS = R152

I_x = R(225+x), ΔI_x = R(275+x)

II_x = R(325+x), ΔII_x = R(375+x)

SS = R402, ΔSS = R452

```
0:
ENT "RATE 1",R1,
"RATE 2",R2⊢
1:
ENT "V MAX",R3,"
K M",R7,"I(S)",R
4;FXD 4⊢
2:
0→R151;0→C;ENT "
CPM(0)",R101;0→R
102;0→R152;0→R15
1;0→R51⊢
3:
1/R1→R5;1/R2→R6;
1→X;1→Y;0→R50⊢
4:
0→R(200+X);0→R(2
50+X);0→R(225+X)
;0→R(275+X);0→R(
125+X);0→R(175+X
)⊢
5:
X+1→X;IF X≤R5+1;
GTO 4⊢
6:
0→R(300+Y);0→R(3
50+Y);0→R(325+Y)
;0→R(375+Y);0→R(
425+Y);0→R(475+Y
)⊢
7:
Y+1→Y;IF Y≤R6+1;
GTO 6⊢
8:
0→R401;0→R451;0→
R402;0→R452;ENT
"PULSE START",R5
3;ENT "CHASE",R5
4⊢
9:
PRT "RATE 1",R1,
"RATE 2",R2⊢
```

```
10:
PRT "V MAX",R3,"
K M",R7,"I(S)",R
4⊢
11:
PRT "PULSE TIME(
HR)",R53,R54;
SPC 2⊢
12:
R(300+R6)+R(200+
R5)-2*R3/(R7+R10
1)*R101→R151⊢
13:
2*R3/(R7+R101)*R
101-R201→R251⊢
14:
2→X⊢
15:
R(199+X)-R(200+X
)→R(250+X)⊢
16:
X+1→X;IF X≤R5+1;
GTO 15⊢
17:
R4*R401-R301→R35
1⊢
18:
2→Y⊢
19:
R(299+Y)-R(300+Y
)→R(350+Y)⊢
20:
Y+1→Y;IF Y≤R6+1;
GTO 19⊢
21:
R(200+R5)-R4*R40
1→R451⊢
22:
R51*R(300+R6)+R(
325+R6)+1.0*R51*
R(200+R5)+R(225+
R5)→R152⊢
23:
R152+R(125+R5)*0
.5-2*R3*R102/(R7
+R101)+R(425+R6)
→R152⊢
24:
2*R3/(R7+R101)*R
102-R126→R176⊢
25:
2→X⊢
26:
R(224+X)-R(225+X
)→R51*R(199+X)→R
(275+X);R(124+X)
-R(125+X)→R(175+
X)⊢
27:
X+1→X;IF X≤R5+1;
GTO 26⊢
28:
R4*R402-R426→R47
6⊢
29:
2→Y⊢
30:
R(324+Y)-R(325+Y
)→R51*R(299+Y)→R
(375+Y);R(424+Y)
-R(425+Y)→R(475+
Y)⊢
31:
Y+1→Y;IF Y≤R6+1;
GTO 30⊢
32:
R(125+R5)*0.5-R4
*R402→R452⊢
33:
R101+R151→R101;R
102+R152→R102⊢
34:
1→X⊢
35:
R(200+X)+R(250+X
)→R(200+X);R(225
+X)+R(275+X)→R(2
25+X)⊢
36:
R(125+X)+R(175+X
)→R(125+X);X+1→X
;IF X≤R5+1;GTO 3
5⊢
37:
1→Y⊢
38:
R(300+Y)+R(350+Y
)→R(300+Y);R(325
+Y)+R(375+Y)→R(3
25+Y)⊢
39:
R(425+Y)+R(475+Y
)→R(425+Y);Y+1→Y
;IF Y≤R6+1;GTO 3
8⊢
```

```
40:
R401+R451→R401;R
402+R452→R402⊢
41:
IF R50/60≤R53;
GTO "AA"⊢
42:
IF R50/60>R54;
GTO "AA"⊢
43:
1E-2→R51;GTO "AB
"⊢
44:
"AA";0→R51⊢
45:
"AB";1+R50→R50⊢
46:
IF R50>R53*60;
GTO "AC"⊢
47:
C+1→C;IF C≤29;
GTO 12⊢
48:
"AC";C+1→C;IF C≤
2;GTO 12⊢
49:
0→C;R50/60→Z;
FXD 2⊢
50:
PRT "TIME (HR)",
Z;SPC 1;FLT 3⊢
51:
0→Z;1→X;0→B⊢
52:
Z+R(200+X)→Z;B+R
(225+X)+R(125+X)
→B⊢
53:
X+1→X;IF X≤R5+1;
GTO 52⊢
54:
PRT R101,Z⊢
55:
0→A;0→X;1→Y⊢
56:
A+R(300+Y)→A;X+R
(325+Y)+R(425+Y)
→X⊢
57:
Y+1→Y;IF Y≤R6+1;
GTO 56⊢
58:
PRT A,R401⊢
59:
R101+A+Z+R401→A⊢
60:
PRT "TOTAL DNA",
A⊢
61:
(A-R101)/A*100→A
;PRT "PCT REP",A
⊢
62:
R3/(R7+R101)→A;
PRT "I =",A⊢
63:
SPC 2;PRT "PULSE
 CPM"⊢
64:
PRT R102,B,X,R40
2⊢
65:
R102+X+B+R402→R6
5⊢
66:
PRT "TOTAL PULSE
 DNA",R65⊢
67:
(R65-R102)/(R65+
.1)*100→R55⊢
68:
PRT "PCT REP PUL
SE",R55⊢
69:
1→X;0→B⊢
70:
R(125+X)*X*R1/(X
+R1+2)+B→B⊢
71:
X+1→X;IF X≤R5+1;
GTO 70⊢
72:
1→Y⊢
73:
R(425+Y)*Y*R2/(Y
*R2+1)+B→B⊢
74:
Y+1→Y;IF Y≤R6+1;
GTO 73⊢
75:
B→R402→B⊢
76:
B/(R65+.01)*100→
A⊢
```

```
77:
PRT "PCT SI SENS
.";A⊢
78:
SPC 2;GTO 12⊢
79:
END ⊢
S26026
R901
```

Matrix Solution for Rate Constants Using EM Data

This program calculates the relative pool sizes for the various replicative forms for input values of i, i_s, r_I, and r_{II}. The program uses the pivot method for solution of a matrix (Cullen, 1967), assumes defective DNA produced by the premature strand displacement mechanism, and uses the matrix in Part III, Figure 7 (with an additional pool for defective DNA).

The following variables are used:

r_I = R1

r_{II} = R2

i = R3

i_s = R4

Matrix element (X, Y) = R (20*X+Y)

```
0:
ENT "RATE 1",R1;
FXD 4;PRT "RATE
1",R1⊢
1:
ENT "RATE 2",R2;
PRT "RATE 2",R2⊢
2:
ENT "I",R3;PRT "
2 STRAND INIT",R
3⊢
3:
ENT "I (S)",R4;
PRT "1 STRAND IN
IT",R4⊢
4:
1→X;1→Y;R2(R1-R2
)/R1→R496⊢
5:
0→R(20*X+Y)⊢
6:
Y+1→Y;IF Y<12;
GTO 5⊢
7:
X+1→X;1→Y;IF X<1
2;GTO 5⊢
8:
-2→R3→R21;R2→R23
;R1→R25;1→R32;R2
/R3(R1+R3)/(R1-R
2)→R252⊢
9:
-R3*R496/R2-R1+R
2→R42;R3*R496/R2
→R43;R496→R50;2*
R2→R51;1→X⊢
10:
R1-R2→R62;-R3-R2
→R63;R4→R64;4*R1
→R68;2*R1→R71;1→
Y⊢
```

```
11:
-R4→R84;R1→R85;R
1→R86;R1→R87;1→C
;0→R500⊢
12:
2*R3→R101;-R2*R3
/R1→R102;R2*R3/R
1→R103;-R1-2*R3→
R105⊢
13:
R1→R107;R496→R11
0;2*R2→R111;-R1→
R126;R3→R127;R2*
R3/R1→R130⊢
14:
R2*R3/R1→R142;R3
→R145;R1→R146;-R
1-2*R3→R147;R496
→R149⊢
15:
-R2*R3/R1→R150;R
3→R165;-2*R3-2*R
1→R168;-R1+R2→R1
89⊢
16:
R3(1-R2/R1)→R190
;R3(1-R2/R1)→R20
2;(R1-R2)(1-R2/R
1)→R209⊢
17:
-R1+R2-R3(1-R2/R
1)→R210;R3→R227;
2*R3→R228;-2*R1→
R231;1→X⊢
18:
0→R800⊢
19:
IF C=X;GTO "AA"⊢
20:
R(20*X+C)→R500⊢
21:
R(20*C+C)→R(20*X
+Y)-R500*R(20*C+
Y)→R(20*X+Y)⊢
22:
Y+1→Y;IF Y≤12;
GTO 21⊢
23:
1→Y⊢
24:
"AA";X+1→X;IF X≤
12;GTO 18⊢
25:
1→X⊢
26:
1→A;1→B⊢
27:
R(20+B+B)→R6⊢
28:
R(20*B+A)/R6→R(2
0*B+A)⊢
29:
A+1→A;IF A≤12;
GTO 28⊢
30:
B+1→B;1→A;IF B≤1
2;GTO 27⊢
31:
C+1→C;IF C≤11;
GTO 18⊢
32:
1→X;0→R425;R3*(R
1-R2)/(R2*(R1+R3
))→R414⊢
33:
R(20*X+12)→R(400
+X)⊢
34:
R(400+X)+R425→R4
25⊢
35:
X+1→X;IF X≤12;
GTO 33⊢
36:
1→X;FXD 2;PRT "P
CT DNA TYPE";R40
1/R425*100*R414→
R413⊢
37:
R(400+X)/R425*10
0→R(400+X)⊢
38:
PRT R(400+X)⊢
39:
X+1→X;IF X≤11;
GTO 37⊢
40:
PRT R413,"PCT RE
P POOL"⊢
41:
.875*R402+.75*R4
03+.5*R404+1.25*
R405+1.75*R406+1
.5*R407→Z⊢
```

```
42:
1.25*R408+1.25*R
409+R410+1.75*R4
11+.25*R413+Z→R4
97⊢
43:
R497/(R497+R401)
*100→Z;PRT Z;
ENT "NR MOL.",R4
99⊢
44:
PRT "NR REP MOLE
CULES",R499⊢
45:
R402+R403+R405+R
406+R407+R408+R4
09+R410+R411→R49
8⊢
46:
(R405+R406+R407+
R408+R411)/R498*
R499→A⊢
47:
PRT "TOTAL TYPE
1",A⊢
48:
R405/R498*R499→A
⊢
49:
PRT "   1 SS DNA
 ","   BRANCH",A
⊢
50:
(R407+R408)/R498
*R499→A⊢
51:
PRT "   2 SS DNA
","   BRANCH",A⊢
52:
(R406+R411)/R498
*R499→A⊢
53:
PRT "   3 SS DNA
","   BRANCH",A⊢
54:
R403/R498*R499→A
⊢
55:
PRT "TYPE 2",A⊢
56:
SPC 1⊢
57:
(R402+R409+R410)
/R498*R499→A⊢
58:
PRT "TOTAL TYPE
1/2",A⊢
59:
R402/R498*R499→A
⊢
60:
PRT "   1 SS DNA
","   BRANCH",A⊢
61:
R410/R498*R499→A
⊢
62:
PRT "   2 SS DNA
","   BRANCH",A⊢
63:
R409/R498*R499→A
⊢
64:
PRT "   3 SS DNA
","   BRANCH",A⊢
65:
2*R402+R403+R405
+3*R406+2*R407+2
*R408+4*R409+3*R
410→A⊢
66:
(A+3*R411)/R498→
A⊢
67:
PRT "INITIATION"
,"SITES PER DNA"
,A⊢
68:
.429*.875*R402+.
333*.750*R403+.5
00*R404+.200*1.2
5*R405→Z⊢
69:
Z+.429*1.75*R406
+.333*1.5*R407+.
111*1.25*R408→Z⊢
70:
Z+.333*1.25*R409
+.250*1.00*R410+
.429*1.75*R411+.
25*R413→Z⊢
71:
Z/(R497+R401)*10
0→Y;PRT "PCT OF
TOTAL","DNA AS S
S DNA",Y⊢
```

```
72:
(.5*R404+.25*R41
3)/(R497+R401)*1
00→Y⊢
73:
PRT "PCT COMPLET
ELY","SS DNA",Y⊢
74:
2/R497*100→Y;
PRT "PCT SS DNA
IN"," REP POOL",
Y⊢
75:
GTO 0;SPC 14⊢
76:
END ⊢
24459
R851
```

Specific Activity of Pulse
Labeled SV40 DNA Fragments

This program calculates the relative specific activity of pulse labeled restriction fragments for SV40 DNA using the model derived in Part IV, Theory. The variables used are:

r = R3

t = R4

Normalization Factor (to relate activities to highest specific activity = R1Ø

Left end of restriction fragment = R5

Right end of restriction fragment = R6

Note that all input and output genome positions use the normal SV40 coordinates, but that within the program the zero is the origin of replication.

```
Ø:
ENT "RATE",R3;
SPC 4;PRT "SV 40
 TERMINI";SPC 2;
PRT "RATE",R3⊢
1:
ENT "PULSE TIME"
,R4,"NORM FACTOR
",R10;PRT "PULSE
 TIME",R4⊢
2:
ENT "LEFT END",R
5⊢
3:
IF R5<.17;GTO 5⊢
4:
R5+.33-1.0→R1;
GTO 6⊢
5:
R5+.33→R1⊢
6:
ENT "RIGHT END",
R6;FXD 4;0→A;0→B
⊢
7:
IF R6<.17;GTO 9⊢
8:
R6+.33-1.0→R2;
GTO 10⊢
9:
R6+.33→R2⊢
10:
IF R2≤R3+R4-0.5;
GTO "AA"⊢
11:
IF R1≤R3+R4-0.5;
GTO "AD"⊢
12:
0→A;GTO "BA"⊢
13:
"AA";IF R1≤0;
GTO "AB"⊢
```

```
14:
IF R2≤0;GTO "AF"
⊢
15:
0→A;GTO "BA"⊢
16:
"AF";(-0.5(R2-0.
5)+R3*R4-0.5)*
ABS (R2+0.5)→A;
GTO "BA"⊢
17:
(-0.5(0-0.5)+R3*
R4-0.5)0.5→A;
GTO "BA"⊢
18:
IF R2>0;GTO "AF"
⊢
19:
"AB";IF R2≤0;
GTO "AC"⊢
20:
-0.5(0+R1)+R3*R4
-0.5→A;A*ABS R1→
A;GTO "BA"⊢
21:
"AC";-0.5(R1+R2)
+R3*R4-0.5→A;A*
ABS (R2-R1)→A;
GTO "BA"⊢
22:
"AD";IF R3*R4≤0.
5;GTO "AE"⊢
23:
IF R2>0;GTO "AG"
⊢
24:
-0.5(R1+0)+R3*R4
-0.5→A;A*ABS R1→
A;GTO "BA"⊢
25:
"AG";0→A;GTO "BA
"⊢
26:
"AE";(-0.5(R1+R3
+R4-0.5)+R3*R4-.
5)*ABS (R3*R4-.5
-R1)→A;GTO "BA"⊢
27:
"BA";IF R2≤0.5-R
3*R4;GTO "BB"⊢
28:
IF R1≤0.5-R3*R4;
GTO "BD"⊢
29:
IF R2≤0;GTO "BG"
⊢
30:
IF R1≤0;GTO "BH"
⊢
31:
(0.5(R1+R2)+R3*R
4-0.5)(R2-R1)→B;
GTO "CA"⊢
32:
"BB";IF R1≤R2;
GTO "BC"⊢
33:
(0.5(R1+0.5)+R3*
R4-0.5)(0.5-R1)→
B;GTO "CA"⊢
34:
"BC";0→B;GTO "CA
"⊢
35:
"BD";IF R3*R4>0.
5;GTO "BE"⊢
36:
(0.5(0.5-R3*R4+R
2)+R3*R4-0.5)(R2
-0.5+R3*R4)→B;
GTO "CA"⊢
37:
"BE";IF R2≤0;
GTO "BF"⊢
38:
(0.5(0+R2)+R3*R4
-0.5)(R2-0)→B;
GTO "CA"⊢
39:
"BF";0→B;GTO "CA
"⊢
40:
"BG";0→B;GTO "CA
"⊢
41:
"BH";(0.5(0+R2)+
R3*R4-0.5)(R2-0)
→B;GTO "CA"⊢
42:
"CA";IF R5>R6;
GTO "CB"⊢
43:
(A+B)/(R6-R5)*R1
0→C;GTO "CC"⊢
```

```
44:
"CB";(A+B)/(R6-1
+R5)*R10→CH
45:
"CC";PRT "ENDS",
R5,R6,"REL ACT",
CH
46:
GTO 2H
47:
END H
Σ21765
R996
```

SV40 Growth Curve Simulation

This program simulates total accumulation of SV40 DNA using saturable kinetics by the method described in Part IV, Theory. The variables used are:

r	= R1	Δ[MAT]	= R151
V_{max}	= R2	$\Delta[REP_x]$	= R(250+x)
K_m	= R3	time counter	= C
MOI	= R4		
[MAT]	= R101		
$[REP_x]$	= R(200+x)		

```
0:
SPC 2;PRT "SV 40
 GROWTH";SPC 2⊢
1:
ENT "RATE",R1⊢
2:
ENT "V MAX",R2,"
K M",R3;FXD 4⊢
3:
0→R151;0→C;ENT "
CPM(0)",R101;
ENT "MOI",R4⊢
4:
1/R1→R6;1→X;0→R5
0⊢
5:
0→R(200+X);0→R(2
50+X)⊢
6:
1+X→X;IF X<R6+1;
GTO 5⊢
7:
PRT "RATE",R1,"V
 MAX",R2,"K M",R
3,"MOI",R4⊢
8:
R2*(1-EXP (-R4))
→R5⊢
9:
SPC 2⊢
10:
2→R(200+R6)-R5/(
R3+R101)*R101→R1
5⊢
11:
2→X⊢
12:
R(199+X)-R(200+X
)→R(250+X)⊢
13:
1+X→X;IF X<R6+1;
GTO 12⊢
14:
R5/(R3+R101)*R10
1-R201→R251⊢
15:
R101+R151→R101⊢
16:
1→X⊢
```

```
17:
R(200+X)+R(250+X
)→R(200+X)⊢
18:
1+X→X:IF X≤R6+1:
GTO 17⊢
19:
1+R50→R50:1+C→C:
IF C≤59:GTO 10⊢
20:
0→C:R50/60→Z:
FXD 2⊢
21:
PRT "TIME(HR)",Z
:SPC 1:FLT 3⊢
22:
0→Z:1→X⊢
23:
Z+R(200+X)→Z⊢
24:
1+X→X:IF X≤R6+1:
GTO 23⊢
25:
R101+Z→Y⊢
26:
PRT "TOTAL DNA",
Y⊢
27:
PRT "MAT,REP",R1
01,Z⊢
28:
Z/Y*100→A:PRT "P
CT REP",A⊢
29:
R5/(R3+R101)→A:
PRT "I",A⊢
30:
GTO 10⊢
31:
END ⊢
Σ18668
R1098
```